Volume: 1
Issue: 1
Serial Number: 1
Winter 2025

Online ISSN: 3092-7277

Interdisciplinary Journal of Civil Engineering

Publisher:
Shahid Beheshti University

Address:
Faculty of Civil, Water, and Environmental Engineering, Shahid Beheshti University, Shahid Abbaspour Technical Campus, Shahid Abolreza Blvd., Hakimieh, Tehran, Iran

P.O. Box:
1658953571

Tel:
+98(21) 73932453
+98(21) 73932401

Fax:
77006660

Website:
http://ijce.sbu.ac.ir

Interdisciplinary Journal of Civil Engineering
Shahid Beheshti University

Interdisciplinary Journal of Civil Engineering

Online ISSN: 3092-7277
Vol. 1, Issue. 1, Winter 2025

About Journal

The **Interdisciplinary Journal of Civil Engineering (IJCE)** is a prestigious scientific research journal published quarterly by Shahid Beheshti University. Supported by a distinguished team of experts from both academia and industry, IJCE focuses on the social science dimensions of civil engineering. The journal covers a broad range of topics, including structural engineering, earthquake engineering, transportation, geotechnics, mapping, environmental engineering, water and wastewater management, and water resources. IJCE invites all researchers to submit their research in the form of articles, review articles, and case studies. The editors will welcome papers from all countries, hoping that this will advance the scientific standards of the journal and provide a channel of communication between Iranian Scholars and their colleagues in other parts of the world.

IJCE is a peer-reviewed journal that offers open access to all interested readers. This journal follows a double-anonymized review process. Also, this journal adheres to the guidelines set by the Committee on Publication Ethics (COPE) and upholds the highest ethical standards in compliance with relevant ethical laws.

Message from the Editor-in-Chief

It is both an honor and a privilege to serve as the Editor-in-Chief of The Interdisciplinary Journal of Civil Engineering. This journal was founded with the vision of establishing a distinguished forum for the dissemination of high-quality research and the exchange of transformative ideas in the field of civil engineering. By fostering an interdisciplinary perspective, we aim to bridge diverse areas of expertise through promoting collaboration across academic and professional communities, addressing the complex challenges that define our rapidly evolving world.

Our mission is to advance the frontiers of civil engineering through scholarly rigor, innovation, and a persistent commitment to excellence. Each contribution to this journal represents a collective pursuit of knowledge that transcends conventional boundaries, driving progress toward sustainable, resilient, and future-ready infrastructures. I extend my sincere gratitude to our authors, reviewers, and the editorial team for their close collaboration and to our readers for their continued engagement in shaping the future of our discipline.

Dr. Nemat Hassani
Editor-in-Chief

Contents

May 2025
Volume 1
Issue 1

DOI: 10.48308/ijce.2025.105740

Interdisciplinary Journal of Civil Engineering
Shahid Beheshti University

Developing a Practical Pricing Framework for Airport Parking Infrastructure

Authors:

Alireza Mahpour[1, *], Amirhossein Baghestani[1], Sahand Heshami[1]

Abstract

This study proposes a practical pricing framework for airport parking infrastructure, with a particular focus on aging airports where construction costs have been amortized. Employing a benefit-cost analysis approach, the study investigates the case of Mehrabad Airport in Tehran, Iran—an operational airport since 1938 with a well-established parking system. Financial data, including annual operational costs and revenue figures from parking lot contractors, were obtained from airport management to assess current profit margins and determine a fair equilibrium price for parking services. The results reveal an average profit margin of approximately 40% for contractors, suggesting a pricing imbalance that favors private operators at the expense of both customers and the airport authority. Based on these findings, the study recommends a set of policy interventions, such as adjusting parking tariffs to reflect real traffic conditions, increasing lease rates for contractors, and enforcing service quality regulations. These measures aim to enhance transparency, promote equitable pricing, and align stakeholder interests in the airport parking sector. The proposed methodology offers a replicable model for pricing public-use infrastructure assets at both mature and emerging airports globally.

Keywords: Airport Infrastructure, Parking Pricing, Benefit-Cost Analysis, Public Asset Management, Mehrabad Airport

1. Faculty of Civil, Water, and Environmental Engineering, Shahid Beheshti University, Tehran 1983969411, Iran

*Corresponding Author: a_mahpour@sbu.ac.ir

1. Introduction

The pricing of transportation infrastructure is a critical issue that impacts the efficiency, equity, and sustainability of transportation systems. Among the various types of transportation infrastructure, parking facilities, particularly at airports, play a vital role as they generate significant revenues for airport authorities (Mahpour et al., 2024). With the growing demand for air travel, the use of airport parking has also increased (Becken & Carmignani, 2020). However, determining the optimal pricing for transportation infrastructures (e.g., Haery et al., 2024; Tayarani Yousefabadi et al., 2020; Tayarani Yousefabadi et al., 2021), especially airport parking, depends on several factors, such as demand, supply, location, and the quality of parking services (Love et al., 2014). One important question in this context is whether the same pricing strategy should be applied to airports that have long been established and have a solid market position, compared to those that are newly built or still under construction.

Airport parking projects that are currently under construction or have recently begun operations incur various costs, including construction, overhead, and investment expenses (Liu, 2003). Several methods can be employed to establish the optimal pricing for these projects. These methods include analyzing the supply and demand function, comparing similar infrastructures in different countries, and utilizing techniques such as linear regression or benchmarking (Straker, 2006). However, understanding the supply and demand function and determining the equilibrium price can prove to be challenging (Xie et al., 2017). Therefore, a more practical approach is to use linear regression to gather relevant data from multiple countries and then apply a transferability method to adjust the pricing for airport parking accordingly (Mamdoohi et al., 1393).

Due to the long lifespan of older transportation infrastructure, costs such as construction expenses and interest rates have been amortized. Therefore, it would be unfair to consider only the construction costs in evaluating such projects (Jones et al., 2014). Various methodologies can be used to determine the pricing of aging airport parking facilities. These include the benchmark method employed by established airports, the benefit-to-cost method, and multiple linear regression (Fan, 2004; lo Storto, 2017). This paper aims to price the parking services at Mehrabad Airport in Tehran, Iran, using the benefit-to-cost method. Mehrabad Airport, which began operations in 1938, currently has 6 terminals, 15 active airlines, and 4 parking lots.

In the next section of the study, we will discuss the review of previous literature on pricing. The third section will explain the methods of data collection, data analysis, and the methodology, focusing on the benefit-to-cost. The fourth section will present the results of the study, followed by a discussion and conclusions in the fifth section.

2. Literature Review

Numerous studies have been conducted on parking pricing in various locations. For instance, Mark Friesen and colleagues examined dynamic pricing in Europe. They concluded that in

order to effectively implement dynamic pricing on a larger scale, private parking operators currently using a fixed pricing model should follow three essential stages: understanding, evaluation, and communication (Friesen & Mingardo, 2020). Moreover, researchers examined data from 14 garages participating in the SF-park program in San Francisco. They found that by implementing price management for parking, public usage of the garages could increase by over a third. Additionally, this approach helped reduce the average costs for drivers while maintaining a stable revenue stream for the city (Pierce et al., 2015).

Hao Wang and colleagues conducted a study analyzing field data collected over four time periods, both before and after the implementation of a new parking pricing policy in Nanning. Their findings indicate that as parking prices increase, the duration of parking time decreases. This relationship demonstrates an elasticity effect, which suggests that the responsiveness of parking circulation may fluctuate based on the influence of vehicle ownership (Wang et al., 2020). The pricing of parking lots has a significant effect on the amount of demand and the quality of services, and more studies have been conducted in this field (Mo et al., 2021; Nourinejad & Roorda, 2017; Ottosson et al., 2013; Pierce & Shoup, 2013; Shu et al., 2021).

Various studies focused on airport parking pricing. For instance, Andreas Papayiannis introduced innovative methodologies to develop recommended pricing structures based on parking capacity and the time remaining until departure. Within the field of airport parking sales, three main revenue management methods have been analyzed: Stochastic Multi-Resource (SMR), Stochastic Single-Resource (SSR), and Deterministic Single-Resource (DSR). These methods aim to assess the expected marginal values of parking spaces, which can then be used to regulate bid prices in an ongoing experimental framework (Papayiannis et al., 2019).

Litman conducted an investigation into determining the most effective pricing for various types of parking services, taking into account several factors that influence the final cost (Litman, 2018). This study recommends that parking services should be priced based on the costs associated with land acquisition or rental, construction, maintenance, and operations. This includes the expenses for utilities such as water, electricity, and gas. Additionally, another study examines how the maximum daily fee charging strategy has impacted the quality of parking services at Hongqiao International Airport, using automated transaction data from before and after the strategy was implemented (Cheng & Qi, 2019). The estimation results indicate that the new pricing method will significantly decrease the demand for long-term parking and enhance the availability of airport parking facilities, particularly during extended vacations. As a result, both throughput and revenue at the airport have seen substantial increases, though there are additional time costs associated with vehicles departing. Furthermore, the price elasticity for parkers with varying parking durations was estimated. The findings revealed that price sensitivity is relatively inelastic but varies depending on the parking duration.

In the absence of a comprehensive pricing method for airport parking, it is imperative to consider a multitude of additional factors. These may encompass the supply and demand

dynamics of transportation at the airport, as well as various socioeconomic factors (Keefe, 2014). Research has indicated that the characteristics of airports and air transportation, as well as the socioeconomic attributes of countries and cities, could exert an influence on the pricing and revenue of services (Iyer & Jain, 2019; Zuidberg, 2017).

A significant amount of research has focused on airport parking pricing; however, it is uncommon to find studies that exclude depreciated costs or reference outdated airports in their pricing analysis, particularly when using the benefit-to-cost method. Therefore, this issue represents a research gap that deserves more attention in order to establish fair pricing practices.

3. Methodology

In this section, the method of data collection is described and the collected information is described. In addition, the method used in the study is explained.

3.1. Data

The data on the parking information for terminals 1, 2, 4, and 6 of Mehrabad Airport were obtained with the cooperation of the airport management. The parking lots of the airport are rented annually to two contractors. The data were collected in two sections. The first section includes the annual costs of the contractor, such as annual rent, number of staff, general expenses, salaries of employees, insurance costs, maintenance costs, and equipment costs. The second section includes the income information of the contractor, such as the number of vehicles exiting with less than 24 hours of parking and more than 24 hours of parking, the entrance fee, the parking fee per day or hour, the average parking time of less than 24 hours, and the average parking time of more than 24 hours.

3.2. Benefit-to-Cost

A benefit-cost model used previously in numerous research (e.g., Mahpour et al, 2018; Mahpour et al, 2019; Mahpour et al, 2020; Mahpour et al, 2021). In this study, a benefit-cost model was utilized to evaluate the current profitability of Mehrabad Airport's parking lots and to project future pricing for these lots. Initially, we calculated the current costs and annual rent associated with the parking areas. Following this, we determined the annual revenue generated from the parking lots. This allowed us to establish the current annual profit. Subsequently, we estimated the equilibrium price in relation to costs. The annual profit was calculated using equation 1, while the annual profit rate was derived from equation 2:

$$\text{Annual Profit} = \text{Annual Income} - \text{Annual Cost} \quad (1$$

$$\text{Annual profit rate} = (\text{Annual Profit} / \text{Annual Cost}) * 100 \quad (2$$

4. Results

The costs associated with Mehrabad Airport are detailed in Table 1. The total number of parking staff across all shifts is 99 individuals, and the average monthly salary of each staff member is 65 million IRR. Also, the majority of the contractor's expenses for one year are attributed to

the annual rent for the parking lots, which amounts to 21,000 million IRR[1], along with the salary of all staff members totaling 77,220 million IRR, and insurance costs totaling 18,000 million IRR.

Additionally, the general expenses amount to 500 million IRR per month. The monthly costs for building maintenance are 300 million IRR, while the monthly expenses for equipment maintenance and repair are 200 million IRR. Therefore, the total annual expenditure for general expenses, building maintenance costs, and equipment maintenance costs is 12,000 million IRR. In total, the annual expenses for the parking lots at Mehrabad Airport, which include maintenance, equipment costs, and general expenses such as water, electricity, and gas, reach 317,220 million IRR.

Table 1. Mehrabad Airport parking cost

Detail	Amount (Million IRR)	Month/ Year/ Person	Total Cost (Million IRR)
Terminal 4 and 6 parking lot rental (total capacity: 1700)	70,000	1 year	70,000
Terminal 1 and 2 parking lot rental (total capacity: 3220)	140,000	1 year	140,000
Monthly general expenses (water, electricity, gas, telephone, etc.)	500	12 Month	6,000
Monthly insurance	1,500	12 Month	18,000
Monthly building maintenance	300	12 Month	3,600
Monthly equipment maintenance	200	12 Month	2,400
Average monthly salary of each staff member	65	12 Month * 99 Person	77,220
Total cost (Per 1 year)			317,220

The income characteristics of contractors are outlined in Table 2. Parking for drivers is available in two formats: daily stops (lasting more than 24 hours) and hourly stops (lasting less than 24 hours). The parking lot experiences a departure of 3,500 cars for hourly stops, while 1,500 cars leave for daily stops. The average stopping time for hourly stops is 4 hours, whereas daily stops average 2 days. Consequently, the revenue generated from hourly parking amounts to 76,650 million IRR, while the revenue from daily parking totals 558,450 million IRR. Overall, the total revenue from Mehrabad Airport parking is 635,100 million IRR.

Given that the full parking capacity may not be available throughout the year due to factors such as maintenance or seasonal fluctuations in demand, this study applies a correction factor of 0.7 to the annual revenue. Consequently, the total corrected annual revenue amounts to 44,570 million IRR. The results show that in order for the amount of income and cost to be equal, drivers must pay 24,142 IRR for each hour of parking, which is equal to the equilibrium

[1] 500,000 IRR is equal to 1 Dollars in Jan 2024

price. Considering the cost and income obtained, the amount of profit calculated for the contractor is 127,350 million IRR per year, and the annual profit rate is 40.15%.

Table 2. Mehrabad Airport parking income

Parking	Departure	Average stop	Income price	Hourly or daily price	Amount (Million IRR)
Hourly stops	3500	4 hours	20,000 IRR	10,000 IRR	76,650
Daily stops	1500	2 days	20,000 IRR	500,000 IRR	558,450
Total income					635,100
Adjusted Total Income (Correction factor = 0.7)					444,570

5. Policy and Conclusion

This paper addresses the issue of pricing for outdated transportation infrastructure, arguing that it is unfair to factor in construction costs that have already been amortized. It proposes a benefit-cost model for pricing the parking lot at Mehrabad Airport in Tehran, which is an older airport, explicitly excluding construction costs from the calculations. This paper gathers annual cost and income data from the contractors who lease the parking lot from the airport management and analyzes the profitability of the parking business. The findings indicate that the contractors generate a net profit of 40.15% from the airport parking operations.

This paper offers policy recommendations for airport sector managers based on the findings of a benefit-cost analysis of parking lot pricing. It suggests that airport service department managers should closely monitor and regulate both the quality of parking services and the profit margins of contractors who operate the parking lots. Addressing these issues can enhance customer satisfaction and loyalty, as well as increase demand for parking services (Nourinejad & Roorda, 2017)(Qin et al., 2022).

Additionally, the paper recommends that parking lot pricing be adjusted to reflect the traffic conditions surrounding the airport, contributing to an overall improvement in traffic flow (Jakob & Menendez, 2020). Furthermore, it suggests increasing the annual fees and rent for contractors to ensure a fair and reasonable profit margin while preventing excessive profiteering in the parking business. In conclusion, these policies can enhance the management and performance of the airport parking sector, aligning them with the interests and expectations of stakeholders.

6. References

Becken, S., & Carmignani, F. (2020). Are the current expectations for growing air travel demand realistic? *Annals of Tourism Research*, *80*. https://doi.org/10.1016/j.annals.2019.102840

Cheng, C., & Qi, P. (2019). Impact analysis of parking price adjustment on the quality of service of airport parking lots for light vehicles. *Journal of Advanced Transportation*, *2019*. https://doi.org/10.1155/2019/3847837

Fan, T. P. (2004). *Market-based airport demand management: theory, model, and applications*. Massachusetts Institute of Technology.

Friesen, M., & Mingardo, G. (2020). Is parking in Europe ready for dynamic pricing? A reality check for the private sector. *Sustainability (Switzerland)*, *12*(7). https://doi.org/10.3390/su12072732

Iyer, K. C., & Jain, S. (2019). Performance measurement of airports using data envelopment analysis: A review of methods and findings. *Journal of Air Transport Management*, *81*. https://doi.org/10.1016/j.jairtraman.2019.101707

Jakob, M., & Menendez, M. (2020). Parking Pricing vs. Congestion Pricing: A Macroscopic Analysis of their Impact on Traffic. *Transportmetrica A: Transport Science*. https://doi.org/10.1080/23249935.2020.1797924

Jones, H., Domingos, T., Moura, F., & Sussman, J. M. (2014). *Transport infrastructure evaluation using cost-benefit analysis: improvements to valuing the asset through residual value—a case study*.

Keefe, J. (2014). What are the key considerations for an airport in implementing a direct channel for car park and ancillary pre-booking, and what are the potential resulting incremental revenue benefits? *Journal of Airport Management*.

Litman, T. (2018). Parking Pricing Implementation Guidelines. *Victoria Transport Policy Institute*.

Liu, S. T. (2003). The total cost bounds of the transportation problem with varying demand and supply. *Omega*, *31*(4). https://doi.org/10.1016/S0305-0483(03)00054-9

lo Storto, C. (2017). Product benchmarking in the air cargo industry: Non-parametric measurement of an aircraft value for money. *Benchmarking: An International Journal*, *24*(4), 857–881.

Love, P. E. D., Sing, C. P., Wang, X., Irani, Z., & Thwala, D. W. (2014). Overruns in transportation infrastructure projects. *Structure and Infrastructure Engineering*, *10*(2). https://doi.org/10.1080/15732479.2012.715173

Mahpour, A., Asadi, M., & Baghestani, A. (2024). Are supply and demand the main key drivers of airport parking prices? The quantitative study. *Journal of Air Transport Management*, *114*, 102505.

Mamdoohi, A. R., Seyedabrishami, S., & Baghestani, A. (1393). *Final Analytical Comparison of Aggregate and Disaggregate Mode Choice Models Transferability*.

Mo, B., Kong, H., Wang, H., Wang, X. (Cara), & Li, R. (2021). Impact of pricing policy change on on-street parking demand and user satisfaction: A case study in Nanning, China. *Transportation Research Part A: Policy and Practice*, *148*. https://doi.org/10.1016/j.tra.2021.04.013

Nourinejad, M., & Roorda, M. J. (2017). Impact of hourly parking pricing on travel demand. *Transportation Research Part A: Policy and Practice*, *98*. https://doi.org/10.1016/j.tra.2017.01.023

Ottosson, D. B., Chen, C., Wang, T., & Lin, H. (2013). The sensitivity of on-street parking demand in response to price changes: A case study in Seattle, WA. *Transport Policy*, *25*. https://doi.org/10.1016/j.tranpol.2012.11.013

Papayiannis, A., Johnson, P. V., Yumashev, D., & Duck, P. (2019). Revenue management of airport car parks in continuous time. *IMA Journal of Management Mathematics*, *30*(1). https://doi.org/10.1093/imaman/dpy015

Pierce, G., & Shoup, D. (2013). Getting the prices right. *Journal of the American Planning Association*, *79*(1). https://doi.org/10.1080/01944363.2013.787307

Pierce, G., Willson, H., & Shoup, D. (2015). Optimizing the use of public garages: Pricing parking by demand. *Transport Policy*, *44*. https://doi.org/10.1016/j.tranpol.2015.07.003

Qin, H., Zheng, F., Yu, B., & Wang, Z. (2022). Analysis of the Effect of Demand-Driven Dynamic Parking Pricing on on-Street Parking Demand. *IEEE Access*, *10*. https://doi.org/10.1109/ACCESS.2022.3187534

Shu, P., Sun, Y., Xie, B., Xu, S. X., & Xu, G. (2021). Data-driven shuttle service design for sustainable last-mile transportation. *Advanced Engineering Informatics*, *49*, 101344. https://doi.org/https://doi.org/10.1016/j.aei.2021.101344

Straker, I. A. (2006). *Airport Car Parking Strategy: Lessons From The Non-Airport Sector* (p. 333).

Wang, H., Li, R., Wang, X. (Cara), & Shang, P. (2020). Effect of on-street parking pricing policies on parking characteristics: A case study of Nanning. *Transportation Research Part A: Policy and Practice*, *137*. https://doi.org/10.1016/j.tra.2020.04.003

Xie, F., Butt, M. M., Li, Z., & Zhu, L. (2017). An upper bound on the minimal total cost of the transportation problem with varying demands and supplies. *Omega (United Kingdom)*, *68*. https://doi.org/10.1016/j.omega.2016.06.007

Zuidberg, J. (2017). Exploring the determinants for airport profitability: Traffic characteristics, low-cost carriers, seasonality, and cost efficiency. *Transportation Research Part A: Policy and Practice*, *101*. https://doi.org/10.1016/j.tra.2017.04.016

May 2025
Volume 1
Issue 1

Interdisciplinary Journal of Civil Engineering
Shahid Beheshti University

DOI: 10.48308/ijce.2025.105775

Design and Analysis of Riverbank Filtration Systems Using Linear Systems Response Functions

Authors:

Saeed Alimohammadi[1, *], Masoumeh Behrouz[1]

Abstract

Riverbank filtration systems offer a useful and reliable method for meeting domestic and industrial demands. In these systems, some wells are constructed in the bank of a river, where the water that flows across porous media into them has a very low pollutant level compared to the river. This study develops a cost-effective optimization model to minimize total cost. A simulation model for analyzing these systems is developed as well. In these models, the analytic solutions of the groundwater flow equations and pollutant transport are used. Using the concept of response functions of linear systems, these solutions are generalized in the case of variable pumping. In common RBF systems, the unit pulse response function of drawdown is independent of wells' location, and the transient flow equation reaches pseudo steady-state conditions. Two hypothetical example problems are presented; in the first, the design of a system is considered for meeting a given demand. The model solutions give the distance of wells' alignment from the river, the distance between wells, and the wells' pumping rates. The model also outputs the pollutant concentration in the wells. The results of the steady optimization problem reveal that, unexpectedly, the central well's discharge is greater than the side wells' discharges. The resulting pumping, conveyance, and treatment costs showed that all three cost terms are important. The sensitivity analysis revealed that all four considered parameters are sensitive, with the sensitivity ranking of: T (transmissivity), λ (decay rate), Θ (porosity), and R_d (retardation factor). In the second problem, an existing RBF system was analyzed by a simulation model, and the variations of the well's concentration were assessed by altering the four sensitive parameters. The proposed models are useful tools for primary design and analysis of RBF systems and assessing the effects of changing parameters on the system behavior.

Keywords: Riverbank Filtration, Response Function of Linear Systems, Analytic Solution, Optimization

1. Faculty of Civil, Water, and Environmental Engineering, Shahid Beheshti University, Tehran 1983969411, Iran

*Corresponding Author: s_alimohammadi@sbu.ac.ir

1. Introduction

Rivers are one of the most important sources of domestic water supplies. Entry of different pollutants, such as agricultural, industrial, and urban wastewaters, into the rivers dramatically compromises their quality. Typically, a great deal of budget is spent on the treatment of river water withdrawals in water treatment plants.

Riverbank filtration (RBF) is one of the efficient methods for the pretreatment of river water pollution. RBF systems are widely used for drinking water provision and treatment in several cities around the world, especially in European countries, where they provide a cost-effective and sustainable alternative compared to direct surface water intake and treatment. As illustrated in Fig. 1, in this method, some wells are constructed adjacent to a permanent river, which together have the capacity to meet a given demand. During transport and seepage of water from rivers to wells through porous media of riverbanks, a considerable level of pollutants can be removed. Although this method is largely classified as physical treatment, in most cases, it removes or reduces most chemical and biological pollutants.

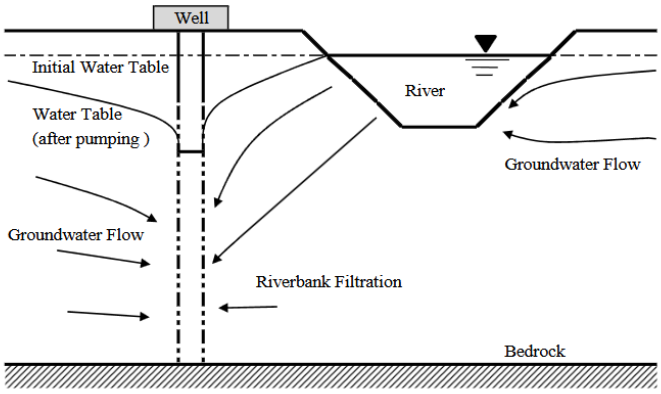

Figure 1. Schematic of an RBF system

Another important feature of RBF systems is their use in accidents through which dangerous pollutants, such as chemical tanks, enter the river. These events have less intense effects on the performance of RBF systems because of the relatively long delay for river water reaching wells. In conventional RBF systems, vertical wells are usually constructed in a straight line parallel to the river line; however, in some situations, the use of horizontal (collector) wells increases the discharge rate to wells (Ray et al., 2003).

Most RBF systems are constructed in alluvial sandy aquifers (banks). In addition to enhancing water quality, reducing water temperature, and protecting fish and other aquatic creatures are other advantages of RBF systems. The major elements of an RBF system that must be considered include the number of production wells and their capacities (discharges), the distance between the river course and the wells' alignment, and the distance between wells.

When the desired quantity (discharge) and quality (concentration) are given, the system could be designed with a minimum cost (cost-effective design). As demonstrated in Fig. 2, the system costs include the costs of constructing wells and OMR, the costs of constructing pipelines and OMR, the pumping cost of wells, and the water treatment cost.

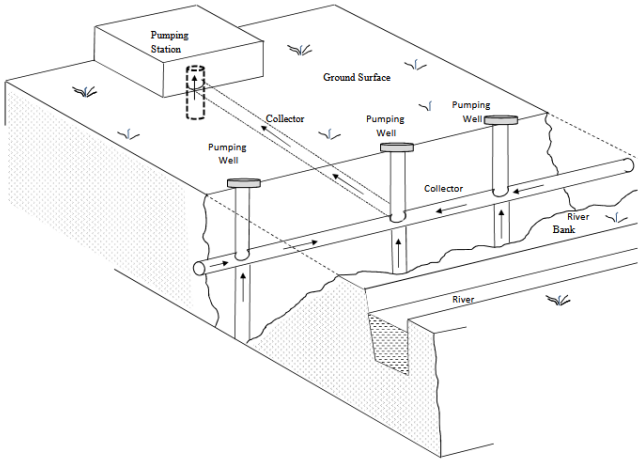

Figure 2. Component of an RBF system

2. Literature Review

It appears that the Glasgow Water Supply Company was the first known firm to develop and utilize an RBF system in 1810 (Ray et al., 1999). Moser et al. (1990) studied an aquifer that used two adjacent rivers for an RBF system. Using an advection-dispersion-based model, they computed the transfer time from the river to the aquifer, and they concluded that by knowing this delay time, there is enough time to control and prevent river pollution of the pumping wells.

Doussan et al. (1997) assessed the general characteristics of RBF systems in a portion of the Seine River in France. They simulated the oxidation and reduction reactions as well as the nitrogen transfer reaction, using a numerical model. They reported the importance of the rate of water (discharge), sediment, and organic carbon in the quality of transferred water.

Dillon et al. (2001) studied the potential of the RBF for domestic water supply, considering the removal of microcystins in the Murray River in Australia. They briefly reported on the decomposition of cyanobacterial hepatotoxin microcystins in porous media.

In RBF systems, removing organic pollutants is an important task when water is used for domestic purposes. Absorption and colonization of an organic pollutant could reduce its transfer. Kim et al. (2002) used a kinetic model for the simulation of the fate and transport of dissolved organic pollutants and bacteria. They modeled the porous media using four phases: two colloidal phases, one aquatic phase, and a solid phase. The result of this study shows that the transfer of pollutants in the vicinity of dissolved organic matter is considerably high.

Schon (2006) studied the RBF systems in Austria and India. He concluded that the layout and arrangement of pumping wells based on morphology have a considerable effect on the extension of the treatment area in wells located on the inside of a meander, and the filtration from the riverbank has more sensitivity than wells located outside the meander.

Abdel Fattah et al. (2007) used tracer techniques to trace and evaluate the transfer of water through the alluvial aquifer in El Paso, Texas. They conducted several simulations to show the effects of well's locations and its pumping rate on the flow path, travel time, pumping radius of influence, and ratio of the volume of water from the river to the volume of water from the

aquifer. Also, they found that the pumping rate has more influence on travel time than the distance between the well and the river.

Shamrukh et al. (2008) investigated the effectiveness of the RBF system in Upper Egypt in the Nile valley for removing particulates, dissolved solids, and microbial pathogens to produce drinking water. For this purpose, they monitored physical, chemical, and microbial measurements. They compared water produced with surface and background natural groundwater and with the RBF system and proved the effectiveness of the RBF technique for potable water supply requiring any further treatment or as pre-treatment for higher water quality in Upper Egypt.

Sandhu et al. (2011) studied the operating bank filtration sites in India and investigated the potential of RBF sites based on water problems and hydrogeological suitability. They found that bank filtrate showed higher quality in RBF water compared to water from surface or groundwater sources. They investigated the different uses and the consequent effect on the quality and quantity of surface and groundwater. They stated the RBF system with an emphasis on the hydrogeological conditions, system capacities, and the main water quality improvements. However, they resulted there are some prospects and limitations for the application of bank filtration in India at the existing sites.

Lee et al. (2011) studied using a radial collector well for taking out a large amount of groundwater in a way that hasn't seen a deep drawdown at the well's center. They investigated the hydraulic interaction between river water and groundwater flow response to pumping the riverbank filtration system in Daesan Myeon, Korea. They performed steady-state and transient simulations to estimate the well yield and well responses to pumping. They also evaluated the effect of well structure on the capacity of the RBF well. They resulted in increasing the length of horizontal arms increases the amount of induced river water, and with increasing pumping rates, the effect of well design is more noticeable.

Prasad et al. (2016) presented an optimization model using genetic algorithms for optimal well distance from the river with minimizing the cost of pumping and treatment. The total suspended solids, endosulfan concentrations, and E. coli were considered as water quality parameters. The total suspended used as microbial contamination and are considered not to be absorbed in the aquifer, and endosulfan is considered to undergo sorption. Also, Sensitivity analysis has been done and resulted in the optimal distance significantly affected at lower hydraulic conductivity values, and the cost of treatment increased with increasing hydraulic conductivity. It was concluded that the hydraulic conductivity of the adjoining aquifer plays a dominant role in deciding the optimal distance of pumping wells in a river bank filtration system.

Mustafa et al. (2024) introduce a 3D analytical model utilizing the Green's function approach to analyze the movement of contaminants from the river towards the extraction well within RBF systems. By accounting for the dynamic interaction between river width and the clogging layer, this model offers a more accurate depiction of contaminant transport in three-dimensional water flow scenarios.

Uwimpaye et al. (2025) assessed the suitability of RBF in regions with limited access to clean water, such as Africa, where it has the potential to alleviate water scarcity and enhance water

security. This study used various studies, highlighting the principles, applications, and advancements of RBF worldwide. The findings of this research revealed that RBF effectively addresses a broad range of contaminants, including microbial pathogens, organic compounds, heavy metals, and micro-pollutants, through natural processes like adsorption, biodegradation, and filtration.

As presented in the literature review, little attention has been paid to using mathematical (optimization) models in designing and analyzing RBF systems. This study undertook this task. Importantly, attempts were made not to give details of the chemical, physical, and biological behavior of pollutants; instead, the governing equations of groundwater flow and contaminant fate and transport were developed here.

Typically, an RBF system's extended area is small compared to the total extension of the aquifer. Thus, the aquifer was assumed homogeneous, and hence the use of lumped models and analytical solutions is reasonable. In the case of inhomogeneous aquifers, the methodology may extend to using numerical methods and distributed models, though the solution of the resulting model is more complicated, usually requiring the utilization of a simulation-optimization scheme to achieve the desired results.

In addition to aquifer homogeneity, other major assumptions in this study included the following: the river discharge is permanent; river and wells are fully penetrated; the river and adjacent aquifer are hydraulically connected and there is no low permeable layer on the bed of river; groundwater flow in porous media is Darcian and Dupoit assumption is applicable; drawdowns in comparison with the initial saturated layer is small; and the system design life cycle and interest rate are given. The river pollutant is a single species and Fickian, and not in the form of biological species (microorganisms) or NAPL. Hence, the advection-dispersion solute transport equation governs here; the flow and solute transport from the river to the aquifer is considered one-dimensional, and the linear sorption mechanism has been considered along with the equilibrium chemical reaction. Finally, assuming that the changes in the solute concentration yielded by the solution of the transport equation cause negligible variations in water density, the flow equation and solute transport equation can be solved independently (Zheng and Bennet, 2002).

3. Methodology

3.1. Model Formulation: Steady–State Conditions

3.1.1. Flow Equations

The flow equations of an RBF system in steady-state conditions are derived by combining the continuity equation, Darcy's law, and the image wells concept. Under steady-state conditions, the total water pumped in wells comes from the river. As demonstrated in Fig. 3, the drawdown at distance *r* from the well pumping equals (McWhorter and Sunada, 1977):

$$s = \frac{Q_w}{2\pi T} Ln \frac{r_i}{r} \quad (1$$

Where, Qw is the constant pumping rate from the well, T represents the aquifer transmissivity, r shows the distance from the river, and ri shows the distance from the image well. Also, the drawdown in the pumping well is derived by incorporating r=rw in Eq. (1).
Fig. 4 indicates a schematic arrangement of the wells near a permanent river as an RBF system. Using Eq. (1) and assuming that the aquifer behaves as a linear system, the required equation could be derived. The drawdown in each well of the system *s(k)* equals the sum of drawdowns due to individual well pumping. Thus, with N_w wells, the drawdown *s(k)* in well *k*, equals:

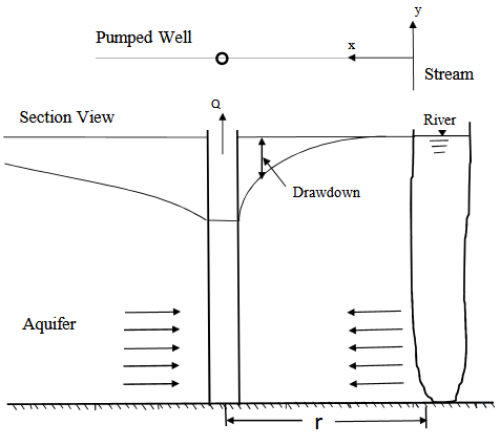

Figure 3. Section view of the system with major components

$$s(k) = \sum_{j=1}^{N_w} s_{k\,j} \qquad (2$$

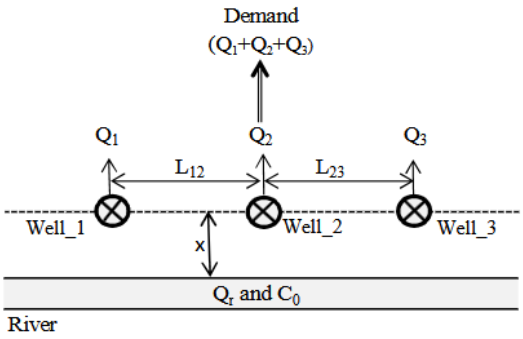

Figure 4. A schematic arrangement of wells near a permanent river

Where, *s(k,j)* is the portion of drawdown in well *k* due to pumping in well *j* (*j* may equal *k*). From Eq. (1), we have:

$$s(k,j) = \frac{Q(j)}{2\pi T} Ln\left(\frac{\sqrt{4x^2 + l_{kj}^2}}{l_{kj}}\right) \qquad (3$$

Where, $Q_w(j)$ is the constant pumping rate in well *j*, l_{kj} represents the distance between wells *k* and *j* (for *k=j*, $l_{kj}=r_w$, where r_w is the well radius), and *x* denotes the distance between the river and wells' alignment (see Fig. 7).

3.1.2. Solute Transport Equations

The governing equation of the solute transport in porous media with sorption and decay was derived by combining the continuity equation, Fick's first and second laws, and the sorption plus decay mechanism. The resulting equation was a variant of the advection-dispersion equation. Assuming a linear sorption isotherm and one-dimensional unidirectional flow in homogeneous isotropic porous media and first-order irreversible rate reaction (decay rate), we have (Zheng and Bennet, 2002):

$$R_d \frac{\partial C}{\partial t} = D_x \frac{\partial^2 C}{\partial x^2} - V_x \frac{\partial C}{\partial x} - \lambda C \quad (4$$

Where, Rd represents the retardation factor, C is the solute concentration, t shows the time, Dx is the dispersion coefficient, Vx denotes seepage velocity in the x direction, and λ is the decay rate. From Darcy's law, we have:

$$V_x = \frac{q_x}{\theta} = \frac{K_x}{\theta} i = \frac{K_x}{\theta} \frac{\bar{s}}{x} \quad (5$$

Where, q_x is Darcy velocity or groundwater flux in the x direction, K_x shows the hydraulic conductivity in the x direction, $\bar{s} = 1/N_w \times \sum_{k=1}^{N_w} s_k$ is the average drawdown of wells, and x is the well's distance to the river. The Retardation factor, R_d, is a function of distribution coefficient (K_d) along with the porosity of the aquifer (θ) and bulk density of the aquifer material (ρ_b), as (Zheng and Bennet, 2002):

$$R_d = 1 + K_d \frac{\rho_b}{\theta} \quad (6$$

The dispersion coefficient D_x is also a function of longitudinal dispersivity (α_L), groundwater velocity (V_x), and molecular diffusivity (D_*) as:

$$D_x = \alpha_L \times V_x + D_* \approx \alpha_L \times V_x \quad (7$$

The longitudinal dispersivity, α_L, is a very uncertain parameter (Gelhar, 1993). However, a well-known equation proposed by Neuman (1990) is applied in the case of data inadequacy as a rough estimate:

$$\alpha_L = 0.0175 \ L^{1.46}, \qquad 100 \ m < L < 3500 \ m \quad (8\text{-a}$$

$$\alpha_L = 0.0169 \ L^{1.53}, \qquad L < 100 \ m \quad (8\text{-b}$$

In which, L is the distance between the contaminant source (river in this case) and contaminant exposure (well in this case). As RBF systems are constructed next to the rivers, thus, Eq. (8-b) is applicable to these systems. Using proper initial and boundary conditions, the analytic solution can be conducted. The initial and boundary conditions in this case are:

$$C(x,0) = 0 \qquad x \geq 0 \quad \textit{initial condition} \quad (9$$

$$C(0,t) = C_0 \qquad t \geq 0 \quad \textit{boundary condition} \quad (10$$

$$C(\infty,t) = 0 \qquad t \geq 0 \quad \textit{boundary condition} \quad (11$$

$$\frac{\partial C(\infty,t)}{\partial x} = 0 \qquad t \geq 0 \quad \textit{boundary condition} \quad (12$$

Where, C_0 is the constant concentration of pollution in the river (*mg/lit*) and *C(x,t)* represents the (reduced) concentration of leaked water in the riverbank at distance *x* after time *t*. The analytical solution for this problem has been given by Batu as (Batu, 2006):

$$C(x,t) = \frac{C_0}{2}\left[\begin{matrix} erfc\left[\frac{R_d x - (V_x{}^2 + 4D_x R_d \lambda)t}{2(D_x R_d t)^{0.5}}\right] \times exp\left(\frac{(V_x - (V_x^2 + 4D_x R_d \lambda))x}{2D_x}\right) + \\ erfc\left[\frac{R_d x + (V_x{}^2 + 4D_x R_d \lambda)t}{2(D_x R_d t)^{0.5}}\right] \times exp\left(\frac{(V_x + (V_x^2 + 4D_x R_d \lambda))x}{2D_x}\right) \end{matrix}\right] \quad (13$$

Under steady-state conditions ($t \to \infty$), the above equation is reduced to:

$$C(x) = C_0 \times exp\left[\frac{x(V_x - (V_x{}^2 + 4D_x R_d \lambda))}{2D_x}\right] \quad (14$$

In which, *C(x)* is the well water concentration at a distance *x* from the river (*mg/lit*).

3.2. Optimization Model

Assuming that the river discharge and its pollution concentration, as well as wells' pumping rates and the resulting drawdowns, are all constant, the steady-state optimization model can be developed. As displayed in Fig. 5, let C_0 be the constant concentration of pollution, *x* the wells' distance to the river, l_{kj} the distance between wells *k* and *j*, $Q_w(k)$ the discharge of well *k* and *Q* the required demand (*Q=Dem*). Then, the objective function of this cost-effective problem is:

$$Min \;\; Z = C_{Inst}^{w} + C_{Pump}^{w} + C_{Inst}^{p} + C_{conv}^{p} + C_{treat} \quad (15$$

Where, C_{inst}^{w} is the cost of installing wells (such as construction of wells, casing, pumps purchased, installation, etc.), C_{pump}^{w} represents the pumping cost of the well, which is a function of the well's discharge ($Q_w(k)$) and the well's total lift height (h_k),C_{inst}^{p} denotes the installation costs of pipelines (construction, purchasing, installation, etc.), C_{conv}^{p} is the cost of the pipeline's water conveyance, which is a function of the well's discharge and distance, and finally C_{treat} shows the cost of treatment of water due to residual concentration (pollution) remaining in the well water. Then, C_{inst}^{w} and C_{inst}^{p} represent the operation and maintenance cost since this cost is usually considered as a fraction of the initial capital cost. All costs are considered in equivalent annual form. C_{pump}^{w} equals to:

$$C_{pump}^{w} = \sum_{k=1}^{Nw} C_{pump}^{w}(k) \quad (16$$

Where, N_w represents the total number of wells and $C_{pump}^{w}(k)$ is the annual pumping cost of well *k*, which is equal to:

$$C_{pump}^{w}(k) = Hour(k) \times UCE \times P_w(k) \quad (17$$

Where, *UCE* is the unit cost of energy *($/kWh)* and $P_w(k)$ is the power utilized for the pump in well *k*. *Hour(k)* denotes the hours that pump *k* works in a year. Also,

$$p_w(k) = \gamma \times Q_w(k) \times (h^{ini}(k) + s(k))/\varepsilon \quad (18$$

Where, γ is the specific weight of water (*9806 N/m³*), $h^{ini}(k)$ is the initial lift (distance between ground surface and groundwater table before pumping) of well *k*, *s(k)* represents the drawdown in well *k* in response to pumping of all wells (Eq. (2)), and ε is the pump's overall efficiency. The conveyance cost equals:

$$C_{conv}^{p} = UCE \times \sum_{k=1}^{Nw} Q_w(k) \times (\Delta H + H_l) \times Hour(k) \quad (19$$

Where, ΔH is the elevation difference between the collector pipe and pumping house (Fig. 2) and H_l represents the total head loss (friction and local head losses) in pipes. Based on the Darcy-Weisbach equation, the friction head loss (H^{frc}) is a function of the pipe's length, diameter and discharge. Similarly, the local head loss (H^{loc}) is a function of the pipe's diameter and discharge (Chin, 2012). Thus:

$$H_l = \sum_{k=1}^{Nw-1} H_{kj}^{frc} + H_{coll}^{frc} + H_{coll}^{loc}; \quad \mathrm{j} = k+1 \quad (20$$

$$H^{frc} = f\frac{16lQ^2}{\pi^2 D^4} \quad (21$$

$$f = \frac{0.25}{\left[\left[log(\frac{k_s}{3.7D}\right] + \frac{5.74}{Re^{0.9}})\right]^2} \quad (\text{for } \ 10^{-6} \le \frac{k_s}{D} \le 10^{-2}, \quad 5000 \le \mathrm{Re} \le 10^8) \quad (22$$

$$Re = VD/\upsilon = 4Q/(\pi D\upsilon) = 1273240Q/D \quad (23$$

$$H_{coll}^{loc} = K\frac{16l_{coll}Q_{coll}^2}{\pi^2 D_{coll}^4} \quad (24$$

Where, *f* is the pipe friction factor, k_s shows the pipe roughness, *l* is the pipe length, *Q* denotes the pipe discharge, *D* indicates the pipe diameter, and *Re* is the Reynolds number. Equations 21-23 must be written for each pipe (using l_{kj}, Q_{kj} , D_{kj} , f_{kj}, and Re_{kj} for each pipe *k-j* located between wells *k* and *j*, as well as using l_{coll}, Q_{coll} , D_{coll} , f_{coll}, and Re_{coll} for the collector pipe). Also, *V* is the pipe water velocity and υ shows the kinematic viscosity of water (equals 10^{-5} m^2/s at 20^oC). Note that $Q_{coll} = \sum Q_w(k) = Dem$ and Q_{kj} is related to the pipe *k-j* position in the system. For example, in the 5-well configuration of Fig. 7, by considering that the collector pipe is located back of the well 3, we have $Q_{12}=Q_w(1)$, $Q_{23}=Q_w(1)+Q_w(2)$, $Q_{34}=Q_w(4)+Q_w(5)$, and $Q_{45}=Q_w(5)$. Thus,

$$\underset{(j=k+1)}{Q_{kj}} = \begin{cases} Q_w(1), & for\ the\ first\ pipe \\ \sum_{k=1}^{\left[\frac{N_w-1}{2}\right]} Q_w(k), & for\ the\ middle\ pipes\ between\ well 1\ and\ well\ [(N_w-1)/2]; \\ \sum_{k=[(N_w+1)/2]}^{N_w} Q_w(k), & for\ the\ middle\ pipes\ between\ well\ \left[\frac{N_w+1}{2}\right]\ and\ well\ N_w; \\ Q_w(N_w), & for\ the\ last\ pipe \end{cases} \quad (25$$

Where, [u] is the integer value of u.

Obviously, the water treatment cost increases by the elevating the water volume (*Dem*) and solute concentration (C), as more chemicals are needed to reduce the concentration up to the standard levels. Thus, this term is a function of the remaining concentration *C(x)* (as depicted in Eq. (13)) and the volume of water that would be treated.

$$C_{treat} = f_1(C(x), Dem) \quad (26$$

The main attractive feature of RBF systems is the property of removing large amounts of pollutants in flowing river water. Indeed, most of the river water pollutants that enter the aquifer and then the wells can be removed through porous media. However, some pollutants remain in the wells from which removing these residual pollutants is necessary to achieve standard levels. There are various treatment methods for removing residual pollutants in water, and here the disinfection with Chlorine and Chloramine (Wilbert et al. 1999) has been used as a common method of treatment. Cost estimation for Chlorine and/or Chloramine disinfection is based on the amount of chemicals used per day. Chlorine demand is determined from the concentration of nitrite and reduced inorganic transition metals, including chromium, copper, iron, and manganese present in the water (Wilbert et al. 1999). The detailed relations of disinfection by chlorine and ammonia have been given by Wilbert et al. (1999), and its companion, a Microsoft Excel file (WaTER). The treatment cost with this method is a multivariate function:

$$C_{treat} = f_2(D, C(x), DCR, AAD, Cl_2Cost, AmmCost) \quad (27$$

Where, Q is the production flow rate to be treated (Q=*Dem*), *C(x)* represents the pollutant concentration in water, *DCR* denotes the desired chlorine residual, *AAD* is the alternative ammonia dose, Cl_2*Cost* shows the cost of Cl_2 and *AmmCost* indicates the cost of NH_4OH. The product flow rate (Q) and porous media characteristic (Θ, *S, T*) are known, but the pollution concentration in the well water is unknown. The farther the distance to the river, the more natural the treatment in porous media will be, thus reducing treatment costs. Also, more drawdown in wells increases the pumping cost. Thus, there is an optimum distance that minimizes the total cost of treatment and pumping.

Finally, the required demand (*Dem*) must be met. Thus,

$$\sum_{k=1}^{N_w} Q_w(k) = Dem \quad (28$$

For a given demand (Q=*Dem*) and number of wells (N_w), $C_{Inst}^{w}$and C_{Inst}^{p} are constant and do not alter the model result.

3.3. Model Formulation; Transient Conditions

Unlike the steady-state conditions, in transient conditions, here the variability of river discharge and solute concentration, well pumping, and the obtained drawdowns were considered. To develop transient flow and solute transport equations, the concept of linear systems theory was applied. The Cooper-Jacob equation for computing drawdown of wells (Todd and Mays, 2005), the image wells concept for computing river aquifer interaction, and Eq. (12) for computing the solute concentration were used under transient conditions. The linear systems theory was

used to derive the required equations in variable pumping as well as variable solute concentration.

3.4. Response Functions of Linear Systems

The linear systems are those whose behavior may be predicted by a linear differential equation. Linear systems have two basic properties, which are proportionality and additivity. Indeed, the response function of a linear system is a solution of its governing differential equations. In many situations, such as computing drawdown or solute concentration in an aquifer, the governing equation is indeed linear; thus, the rules of linear systems can be used in deriving the desired relations.

If a system receives an input of unit value applied instantaneously (a unit impulse) at time τ, the response of the system at a later time t is described by the unit impulse response function $u(t-\tau)$. The response to the complete input time function $I(\tau)$ can then be obtained by integrating the response to its constituent impulses, which is called the convolution integral (Chow et al. 1988):

$$Q(t) = \int_0^t I(\tau)u(t-\tau)d\tau \quad (29$$

A unit step input response function $g(t)$ is found from (29) with $I(\tau)=1$ for $\tau \geq 0$ as:

$$g(t) = \int_0^t u(t-\tau)d\tau = \int_0^t u(l)dl \quad (30$$

Also, the unit pulse response function $h(t)$ equals" (Chow et al. 1988):

$$h(t) = \frac{1}{\Delta t}[g(t) - g(t-\Delta t)] \quad (31$$

If Δt set equals unity ($\Delta t=1$), then:

$$h(t) = g(t) - g(t-1) \quad (32$$

Further, for $t<0$, $g(t)=0$. The drawdown derived from Theis or Cooper-Jacob equations, assuming $Q=1$ is a unit step response function. If the unit pumping shuts down at the end of $t=1$, the derived drawdown is the unit pulse response function. Fig. 5 displays the unit step and unit pulse response functions of a confined aquifer.

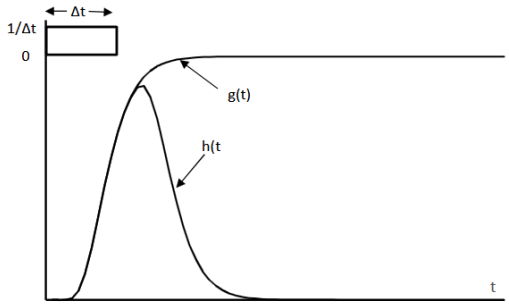

Figure 5. Unit step ($g(t)$) and unit pulse ($h(t)$) response functions of a confined aquifer

3.5. Flow Equation, Transient Condition

The flow equation in RBF systems in transient conditions is required for computing the drawdown of wells and river seepage to each well. These equations, derived by integrating the Cooper-Jacob equation, the concept of image wells, and the unit pulse response function, are as follows:

The drawdown in a confined aquifer due to constant well discharge Q may be derived using the Cooper-Jacob equation (assuming $u = \frac{r^2 S}{4Tt} < 0.01$),

$$s(t) = \frac{Q_w}{4\pi T} ln(\frac{2.246Tt}{r^2 S}) \quad (33$$

Where, $s(t)$ represents the drawdown at distance r from the pumping well at time t after the start of pumping, T and S show the aquifer transmissivity and storativity, respectively, and t is the time passed since the beginning of pumping. This equation is linear due to the pumping rate Q_w. By setting $Q_w=1$, the derived drawdown is a unit step response function:

$$g_w(t) = \frac{1}{4\pi T} ln(\frac{2.246Tt}{r^2 S}) \quad (34$$

Following that, the related unit pulse response function yields:

$$h_w(t) = g_w(t) - g_w(t-1) = \frac{1}{4\pi T} ln(\frac{t}{t-1}) \quad (35$$

Note that for $t>1$, the unit pulse response function $h_w(t)$ is independent of space, i.e., the locations of wells and aquifer storativity. Fig. 6 demonstrates $g_w(t)$ and $h_w(t)$ functions for a confined aquifer with $T=1000\ m^2/day$ and $S=0.01$ for different distances from $r=1m$ to $r=100\ m$.

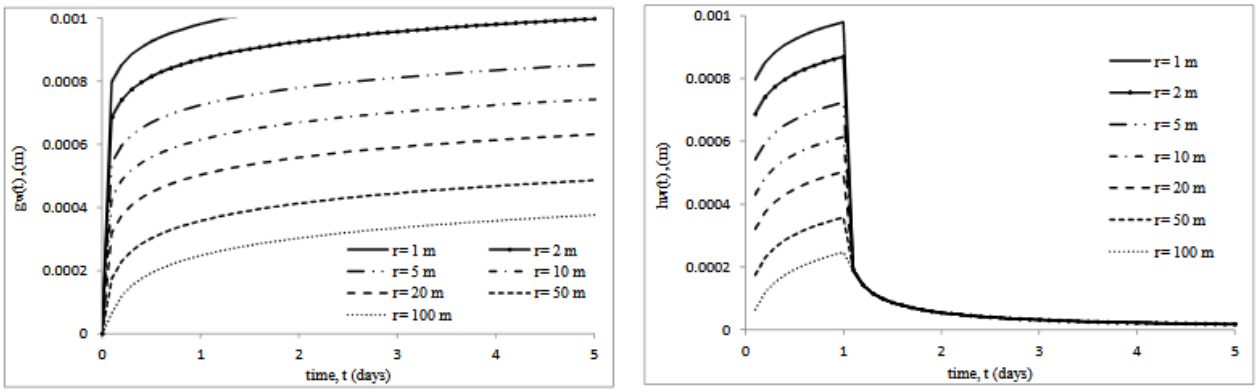

Figure 6. Unit step response ($g_w(t)$) and unit pulse response ($h_w(t)$) functions for a confined aquifer with T=1000 m^2/day and S=0.01

For variable pumping, $Q_w(t)$, the resulting drawdown is derived as:

$$s(n) = \sum_{t=1}^{N} h_w(n-t+1) Q_w(t) \quad (36$$

This is a form of discrete convolution equation for a linear system (Chow et al., 1988).

When a set of N_w wells exists, each with $Q_w(j,t)$, $j=1, 2,..., N_w$, by substituting $h_w(n-t+1)$ by $h_w(k, j, n-t+1)$, which is now called "unit response coefficient" of drawdown of wells, the obtained equation is:

$$s(k,n) = \sum_{t=1}^{n}\sum_{j=1}^{Nw} h_w(k,j,n-t+1)Q_w(j,t) \quad (37$$

This equation is known as the unit response matrix method, which was first introduced in groundwater systems optimization by Maddock (1972). Alimohammadi et al. (2009) later developed general equations for deriving response equations for point, linear, and surface excitations in aquifers.

When there are some sources, such as return flows or river leakage, these sources should also be considered. In RBF systems, river leakage exists and thus this river-aquifer interaction must be considered. One approach is to use the concept of image wells. Fig. 7 illustrates a series of pumping wells ($k,j,...$) near a permanent river and its corresponding image wells ($k',j',...$). The drawdown in well k due to constant pumping (Q_w) in well j based on the concept of image wells and Cooper-Jacob equation equals:

$$s_r(t) = \frac{Q_w}{4\pi T}\left[ln(\frac{2.246Tt}{r^2S}) - ln(\frac{2.246Tt}{r_i^2S})\right] = \frac{Q_w}{2\pi T}ln(\frac{r_i}{r}) = \frac{Q_w}{2\pi T}ln(\frac{L_{kj'}}{L_{kj}}) = Cte. \quad (38$$

$$L_{kj'} = \begin{cases} 2x, if j' = k' \\ \sqrt{L_{kj}^2 + 4x^2}, if j' \neq k' \end{cases} \quad (39$$

Where, r and r_i represent the distance from the pumping well and image well, respectively. Also, $L_{kj}=r_w$ for $k=j$. Eq. (38) is the same as Eq. (1). Note that $s_r(t)$ is independent of time. This condition is known as pseudo steady-state conditions (McWhorter and Sunada, 1977). In Eq. (38), Q_w is constant, and the equation is linear due to Q_w. Therefore, the properties of linear systems could be used again in this case. By setting $Q_w=1$, the derived net drawdown is a unit step response function as:

$$g_r(t) = \frac{1}{2\pi T}ln(\frac{L_{kj'}}{L_{kj}}) \quad (40$$

Also,

$$h_r(t) = \begin{cases} g_r(t), \text{for } t \leq 1 \\ 0, \text{for } t > 1 \end{cases} \quad (41$$

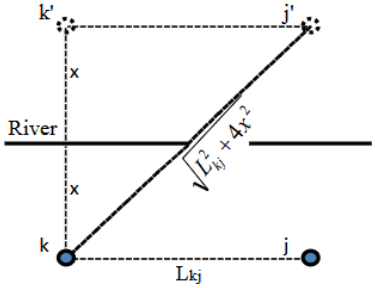

Figure 7. Pumping wells (*k,j,..*), and corresponding image wells (*k',j',…*)

For a set of N_w wells, we have:

$$g_r(k,j,t) = g_r(k,j) = \frac{1}{4\pi T}\left[\sum_{j=1}^{Nw} ln(\frac{2.246Tt}{L_{kj}^2 S}) - \sum_{j'}^{Nw} ln(\frac{2.246Tt}{L_{kj'}^2 S})\right] = \frac{1}{4\pi T}\left[\sum_{j=1}^{Nw} ln(\frac{L_{kj'}^2}{L_{kj}^2})\right] =$$

$$\frac{N_w}{2\pi T} ln\left(\frac{\prod_{j'=1}^{Nw} L_{kj'}}{\prod_{j=1}^{Nw} L_{kj}}\right) \quad (42$$

The equation for net drawdown due to variable pumping rates $Q_w(j,t)$ of N_w wells is obtained as:

$$s_r(k,n) = \sum_{t=1}^{n}\sum_{j=1}^{Nw} h_r(k,j,n-t+1)Q_w(j,t) \quad (43$$

Based on Eqs. (41) and (42), it is reduced to:

$$s_r(k,t) = \frac{Nw}{2\pi T} ln\left(\frac{\prod_{j'=1}^{Nw} L_{kj'}}{\prod_{j=1}^{Nw} L_{kj}}\right)\sum_{j=1}^{Nw} Q_w(j,t) \quad (44$$

3.6. Solute Transport Equation-Transient Conditions

The term transient here refers to the difference in the river solute concentration. According to Eq. (13), the equation is linear due to the constant concentration C_0. Thus, as with flow equations, in this case, we have:

$$g_c(x,t) = \frac{1}{2}\left[\begin{matrix} erfc\left[\frac{R_d x - (V_x{}^2 + 4D_x R_d\lambda)t}{2(D_x R_d t)^{0.5}}\right] \times exp(\frac{(V_x - (V_x^2 + 4D_x R_d\lambda))x}{2D_x}) + \\ erfc\left[\frac{R_d x + (V_x{}^2 + 4D_x R_d\lambda)t}{2(D_x R_d t)^{0.5}}\right] \times exp(\frac{(V_x + (V_x^2 + 4D_x R_d\lambda))x}{2D_x}) \end{matrix}\right] \quad (45$$

$$h_c(x,t) = g_c(x,t) - g_c(x,t-1) \quad (46$$

Where, $g_c(x,t)$ is the unit step response function and $h_c(x,t)$ is the unit pulse response function or unit response matrix of the river leakage, and:

$$C_c(x,n) = \sum_{t=1}^{n} h_c(x,n-t+1) \times C_0(t) \quad (47$$

Where, $C_c(x,n)$ represents the solute concentration in the well within time period n, and $C_0(t)$ is the river solute concentration within time period t. Similarly, for well j within time period t, we have:

$$C_c(x,j,n) = \sum_{t=1}^{n} h_c(x,j,n-t+1) \times C_0(t) \quad (48$$

Where, $h_c(x, j, n-t+1)$ is the unit pulse response function or unit response matrix of the solute concentration for well j within time period $n-t+1$.
The optimization model in transient conditions is similar to the steady-state model, but using unsteady terms such as $Q_w(k,t)$ and $C_c(x,t)$ instead of $Q_w(k)$ and $C_c(x)$, as well as flow and transport formulation in transient conditions.

4. Results

In this section, two numerical examples have been presented. The first example illustrates the proposed formulation for the design of a hypothetical RBF system. In the design problem, the steady-state conditions, with some critical situations such as river discharge equal to $_7Q_{10}$ (7-day minimum discharge with 10 years return period) and high pollutant concentration, could be considered. The second example represents the analysis of an existing RBF system in a 12-month period. Obviously, for this example, transient conditions must be considered.

4.1. Example Problem 1, Design of an RBF System

A hypothetical example has been considered here to show how the developed proposed model works in the case of design problems. A small city located next to a relatively large permanent river has been considered. Its municipality has a plan for designing an RBF system as a backup water supply system. The design discharge (required demand) equals 0.5 m^3/s. The river's $_7Q_{10}$ discharge is far larger than the design discharge. Five wells have been considered in this plan, with Fig. 7 demonstrating a schematic view of this problem. The radius of the wells equals 0.5 *m,* and the distance between the ground surface and the static groundwater table equals 10 *m*. The aquifer's transmissivity and porosity equal 0.01 m^2/s and 0.3, respectively. The pumping house is located 20 *m* away from the collector pipe and in 10 *m* upper elevation that has required as the local network head. Other data on the problem are reported in Tables 1 and 2. Table 2 shows the parameters of disinfection treatment and piping facilities. Based on construction limitations, equal sizes have been considered here for the diameter of all collector pipes of the wells. The entire optimization model formulation and solution have been implemented in Microsoft Excel® as a spreadsheet model. Table 3 shows the problem solution results using the Solver add-on of Microsoft Excel®.

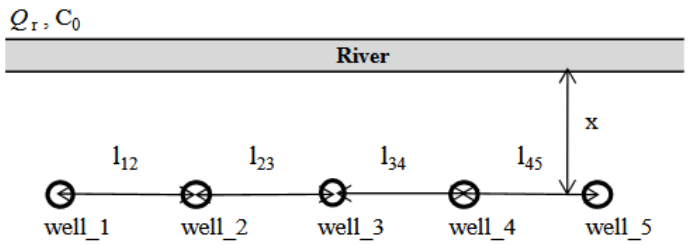

Figure 8. A schematic view of the example problem 1

Table 1. Input parameters

Parameter	Unit	Value
Demand	m^3/s	0.5

Wells radius	m	0.5
Transmissivity	m^3/s	0.05
Porosity	-	0.3
Saturated thickness	m	50
Initial Lift	m	10
Initial concentration	Mg/liter	500
Minimum well distance	m	20
Maximum well distance	m	100
Retardation factor	-	20
Decay rate	-	0.000001
Plan duration	Day	7
Unit cost of energy	4/Kwh	0.00714

Table 2. Parameters of disinfection treatment and pumping facilities

Parameter	Units	Value
Residual chloramines	mg/L	3
Alternative chlorine dose	mg/L	6
Alternative ammonia dose	mg/L	2
Cl_2 needed	mg/L	21.18
Ammonia needed	mg/L	0.99
Cl_2 unit cost	$/ton	50
Basis ammonia	Kg/day	172.8
NH_4OH unit cost	$/ton	250
Plant availability	-	0.95
Collector-motor house distance	m	20
Collector-motor house ΔH	m	10
Pipes roughness	m	0.00015
Pipe velocity	m/s	3

Table 3.The problem solution brief results

Well#	1,5	2,4	3
Discharge (l/s)	68.7	97.6	167.3
Drawdown (m)	1.45	2.54	3.54
Distance from center (m)	85.0	22.7	0
Used power (Kw)	9.65	15.01	27.78
Used energy (Mwh)	1.621	2.522	4.667
Pumping cost ($)	11.577	18.012	33.339
X=36.7 m C=34.10 mg/lit	α_L=4.18 D_x=0.000876 m2/s		
Pipe diameter=12 in. (0.3048 m)*			
Collector diameter=18 in. (0.4572)			
Total pumping cost= 93 $			
Total conveyance cost= 91 $			
Treatment cost=98 $			
Total cost=281 $			

*: Equal sizes have been considered here for all pipe diameters.
(1 inch=2.54 cm)

As presented in Table 3, the results of the model show that in this case, the well alignment should be located 36.7 *m* away from the river. The wells' discharges and distances are symmetric where $Q_1=Q_5$, $Q_2=Q_4$, $l_{12}=l_{45}$, and $l_{23}=l_{34}$. The central well has more while the side wells have less discharge. Also, the pollutant concentration in wells decreases to 34.1 mg/L from the initial 500 mg/L in the river. Unexpectedly, the discharge of the central well is greater than and that of side wells is less than discharge of other wells. Since both pumping and conveyance costs have been considered here, the conveyance cost (which grows with distancing off the wells) outweighs the pumping cost (which decreases with farther distance off the wells) here. This suggests that if only the pumping cost has been considered, opposite results can be expected. Three cost terms (pumping, conveyance, and treatment) approached each other in this case, suggesting that none of them is ignorable.

4.1.1. Sensitivity Analysis

A local sensitivity analysis has been implemented here for assessing the relative importance of the model parameters. Five parameters, including unit cost of energy (*UCE*), retardation factor (R_d), transmissivity (T), porosity (Θ), and decay rate (λ), have been considered. Fig. 9 displays the variations of variable x against the variations of the five above-mentioned parameters. As can be seen, the variations of x versus T are ascending, but for other parameters, they are decreasing. With the elevation of T, the value of K has grown (the thickness of the saturated layer was considered constant). Thus, the seepage or solute transport velocity increases, while for a given concentration, the value of x drops. The variable x is more or less sensitive to all parameters, with the sensitivity being greater on the left-hand side (values of parameters that are less than initial values) than on the right-hand side (values of parameters that are greater than the initial values). The sensitivity of T and *UCE* is almost equal but with opposite directions, and both are less sensitive than the other three variables. R_d, Θ, and λ revealed similar sensitivity.

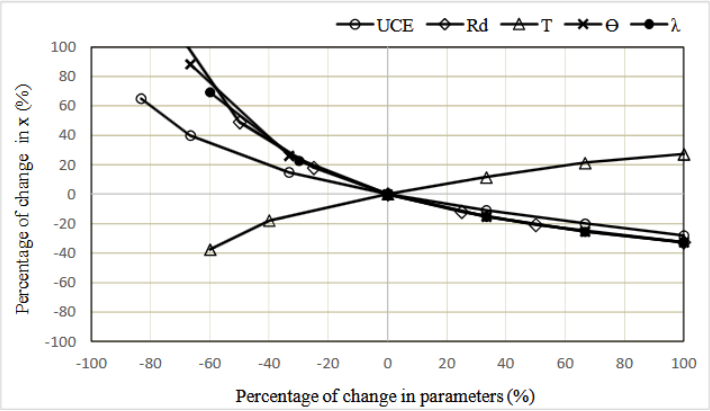

Figure 9. Variations of *x* against the variations of five parameters

Fig. 10 illustrates the variations of variable L_{12} against the variations of the five parameters. L_{12} is not sensitive to variations of T, but is sensitive to other variables. In this regard, UCE is less sensitive than the other three variables, indicating the same behavior. Again, the sensitivity has been greater on the left-hand side.

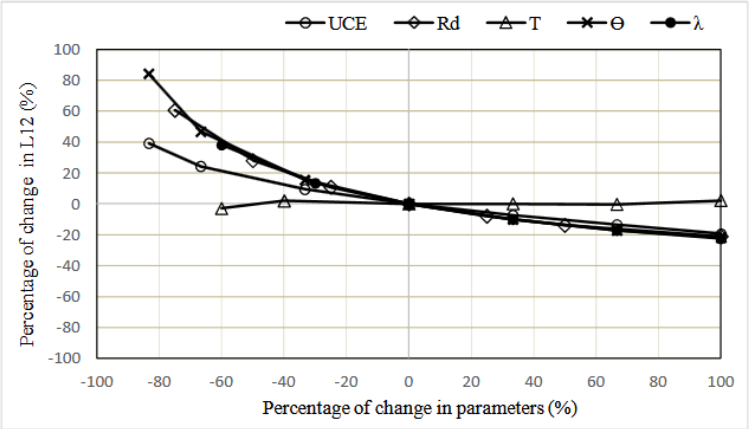

Figure 10. Variations of L_{12} against the variations of five parameters

Fig. 11 reveals the results of sensitivity analysis for concentration C. C is sensitive to all parameters, especially to UCE and T. By increasing UCE, x declines (Fig. 9), thereby augmenting C, but by increasing T, x rises (Fig. 9), thereby lowering C. The sensitivity of C to R_d, Θ, and λ has been similar, i.e., the variations of these parameters show a similar effect on C. Increasing R_d means lengthening retarding and reducing the solute transport velocity, thereby lessening C. Also, increasing Θ means diminished seepage velocity and again lower solute transfer velocity. Finally, increasing λ signifies greater contaminant decay and lower concentration in the wells. To assess this further, Fig. 12 reveals the variations of C/C_0 against the variations of Θ/Θ_0, R_d/R_{d0}, *and* λ/λ_0 where C_0 =500 mg/L, Θ_0=0.3, R_{d0}=20, and λ_0=0.000001. As can be seen, the variations for R_d/R_{d0} and λ/λ_0 are the same (see Eq. (14)), while for Θ/Θ_0, there is a little difference between the two other curves.

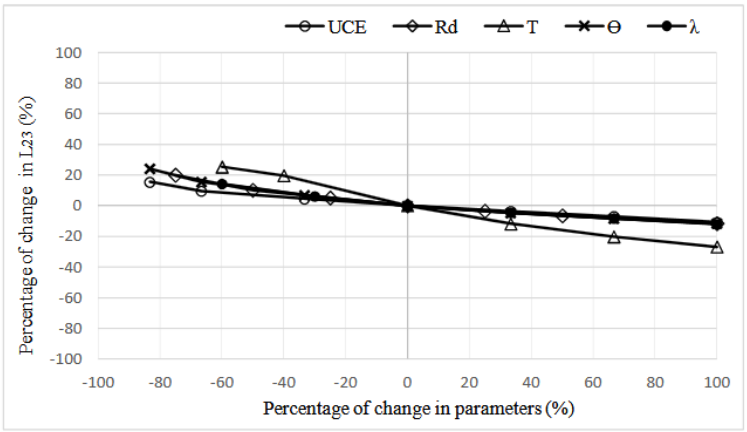

Figure 11. Variations of C against the variations of five parameters

Fig. 13 displays the variations of average drawdown in five wells (*s_ave*) against the variations of the five parameters. Drawdown is an inverse function of transmissivity (Eq. (1)), thus is more sensitive to

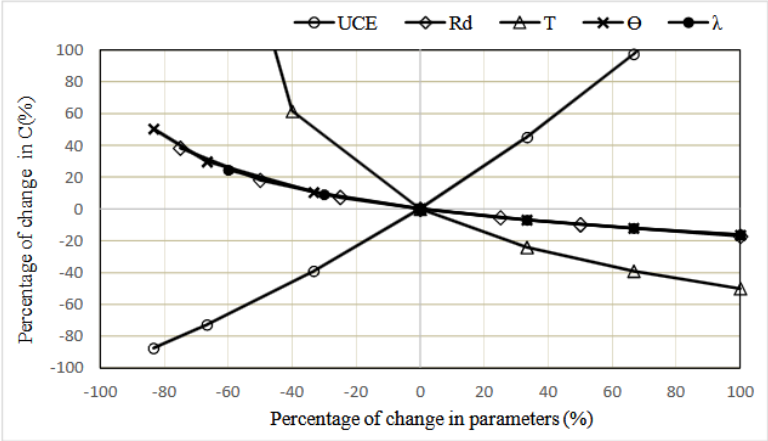

Figure 12. Variations of C/C_0 against the variations of Θ/Θ_0, Rd/Rd_0, and λ/λ_0

T than to other parameters. In smaller values of parameters, *UCE* is less sensitive than R_d, Θ, and λ (these are solute transport parameters and are not directly related to drawdown, but they directly affect distance *x*. Also, because *s_ave* is related to *x* (*i*=*s_ave*/*x* where *i* is the gradient), thus three parameters are indirectly related to *s_ave*.). However, for larger values, *s_ave* is relatively less sensitive to *UCE*, R_d, Θ, and λ.

Fig. 14 indicates the variations of the pumping cost against the variations of the five parameters. Except for *UCE*, other parameters seem to be less sensitive. Since *T* directly affected the drawdown and thus the required energy, it is more sensitive than the other three parameters (which are transport parameters). Also, Fig. 15 exhibits the variations of conveyance cost against the variations of the five parameters. Except for *UCE*, other parameters have been insensitive.

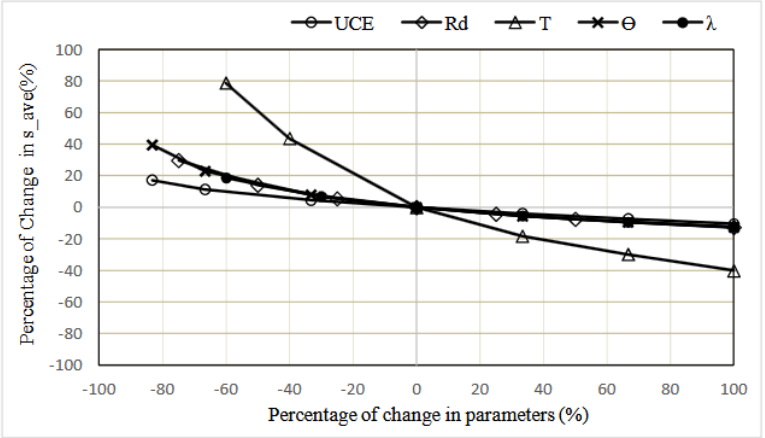

Figure 13. Variations of average drawdown in wells against the variations of five parameters

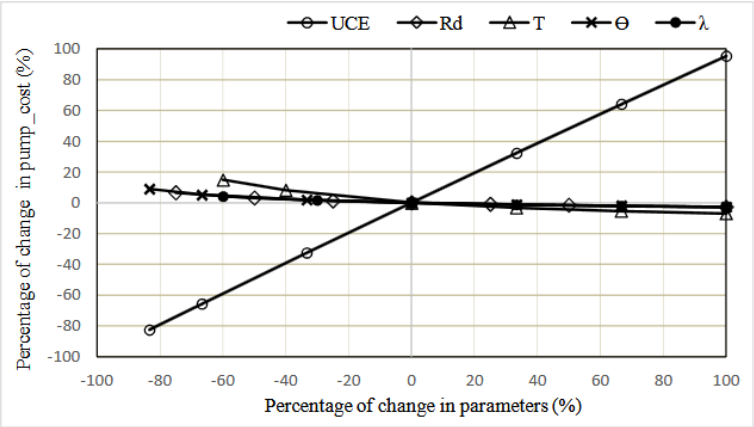

Figure 14. Variations of pumping cost against the variations of five parameters

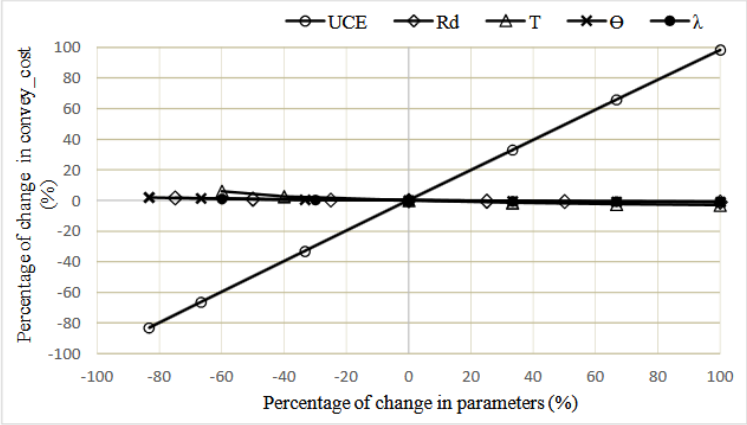

Figure 15. Variations of conveyance cost against the variations of five parameters

Since there are several output variables (*x, C, Costs, …*), for reaching a conclusion on the sensitivity analysis, a dimensionless parameter is defined as:

$$Sens_p = \frac{1}{n_y}\sum_{y=1}^{n_y}\sum_{i=1}^{n_i}\left(\frac{\left|\frac{y_i-y_0}{y_0}\right|}{\left|\frac{x_i-x_0}{x_0}\right|}\right) \quad (49$$

Where, $Sens_p$ is the sensitivity of parameter p, y_i represents the value of variable y ($y \in \{x, C, s, Cost, \ldots\}$) corresponding to the value of parameter x_i ($x \in \{UCE, Rd, T, \Theta, \lambda\}$). Table 4 presents the results of computing Eq. (48). According to this table, *UCE* is a relatively more sensitive while R_d is a relatively less sensitive parameter, but generally all five parameters have been sensitive. Figs. 9-15 are in line with this conclusion.

Table 4. Sensitivity of five parameters

Parameter	Sensitivity	Rank
UCE	0.69	1
Rd	0.30	5

T	0.45	2
ɵ	0.34	4
λ	0.37	3

4.2. Example Problem 2: Analysis of an RBF System

The purpose of this example is to show the ability of the proposed transient formulation in computing the solute concentration in a well next to a river, and the effects of changing parameters on the concentration. A pumping well is located next to a permanent river at a distance $x= 30\ m$. The aquifer and transport parameters are similar to example 1 ($T=0.05\ m^2/s$, $K=0.001\ m/s$, $R_d=20$, $\lambda=10^{-5}$, $\Theta=0.3$). In pseudo-steady conditions, the drawdown in the well equals 9 m. Table 5 reports the variations of the concentration of a solute pollutant in the river within a 12-month period (the concentration had been assumed constant through each month). Then, the concentration should be computed in the well water within each period.

Table 5. Concentration of pollution in the river and in the well

Month (t)	$C_0(t)$	C(t)
1	1000	653.92
2	1300	1008.82
3	1100	928.49
4	800	701.47
5	1000	784.08
6	700	624.83
7	1100	833.29
8	1200	961.33
9	500	520.58
10	1000	736.74
11	800	679.83
12	700	585.67

Using Eq. (45) and considering a computation time step equal to 1 day for greater accuracy, Fig. 16 illustrates the unit step (g_c) and unit pulse (h_c) response functions of the well concentration. Also, Fig. 17 reveals the variations of concentration in the river ($C_0(t)$) and in the well ($C(t)$) in a 12-month period. Attenuation and time lag of concentration in the well's water are clear in the figure.

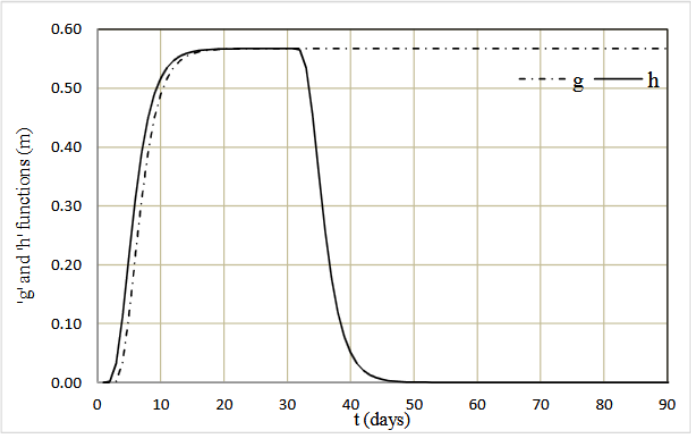

Figure 16. Unit step (g) and unit pulse (h) response functions of the well's concentration

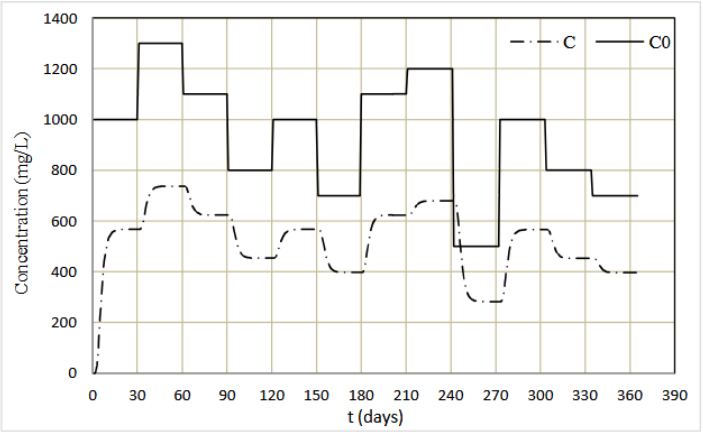

Figure 17. Variations of concentration in the river ($C_0(t)$) and in the well ($C(t)$)

In the first example, it was observed that Rd, T, Θ, and λ are sensitive parameters of flow and transport models. Here, the effect of these parameters on the variations of concentration and solute transport is observed. Fig. 18 displays the gc and hc functions for different values of Rd. By increasing Rd (retardation), the solute is more retarded and thus gc and hc functions decline. Fig. 19 shows the solute concentration variations for different values of Rd.

Fig. 20 shows the g_c and h_c functions for different values of T. By increasing T (increasing seepage velocity), g_c and h_c functions, as well as concentration, grow. Fig. 21 demonstrates the variations of solute concentration for different values of T.

Fig. 22 shows the g_c and h_c functions for different values of Θ. By increasing Θ (decreasing seepage velocity), g_c and h_c functions as well as the concentration drop. Fig. 23 exhibits the variations of solute concentration for different values of T.

Fig. 24 reveals the g_c and h_c functions for different values of λ. By increasing λ (increasing decay), g_c and h_c functions as well as the concentration fall. Fig. 25 indicates the variations of solute concentration for different values of T. At relatively large values of λ (say $\lambda=10^{-5}$), the concentration in the well reaches zero (one method of protecting the well's water is using permeable reactive barriers with nanoparticles with a relatively large λ).

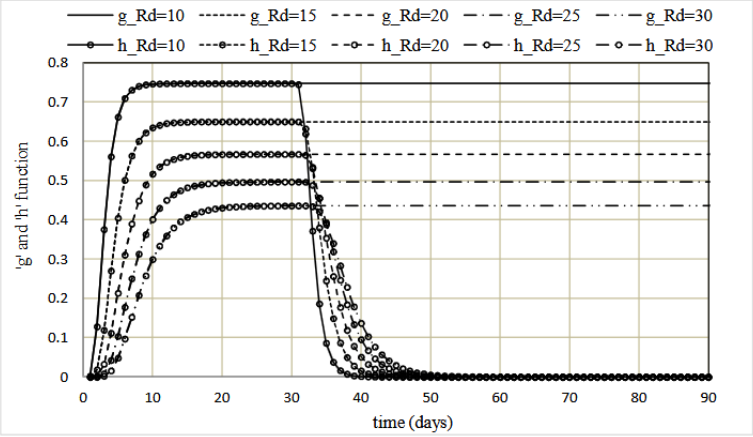

Figure 18. g_c and h_c functions of the well's concentration for different values of R_d

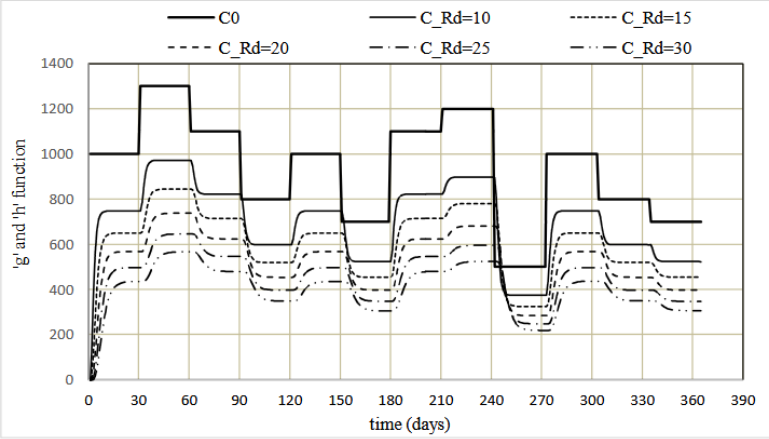

Figure 19. Variations of concentration in the well ($C(t)$) for different values of R_d

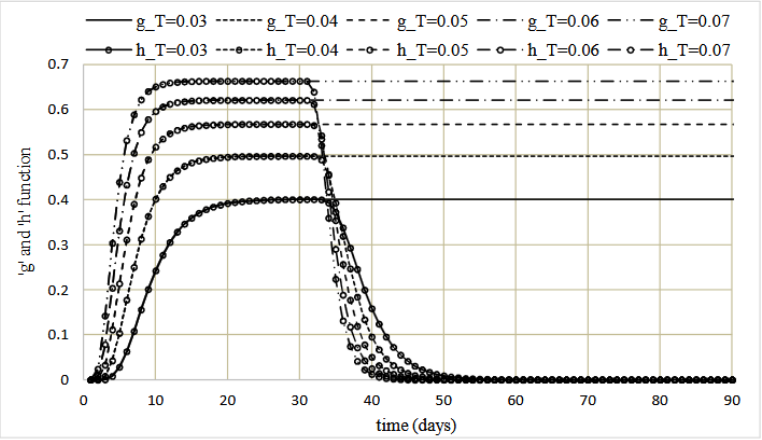

Figure 20. g_c and h_c functions of the well's concentration for different values of T

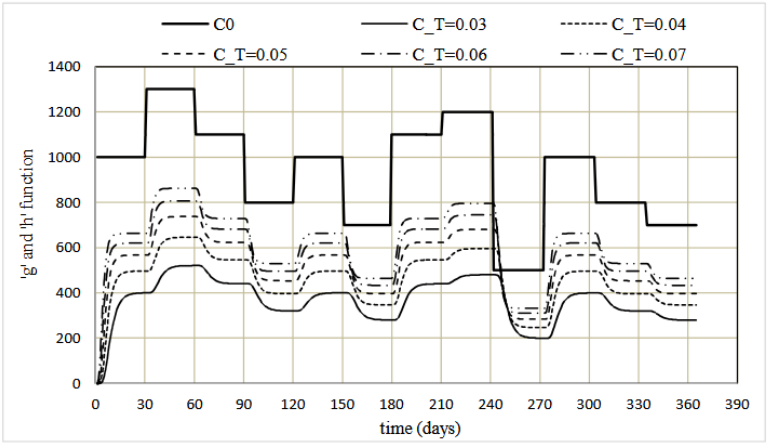

Figure 21. Variations of concentration in the well (*C(t)*) for different values of *T*

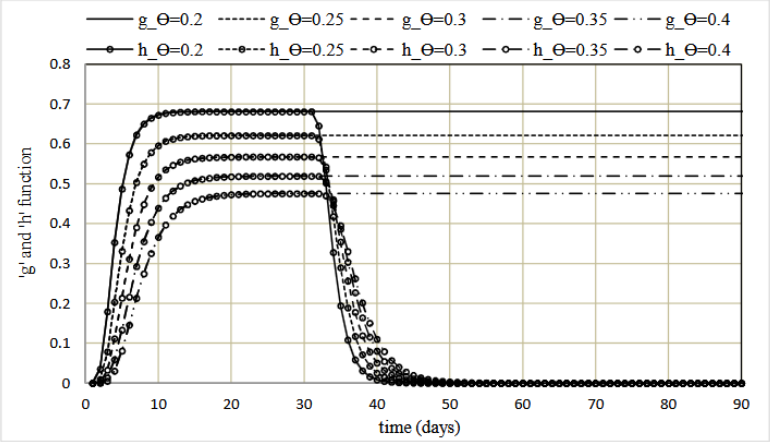

Figure 22. g_c and h_c functions of the well's concentration for different values of Θ

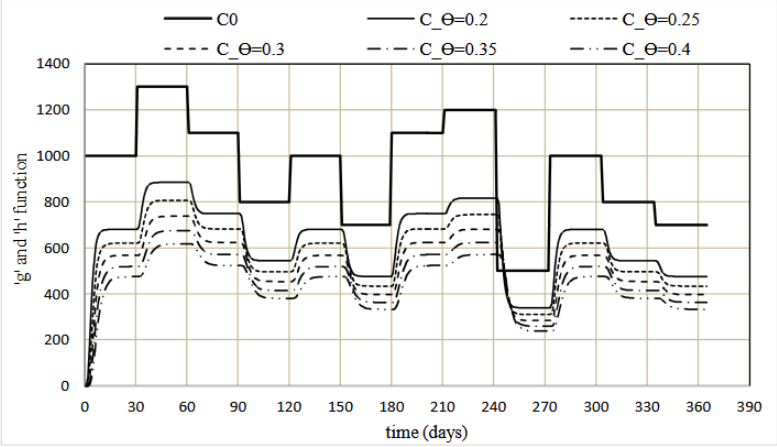

Figure 23. Variations of concentration in the well (*C(t)*) for different values of Θ

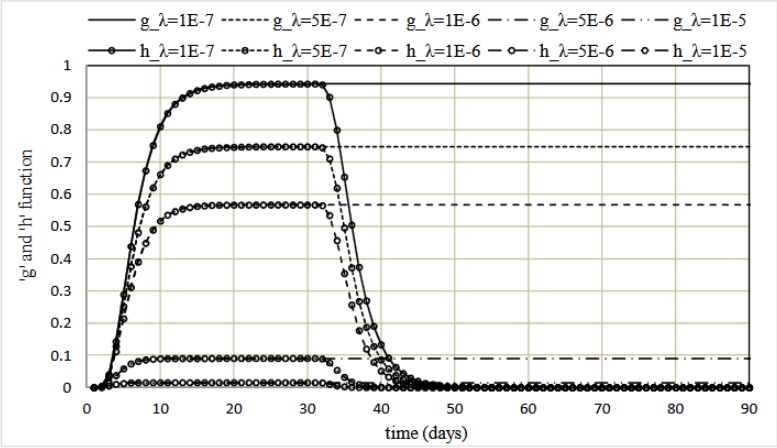

Figure 24. g_c and h_c functions of the well's concentration for different values of λ

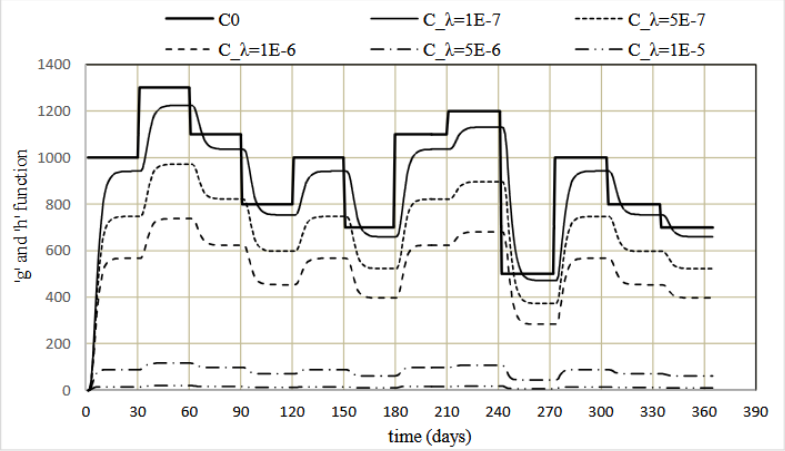

Figure 25. Variations of concentration in the well ($C(t)$) for different values of λ

5. Conclusion

Riverbank Filtration (RBF) systems utilize the natural filtration processes of riverbed and aquifer materials to purify water as it moves from a surface water source to extraction wells. The application of Linear Systems Response Functions in RBF systems enhances their design, management, and operational efficiency, particularly in modeling and predicting groundwater flow and contaminant transport under variable conditions.
Clearly, the novelty of this work is as follows:

Using the concept of response functions of linear systems in the modeling of contaminant transport in groundwater systems. Linear Systems Response Functions, such as unit pulse response functions, are used to model the drawdown of the groundwater table caused by pumping wells, and to predict the solute concentration extending in the aquifer.
In this paper, a comprehensive optimization model for the design of riverbank filtration systems has been developed with the aim of minimizing the total cost of the system, encompassing the locations and pumping rates of wells, as well as the dimensions of other system components. This method enables the analytical calculation of the optimal location and pumping rate of

wells in the RBF system. A simulation model was also developed for analyzing these systems. In these models, the analytic solutions of the equations of groundwater flow and pollutant transport were used.

The analysis indicated that:

- For $t>1$, the unit pulse response function of drawdown $h_w(t)$ is independent of the locations of wells and aquifer storativity.
- The transient flow equation in RBF systems reaches steady (pseudo-steady) conditions. The drawdown in variable pumping for a given transmissivity and distance of wells is only a function of the pumping pattern of wells.
- Solving the steady optimization problem shows that unexpectedly, the discharges of the central and side wells were greater than and smaller than those of other wells. As both pumping and conveyance costs have been considered here, the conveyance cost (which increases with the distance of wells) dominated the pumping cost (which drops with the distance of wells) here, suggesting that if only the pumping cost had been considered, opposite results can be expected.
- The sensitivity analysis revealed that *UCE* (unit cost of energy) is a relatively more sensitive and R_d is a relatively less sensitive parameter, but generally all five parameters are sensitive. For four system parameters (other than *UCE*), the sensitivity ranking was: transmissivity (T), decay rate (λ), porosity (Θ), and retardation factor (R_d) (implementing the transient model by changing these four parameters confirmed the above-mentioned result).
- The proposed simulation model formulations are useful for assessing the computability of the variations of solute concentration in RBF systems, and the effects of changing parameters in the solute concentration in steady-state and transient conditions.

6. References

Abdel-Fattah, A., Langford, R., Schulze-Makuch, D. (2007). Applications of particle-tracking techniques to bank infiltration: a case study from El Paso, Texas, USA.

Alimohammadi, S., Afshar, A., Marino, M. (2009).” Cyclic storage systems optimization: Semi-Distributed Parameter Approach”, Journal of American Water Works Association, 101(2), 90-103.

Batu, V. (2006). Flow and solute transport modeling in aquifers, CRC Press, Taylor & Francis Group, Boca Raton.

Chin, D. A. (2012). Water-quality engineering in natural systems: Fate and Transport Processes in the Water Environment, 2nd Edition, Willy & Sons, Inc., USA.

Chow, V.T., Maidment, D.R., Mays, L.W. (1988). Applied Hydrology, McGRAW-HILL, U.S.

Dillon, P. J., Miller, M., Fallowfield, H., Hutson, J. (2001). “The potential of riverbank filtration for drinking water supplies in relation to microsystin removal in brackish aquifers”, Journal of Hydrology, 266, 209-221.

Doussan, C., Poitevin, G., Ledoux, E., Detay, M. (1997). “River bank filtration: modeling of the changes in water chemistry with emphasis on nitrogen species”, Journal of Contaminant Hydrology, Volume 25 (1-2), 129-156.

Gelhar, L. W. (1993). *Stochastic subsurface hydrology*. Prentice Hall.

Kim, S., B., Yavuz Corapcioglu, M. (2002). “Contaminant transport in riverbank filtration in the presence of

dissolved organic matter and bacteria: a kinetic approach", Journal of Hydrology, 266, 269–283.

Lee, E., Hyun, Y., Lee, K., Shin, J. (2012). "Hydraulic analysis of a radial collector well for riverbank filtration near Nakdong River", Journal of Hydrology, 20(3), 575-589.

Maddock, T. (1972). "Algebraic technological function from a simulation model", Journal of Water Resource Research, 8(1), 129-134.

McWhorter, D.B., Sunada, D.K. (1978). Ground-Water Hydrology and Hydraulics, Water Resources, Littleton, U.S.A.

Moser, P., M., Stickler, W., Bertleef, B., Hedin, K. (1990). "Modeling of groundwater pollution by river bank filtration using oxygen-18 data", Groundwater monitoring and management (Proceedings of the Dresden Symposium, March 1987), IAHS Publ. no. 173.

Mustafa, S., F. Rabah, M. Darwish. (2024). "Modeling contaminant transport in riverbank filtration systems: A three-dimensional analysis with Green's function approach", Ain Shams Engineering Journal, 15 (7).

Neuman, S. P. (1990). "Universal scaling of hydraulic conductivities and dispersivities in geologic media", Journal of Water Resour. Res., 26, 1749–1758.

Prasad, K. S. Hari, Ojha, C. S. P., Nirala, R. K., and Sharma, D. (2016). "Optimal Well Location in a River Bank Filtration System: Sensitivity to Aquifer Characteristics and Decay Rate", Journal of Hazardous, Toxic, and Radioactive Waste, © ASCE, 20(3), 04016001-1-04016001-6.

Ray, C., Melin, G., Linsky, R., B. (2003). River bank filtration – Improving source-water quality, Kluwer Academic Publishers, California, USA.

Sandhu, C., Grischek, T., Kumar, P., Ray C. (2011). "Potential for riverbank filtration in India", Journal of Clean Technologies and Environmental Policy, 13(2), 295-316.

Schön, M. (2006). "Systematic comparison of riverbank filtration sites in Austria and India", Thesis, Leopold Franzens University, Faculty of Civil Engineering Sciences, Austria.

Shamrukh, M., Abdel-wahab, A. (2008). "Riverbank filtration for sustainable water supply: Application to a large-scale facility on the Nile River", Journal of Clean Technologies and Environmental Policy, 10(4), 351-358.

Todd, D. K., Mays, L. W. (2003). Groundwater Hydrology, John Wiley & Sons, Inc., USA.

Uwimpaye, F., Twagirayezu, G., Agbamu, I.O. et al. (2025). Riverbank filtration: a frontline treatment method for surface and groundwater—African perspective. Environ Monit Assess 197, 160.

Wilbert, M. C., Pellegrino, J., Scott, J., Zhang, Q. (1999). Water Treatment Estimation Routine (WATER) User Manual. Water Desalination Research & Development Program Report No. 43, Denver, Colorado, and Lower Colorado Regional Office, Boulder City, Nevada.

Zheng, C., Bennett, G.D. (2002). Applied Contaminant Transport Modeling, 2nd Edition. WILEY, USA

WWW.documbase.com/Water-Treatment-Cost-Estimation-Program-USBR.xls.

May 2025
Volume 1
Issue 1

DOI: 10.48308/ijce.2025.240047.1003

Interdisciplinary Journal of Civil Engineering
Shahid Beheshti University

A Comprehensive Review of Eutrophication in Water Resources: From Identifying Contributing Factors to Proposing Management Strategies

Authors:

Reza Khalili[1], Ali Moridi[1, *]

Abstract

Eutrophication, which refers to the excessive enrichment of water bodies with nutrients, has emerged as a significant global environmental and economic crisis. This complex ecological process primarily results from extensive human activities, including the overuse of chemical fertilizers in agriculture, the discharge of untreated domestic and industrial wastewater, and intensive livestock and aquaculture systems. The influx of large amounts of nitrogen and phosphorus compounds into aquatic ecosystems disrupts natural nutrient cycles, leading to algal blooms and ultimately severe depletion of dissolved oxygen (hypoxia). The devastating consequences of this phenomenon include biodiversity loss, the creation of dead zones in coastal waters, threats to fisheries and aquaculture industries, and substantial increases in water treatment costs for drinking and industrial purposes. To address this multifaceted challenge, various solutions have been proposed, including chemical methods (such as coagulants), physical approaches (like artificial aeration), and biological techniques (using nutrient-absorbing plants and microorganisms). However, international experience demonstrates that only through integrated management strategies—combining smart policymaking, continuous water quality monitoring, and the development of clean technologies in agriculture and industry, and active local stakeholder engagement—can we effectively control this problem and safeguard water resources for future generations.

Keywords: Eutrophication, Harmful Algal Bloom (HAB), Water Quality Management, Nutrient Load.

1. Faculty of Civil, Water, and Environmental Engineering, Shahid Beheshti University, Tehran 1983969411, Iran

*Corresponding Author: a_moridi@sbu.ac.ir

1. Introduction

Water stands as the fundamental building block of life, an irreplaceable resource that sustains all terrestrial ecosystems. This remarkable chemical substance – characterized by its transparency, neutral taste, and absence of color or odor – constitutes approximately 71% of Earth's surface. Its critical importance extends across biological, environmental, and socioeconomic domains, making responsible water management absolutely imperative. Contemporary water resources face unprecedented challenges, including severe scarcity, escalating pollution levels, and inefficient utilization patterns. Implementing robust conservation measures has therefore become essential to safeguard water security for current and future populations. This necessitates adopting sustainable management approaches, promoting water preservation initiatives, and enforcing stringent anti-pollution regulations (Islam et al., 2020).

As a finite yet indispensable resource, water demands meticulous stewardship to maintain its availability. Strategic water storage solutions coupled with rigorous quality control measures form the cornerstone of effective water governance (Elhaga et al., 2020) .The primary objectives of water storage encompass drought mitigation, reliable supply assurance, and climate resilience enhancement (Yousefi et al., 2019) .Subsequent water quality monitoring becomes equally vital, addressing critical considerations for public health protection, environmental conservation, and agricultural/industrial requirements (saboktakin et al., 2022). Water's extraordinary value manifests through its life-sustaining properties, ecosystem support functions, economic facilitation, and community enrichment capabilities. Proper recognition of water's centrality and implementation of science-based conservation frameworks constitute pivotal steps toward achieving planetary sustainability (Elhaga et al., 2020).

Both surface water bodies and groundwater aquifers serve as crucial reservoirs supporting human civilization and natural biodiversity (Ma et al., 2020) . Alarmingly, escalating pollution trends have recently compromised these resources, particularly affecting reservoirs and underground water tables. Contamination occurs through identifiable point sources and diffuse pathways, originating from either natural processes (geological leaching, watershed degradation) or human activities (municipal wastewater, agricultural runoff containing agrochemicals, livestock operations, industrial effluents, and mining byproducts). A comprehensive understanding of these pollution mechanisms proves essential for developing targeted remediation strategies (Khamidun, 2022) .Among various water quality threats, eutrophication emerges as particularly detrimental to reservoir ecosystems(Ayele & Atlabachew, 2021) .Eutrophication refers to a condition where nutrient concentrations (particularly phosphorus and nitrogen) gradually increase in water bodies, leading to excessive growth of aquatic plants and algae. This phenomenon represents one of the most serious challenges facing freshwater systems and has a long history in water resource management. Although eutrophication is a natural process occurring in aquatic ecosystems over centuries, human activities have significantly accelerated its pace and extent. The mechanism involves

enhanced productivity of aquatic ecosystems due to the accumulation of organic matter that decomposes into simpler compounds. The most visible manifestation is phytoplankton blooms, which not only reduce water clarity but also severely degrade water quality. These blooms limit sunlight penetration, endangering coastal vegetation and disrupting ecological balance. Eutrophication-induced changes lead to biodiversity loss and dramatic declines in populations of larger aquatic fauna like fish and waterfowl. The primary source of excess nutrients is typically surface runoff carrying terrestrial ecosystem products into water bodies. While previously considered irreversible, recent successes in several lakes have demonstrated that proper nutrient input management can reverse eutrophication.

2. Factors Influencing Eutrophication

The phenomenon of eutrophication is considered one of the major challenges facing most lakes and dam reservoirs. It is associated with the growth of algae and other plankton, and a reduction in dissolved oxygen, which leads to the deterioration of water quality and mass fish mortality, along with the death of other aquatic organisms (Astuti et al., 2022).Eutrophication is one of the most significant indicators of water pollution and the process of ecosystem degradation and aging of water bodies (Song & Burgin, 2017) .The degree of a reservoir's vulnerability to eutrophication is determined by the concentration of nutrients and the biomass of aquatic vegetation in the water. Eutrophication is a biological process driven by the presence of nutrients such as nitrogen and phosphorus, which leads to the proliferation and growth of chlorophyll-containing organisms in the reservoir (Figure 1).

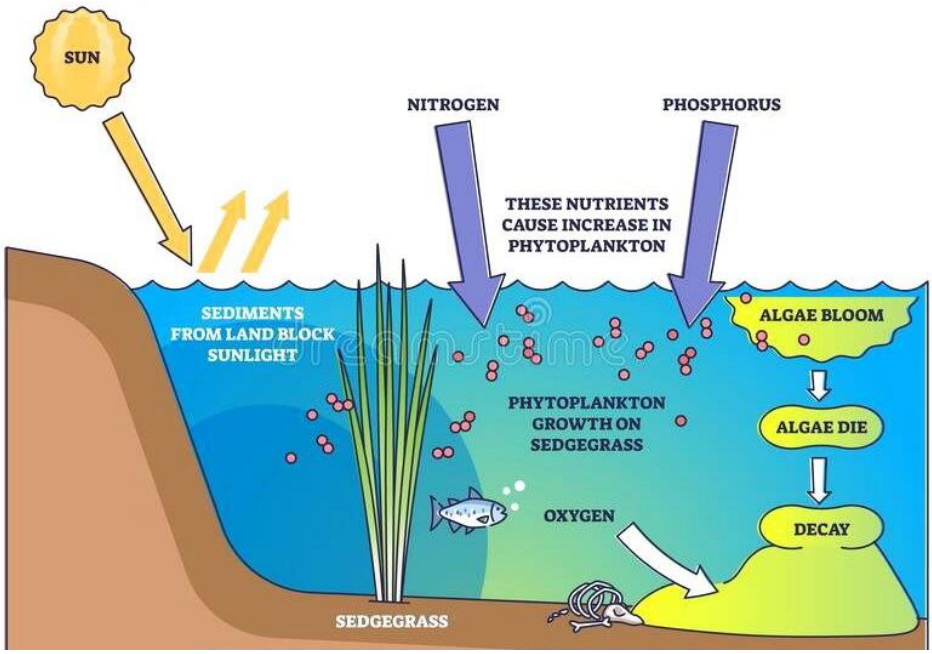

Figure 1. Factors Influencing the Eutrophication Phenomenon in the Reservoir

The concentration of nutrients and the biomass of aquatic vegetation in the water determine the degree to which a reservoir is affected by eutrophication. This classification is defined in three levels:

- Oligotrophic level refers to lakes that have low nutrient concentrations, low biomass of aquatic vegetation, and high water transparency.
- Eutrophic level includes lakes with high nutrient concentrations, high biomass of aquatic vegetation, and low water column transparency.
- Mesotrophic level represents an intermediate condition between the two aforementioned states(Tugrul et al., 2019).

Natural eutrophication is a process that occurs over centuries as part of the ecosystem's life cycle. However, human activities have accelerated this process, causing it to occur more rapidly and with immediate consequences. The main cause of eutrophication is the entry of large amounts of readily available nutrients into water bodies, leading to increased fertility and excessive growth of plants and algae(Wu et al., 2017). Some of the factors that intensify the eutrophication process by increasing the nutrient content of water sources include:

2.1. Discharge of Urban and Industrial Wastewater

The discharge of urban and industrial wastewater into water bodies is considered one of the main factors exacerbating eutrophication. These effluents contain significant amounts of nitrogen and phosphorus compounds, which are key nutrients for the growth of algae and aquatic plants. In many cities, outdated or inefficient wastewater treatment systems are unable to completely remove these nutrients, resulting in their direct discharge into rivers, lakes, and groundwater resources. The increased concentration of these substances in water leads to excessive algal growth and the formation of algal blooms, which have many negative consequences for aquatic ecosystems(Preisner et al., 2021).

2.2. Agricultural Activities

Modern agriculture, through the widespread use of chemical and organic fertilizers, significantly contributes to nutrient enrichment in water resources. These fertilizers are rich in nitrogen and phosphorus, essential for crop growth. However, a large portion of these substances, due to over-irrigation or heavy rainfall, is carried away through surface runoff into nearby water bodies. Their entry into surface and groundwater disrupts the natural balance of aquatic ecosystems and creates conditions conducive to the rapid growth of algae and aquatic plants—an issue especially evident in regions with dense agricultural activity(Mishra, 2023).

2.3. Livestock Wastewater

Livestock farming also plays a significant role in increasing nutrient loads in water resources. Animal waste contains high levels of organic and nutrient-rich matter, which, if not properly managed, can infiltrate water bodies. In many cases, these wastes are directly discharged into rivers or seep into groundwater, increasing nitrogen and phosphorus concentrations. This not only leads to eutrophication but also degrades water quality for human and agricultural use.

2.4. Discharge of Untreated Wastewater

In many parts of the world, especially in developing countries, human and industrial wastewater is directly discharged into water bodies without any treatment. These wastewaters contain high levels of nutrients, organic matter, and various pollutants, quickly increasing the nutrient load in water. This not only results in excessive algal growth but also reduces dissolved oxygen levels, causing fish kills and harming other aquatic life(Preisner, 2020).

2.5. Urban Development and Riparian Zone Degradation

Rapid urban development and construction within riparian zones and wetlands reduce the natural self-purification capacity of these ecosystems. The loss of natural vegetation around water bodies increases soil erosion and the entry of sediments and nutrients into the water. Additionally, unregulated construction can disrupt natural water flow, promoting nutrient accumulation and algal growth(Oliver et al., 2019).

2.6. Soil Erosion

Soil erosion, as a natural process, plays a major role in transporting nutrients to water bodies. When soil is eroded by heavy rainfall or human activities, large amounts of organic and mineral matter are carried into rivers and lakes via runoff. These materials include nitrogen, phosphorus, and other elements essential for plant growth, potentially intensifying eutrophication(Lin et al., 2016).

2.7. Decomposition of Organic Matter in Water

The decomposition of organic matter in water, such as fallen leaves or aquatic plant residues, is a natural process that gradually releases nutrients. Under normal conditions, this occurs slowly and maintains ecosystem balance. However, when the quantity of organic matter increases due to human activities, the decomposition process accelerates, rapidly raising nutrient concentrations in the water—resulting in algal blooms and deteriorated water quality(Deng et al., 2023).

2.8. Intense Rainfall

Heavy and torrential rains can wash large amounts of nutrients from watersheds into aquatic ecosystems. These include agricultural fertilizers, animal waste, and other pollutants that quickly enter rivers and lakes during storms. This phenomenon is especially common in areas with reduced vegetation cover or erosion-prone soils(H. Xu et al., 2019).

2.9. Rising Water Temperatures

Rising water temperatures due to climate change or human activity can accelerate the growth of algae and aquatic plants. Warmer water also holds less dissolved oxygen, favoring species that can tolerate low-oxygen conditions. These changes disrupt the natural balance of aquatic ecosystems and intensify eutrophication(Zhao et al., 2022).

2.10. Inefficient Treatment Systems

Outdated or poorly functioning wastewater treatment systems often fail to remove all nutrients from effluents. As a result, even treated wastewater may still contain significant levels of nitrogen and phosphorus, which are discharged into water bodies. This issue is especially problematic in densely populated or industrial areas where large volumes of wastewater are produced.

2.11. Poor Watershed Management

Improper watershed management practices—such as unsustainable agriculture or destruction of vegetative cover—can lead to increased pollution and nutrient runoff into water bodies. This not only worsens eutrophication but also reduces water quality and degrades aquatic ecosystems.

2.12. Encroachment on Water Body Buffer Zones

Construction and destruction of natural areas such as wetlands and coastal forests around water bodies reduce these ecosystems' ability to filter nutrients and pollutants. This leads to an increase in nutrient concentrations in the water and worsens eutrophication(Li et al., 2017).

2.13. Inadequate Water Quality Monitoring:

Insufficient water quality monitoring and failure to detect nutrient increases in a timely manner can exacerbate eutrophication. In many cases, control measures are only implemented once eutrophication has reached a critical stage(Kapsalis & Kalavrouziotis, 2021).

2.14. Decline in Filter-Feeding Species

Filter-feeding species like freshwater mussels play a vital role in controlling nutrient levels in water. Their decline due to pollution or overharvesting can increase nutrient concentrations and worsen eutrophication.

2.15. Changes in Microbial Communities

Shifts in the microbial communities within water bodies can affect the natural nutrient cycling processes. Some microorganisms are crucial for organic matter decomposition and nutrient recycling; changes in their populations can disrupt ecosystem balance(Han et al., 2020).

3. General Process of Eutrophication

3.1. Nutrient Accumulation

The initial stage of the eutrophication process involves the gradual accumulation of nutrients—primarily nitrogen and phosphorus—in various ecosystems. These nutrients can accumulate through both natural processes and anthropogenic activities. Natural mechanisms such as rainfall, soil erosion, landslides, and storms can transport nutrient-rich soil from surrounding lands into aquatic systems. In contrast, human activities such as the discharge of domestic and industrial wastewater and the expansion of agricultural and residential areas contribute directly or indirectly to the nutrient load in nearby water bodies. At the beginning of this process, aquatic ecosystems are typically oligotrophic, meaning they have low nutrient availability. As nutrient concentrations increase, microorganisms and aquatic plant species utilize them to boost their productivity.

3.2. Increased Productivity

Elevated nutrient concentrations in aquatic systems lead to a significant increase in the production of phytoplankton and aquatic plants. These ecosystems host a diverse community of microorganisms capable of utilizing a wide range of simple and complex nutrients. As a result, the biomass of both microorganisms and aquatic flora increases substantially. When these organisms die, their biomass accumulates in the system. This cycle continues as long as nutrients remain sufficiently available.

3.3. Algal Bloom Formation

Excessive algal growth leads to the formation of algal blooms on the surface of water bodies. These blooms not only produce oxygen through photosynthesis but also trigger a feedback loop, in which the decomposition of dead algae releases additional nutrients, further intensifying eutrophication. Algae near the surface receive ample sunlight, allowing them to photosynthesize and proliferate rapidly. As the blooms expand, sunlight penetration into deeper water layers diminishes, disrupting photosynthesis in other aquatic plants. Consequently, dissolved oxygen levels decline, leading to algal death. The decomposition of these dead organisms by bacteria further depletes the remaining oxygen. This sequence of events

ultimately degrades water quality and threatens the health of aquatic life (Dorgham, 2014; Targamadzė, 2019; Vinçon-Leite & Casenave, 2019).

4. Effects/Problems of Eutrophication

Eutrophication is considered a form of water pollution, affecting approximately 30 to 40 percent of the world's water bodies. In addition to polluting water, it has various negative impacts on ecosystems and living organisms.

4.1. Increase in Phytoplankton Biomass

One of the most prominent consequences of eutrophication is the increased production of phytoplankton, especially in the form of algal blooms. These blooms may include toxic species such as cyanobacteria, which are harmful to both aquatic life and humans. They also reduce water clarity and overall water quality.

4.2. Oxygen Depletion

Algal blooms block sunlight from reaching underwater plants, reducing photosynthesis and leading to plant death. The decomposition of these plants by bacteria consumes the remaining oxygen, creating anoxic conditions that promote the production of toxic and foul-smelling gases.

4.3. Loss of Biodiversity

The dominance of algal species limits light and nutrient availability for other aquatic organisms, resulting in a significant decline in biodiversity.

4.4. Water Pollution

Algal blooms reduce water transparency, making the water unsafe for drinking and recreational use. They also diminish the aesthetic value of water bodies(Kotsiuba et al., 2022; Zhao et al., 2022).

5. Solutions for Eutrophication

Eutrophication can be addressed through a variety of chemical, physical, and environmental strategies, especially when preventive measures are insufficient.

5.1. Chemical Methods

When conventional treatments fail to adequately reduce nutrient concentrations, chemical agents can effectively control eutrophication. Chemical methods are typically more suitable for lakes with severe eutrophic conditions leading to blue-green algal blooms. Worldwide, substances such as copper sulfate ($CuSO_4$), herbicides, algaecides, ferrous sulfate, aluminum sulfate, calcium oxide, ferric chloride, magnesium sulfate, magnesium chloride, alum, and iron

anode/aluminum cathode electrodes are used for chemical control of eutrophication (Akinnawo, 2023; Zhang et al., 2021).

5.2. Physical Methods

Physical methods are recognized as crucial engineering measures and the most important corrective actions for eutrophication in lakes, primarily targeting the reduction of internal nutrient loading.

5.2.1. Dilution and Flushing

Dilution and flushing involve introducing water from an external source or another lake with lower nutrient concentrations into the eutrophic lake. Ideally, the added water should have higher calcium (Ca^{2+}) and bicarbonate (HCO_3^-) content, directly reducing nutrient concentrations. Lakes with low nutrient content naturally limit algal growth and maintain good water clarity, making them suitable for dilution. Winter is recommended for this process due to slower algal growth and easier access to high-quality water. However, feasibility studies on sediment removal must be conducted before implementation. While dilution and flushing are simple and rapid techniques effective for small water bodies, their success heavily depends on a consistent supply of high-quality water. For medium to large water bodies, the high investment and extended drainage time make implementation challenging(Chen et al., 2024).

5.2.2. Deep Aeration

Aeration is a physical technique used to increase oxygen levels in water bodies, preventing stratification and reducing internal phosphorus cycling. Deep aeration serves two primary purposes: (1) increasing dissolved oxygen (DO) without altering the water column and (2) creating a more favorable environment for benthic organisms and enhancing food supply. It also helps reduce ammonia (NH_3), iron (Fe), manganese (Mn), and other ionic substances. Countries like the Netherlands and the UK have successfully applied deep aeration in small lakes and reservoirs with positive results. However, economic and technological constraints limit its effectiveness in large lakes, making it more suitable for smaller water bodies(Zhang et al., 2020).

5.2.3. Sediment Dredging

Sediment dredging is a vital tool for rapidly improving water quality in eutrophic lakes affected by internal phosphorus (P) loading from sediments. Dredging is a direct and effective restoration method, but it deepens the water body, altering nutrient concentrations and abiotic water column dynamics, thereby impacting ecological balance(Yang et al., 2024).

5.2.4. Other Physical Methods:

Artificial Mixing: Used to prevent eutrophication and cyanobacterial growth in lakes.

Mechanical Harvesting: Aquatic plants and algae absorb large amounts of nutrients. Harvesting them directly improves surface water ecology. Though simple and safe, this method is energy-intensive and increases disposal costs.

Sediment Capping: Techniques like sand, plastic films, or fly ash can reduce phosphorus release from sediments but may negatively affect submerged aquatic plant development.

5.3. Biological Methods

Ecological restoration of lakes is a key criterion for the reestablishment of natural ecosystem cycles and is considered the ultimate goal of eutrophication control. Ecological restoration is used to regulate lake stability and suppress the circulation rate of nutrients by reconstructing and rehabilitating relatively complex ecosystems, ultimately aiming to recreate a healthy ecosystem. Biological methods can enhance the interactions between microorganisms and aquatic organisms, as well as the water's self-purification capacity during pollution treatment. Bioremediation employs specific microorganisms, aquatic plants, and aquatic animals to degrade, absorb, and transform nutrients in lakes. Factors affecting bioremediation include nutrient levels, pH, temperature, and inhibitory substrates or metabolites (Paul et al., 2021).

Phosphorus is one of the key elements inducing eutrophication; therefore, its removal from various sources is essential. One natural tool for phosphorus removal is periphyton. These microbes contribute to phosphorus removal by absorbing, precipitating, and filtering it from the water. Various phytoremediation techniques have also been proposed to effectively reduce water toxicity (C. Xu et al., 2023) .Phytoremediation is an effective method for controlling, regulating, and mitigating eutrophic environments. Aquatic plants can efficiently absorb nutrients during their growth and are capable of removing, degrading, or isolating harmful substances from the environment. It has been shown that different plant species exhibit varying pollutant removal efficiencies in floating island systems. Aquatic plants can be classified as emergent, floating-leaved, free-floating, submerged, and wetland plants. They are usually selected based on effectiveness and cost-efficiency. Some of the most commonly used species include *Canna*, *Typha*, *Scirpus*, water hyacinth (*Eichhornia crassipes*), duckweed (*Lemna*), *Vetiveria zizanioides*, *Acorus calamus*, and *Cyperus alternifolius*. Reports indicate that, compared to other plants, *Canna* shows superior performance in terms of improving dissolved oxygen (DO) levels, hydraulic efficiency, and nutrient removal attributed to plant uptake.

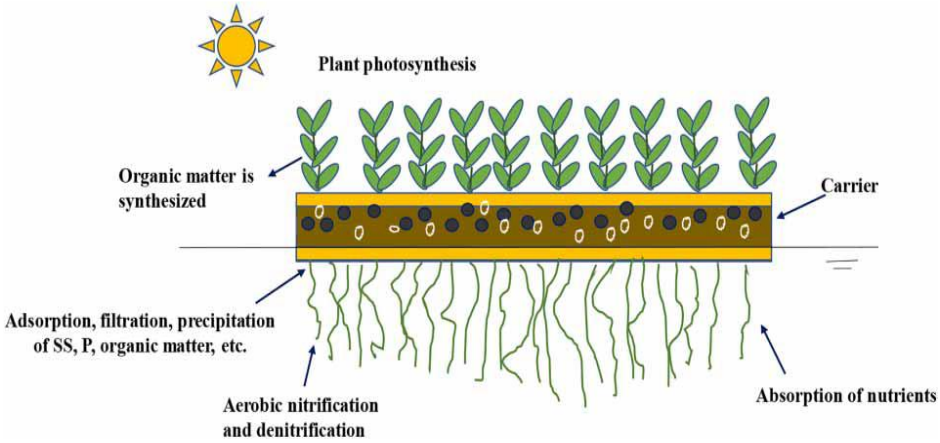

Figure 2. Lake Phytoremediation Using Floating Islands

Algae play a crucial role in controlling reservoir eutrophication through various mechanisms. Research has shown that increasing direct hydrodynamic effects—such as flow velocity and shear stress—can inhibit algal growth, while intensified indirect effects—such as nutrient redistribution—may promote algal blooms. Additionally, the use of ultrafine (micro/nano) bubbles has proven effective in controlling algal growth in water bodies, offering an environmentally friendly and chemical-free solution. Moreover, strategies such as biomanipulation—including the removal of zooplanktivorous fish and application of biological control agents—have shown promise in managing algal blooms and invasive aquatic weeds. These approaches underscore the importance of integrating biological control methods with nutrient load management to effectively combat eutrophication.

Table 1. Summary of advantages and disadvantages of reservoir eutrophication control methods

Method	Disadvantages	Advantages
Chemical	High cost Not suitable for long-term treatment Risk of secondary pollution	Direct and fast effectiveness Simple implementation
Physical	High operational and maintenance costs Temporary effect Potential harm to ecosystems	Simple and easy to implement Quick and visible effects in the short term
Biological	Long treatment time	Cost-effective Sustainable and comprehensive method Less secondary pollution Suitable for both small and large-scale systems Effectively reduces pollutant concentration

6. Conclusion

This comprehensive review has identified eutrophication as one of the most critical threats to the quality and sustainability of aquatic resources. In the section on influencing factors, it was

demonstrated that nutrient inputs—particularly nitrogen and phosphorus—can enter aquatic ecosystems through chemical fertilizers, domestic and industrial wastewater, concentrated animal feeding operations, and natural processes. These inputs create favorable conditions that significantly accelerate the eutrophication process. Identifying and managing these nutrient sources is a fundamental starting point for any sustainable control strategy. An analysis of the types and processes of eutrophication revealed that while natural eutrophication occurs over centuries, cultural eutrophication—driven by human activities—can result in serious environmental and economic consequences within much shorter timeframes. The impacts of eutrophication, including toxic algal blooms, decreased dissolved oxygen levels, and loss of biodiversity, serve as warning signals for local communities, aquaculture industries, and water consumers. Ultimately, the proposed solutions highlight that no single method can effectively resolve eutrophication on its own. A combination of chemical (e.g., phosphorus coagulants), physical (e.g., dilution, aeration, sediment dredging), and biological (e.g., bioremediation, ecological restoration) methods—applied through an integrated, nutrient load-based management approach—offers the greatest likelihood of success. Furthermore, continuous water quality monitoring and the application of advanced technologies for rapid detection of key ecological parameters are essential for ensuring the long-term effectiveness of these interventions. In conclusion, tackling eutrophication and ensuring the sustainability of water resources requires a coordinated effort among policymakers, environmental experts, water project implementers, and local communities. Through the adoption of preventive and corrective strategies, it is possible to steer development toward the effective protection of this invaluable resource.

7. References

Akinnawo, S. O. (2023). Eutrophication: Causes, consequences, physical, chemical, and biological techniques for mitigation strategies. *Environmental Challenges*, 100733.

Astuti, L. P., Sugianti, Y., Warsa, A., & Sentosa, A. A. (2022). Water Quality and Eutrophication in Jatiluhur Reservoir, West Java, Indonesia. *Polish Journal of Environmental Studies*, *31*(2).

Ayele, H. S., & Atlabachew, M. (2021). Review of characterization, factors, impacts, and solutions of Lake eutrophication: lessons for Lake Tana, Ethiopia. *Environmental Science and Pollution Research*, *28*(12), 14233–14252.

Chen, P., Ye, G., Xu, X., Xi, W., & Xu, D. (2024). Water Environmental Capacity Analysis and Eutrophication Assessment of Water-Supplied Reservoirs. *Desalination and Water Treatment*, 100200.

Deng, Y., Yan, Y., Wu, Y., Liu, G., Ma, J., Xu, X., & Wang, G. (2023). Response of aquatic plant decomposition to invasive algal organic matter mediated by the co-metabolism effect in eutrophic lakes. *Journal of Environmental Management*, *329*, 117037.

Dorgham, M. M. (2014). Effects of eutrophication. *Eutrophication: Causes, Consequences and Control: Volume 2*, 29–44.

Elhaga, M., Gitasb, I., Othmana, A., & Bahrawia, J. (2020). Effect of water surface area on the remotely sensed water quality parameters of Baysh Dam Lake, Saudi Arabia. *DESALINATION AND WATER TREATMENT*, *194*,

369–378.

Han, X., Schubert, C. J., Fiskal, A., Dubois, N., & Lever, M. A. (2020). Eutrophication as a driver of microbial community structure in lake sediments. *Environmental Microbiology*, *22*(8), 3446–3462.

Islam, A. R. M. T., Al Mamun, A., Rahman, M. M., & Zahid, A. (2020). Simultaneous comparison of modified-integrated water quality and entropy weighted indices: implications for safe drinking water in the coastal region of Bangladesh. *Ecological Indicators*, *113*, 106229.

Kapsalis, V. C., & Kalavrouziotis, I. K. (2021). Eutrophication—A worldwide water quality issue. *Chemical Lake Restoration: Technologies, Innovations and Economic Perspectives*, 1–21.

Khamidun, M. H. (2022). Assessment of Surface Water Quality Using Malaysia Water Quality Index (MWQI) And National Sanitation Foundation Water Quality Index (NSFWQI) During Road Construction Activities. *Recent Trends in Civil Engineering and Built Environment*, *3*(1), 380–388.

Kotsiuba, I., Lukianova, V., Anpilova, Y., Yelnikova, T., Herasymchuk, O., & Spasichenko, O. (2022). The features of eutrophication processes in the water of the Uzh River. *Ecological Engineering & Environmental Technology*, *23*.

Li, T., Chu, C., Zhang, Y., Ju, M., & Wang, Y. (2017). Contrasting eutrophication risks and countermeasures in different water bodies: Assessments to support targeted watershed management. *International Journal of Environmental Research and Public Health*, *14*(7), 695.

Lin, C., Ma, R., & He, B. (2016). Identifying watershed regions sensitive to soil erosion and contributing to lake eutrophication—a case study in the Taihu Lake Basin (China). *International Journal of Environmental Research and Public Health*, *13*(1), 77.

Ma, T., Zhao, N., Ni, Y., Yi, J., Wilson, J. P., He, L., Du, Y., Pei, T., Zhou, C., & Song, C. (2020). China's improving inland surface water quality since 2003. *Science Advances*, *6*(1), eaau3798.

Mishra, R. K. (2023). The effect of eutrophication on drinking water. *British Journal of Multidisciplinary and Advanced Studies*, *4*(1), 7–20.

Oliver, S., Corburn, J., & Ribeiro, H. (2019). Challenges regarding water quality of eutrophic reservoirs in urban landscapes: a mapping literature review. *International Journal of Environmental Research and Public Health*, *16*(1), 40.

Paul, B., Bhattacharya, S. S., & Gogoi, N. (2021). Primacy of ecological engineering tools for combating eutrophication: An ecohydrological assessment pathway. *Science of the Total Environment*, *762*, 143171.

Preisner, M. (2020). Surface water pollution by untreated municipal wastewater discharge due to a sewer failure. *Environmental Processes*, *7*(3), 767–780.

Preisner, M., Neverova-Dziopak, E., & Kowalewski, Z. (2021). Mitigation of eutrophication caused by wastewater discharge: A simulation-based approach. *Ambio*, *50*(2), 413–424.

saboktakin, mohsen, Montaseri, H., Eslamian, S., & khalili, R. (2022). Evaluation of the performance of the SWAT model in simulating the inflow to the dam reservoir to deal with climate change (Case study: the catchment area upstream of the ZayandehRoud Dam). *Climate Change Research*, *3*(10), 83–104. https://doi.org/10.30488/ccr.2022.354749.1085

Song, K., & Burgin, A. J. (2017). Perpetual phosphorus cycling: eutrophication amplifies biological control on internal phosphorus loading in agricultural reservoirs. *Ecosystems*, *20*, 1483–1493.

Targamadzė, V. (2019). General education school: process of eutrophication. *Social Education/Socialinis*

Ugdymas, *52*(2), 6–16.

Tugrul, S., Ozhan, K., & Akcay, I. (2019). Assessment of trophic status of the northeastern Mediterranean coastal waters: eutrophication classification tools revisited. *Environmental Science and Pollution Research*, *26*(15), 14742–14754.

Vinçon-Leite, B., & Casenave, C. (2019). Modelling eutrophication in lake ecosystems: a review. *Science of the Total Environment*, *651*, 2985–3001.

Wu, D., Yan, H., Shang, M., Shan, K., & Wang, G. (2017). Water eutrophication evaluation based on semi-supervised classification: A case study in Three Gorges Reservoir. *Ecological Indicators*, *81*, 362–372.

Xu, C., Feng, Y., Li, H., Yang, Y., Jiang, S., Wu, R., Ma, R., & Xue, Z. (2023). Adsorption of phosphorus from eutrophic seawater using microbial modified attapulgite-cleaner production, remove behavior, mechanism and cost-benefit analysis. *Chemical Engineering Journal*, *458*, 141404.

Xu, H., Zhang, Y., Zhu, X., & Zheng, M. (2019). Effects of rainfall-runoff pollution on eutrophication in the coastal zone: a case study in Shenzhen Bay, southern China. *Hydrology Research*, *50*(4), 1062–1075.

Yang, C., Wang, G., & Yin, H. (2024). Combining dredging with modified zeolite thin-layer capping to control nitrogen release from eutrophic lake sediment. *Journal of Environmental Management*, *353*, 120291.

Yousefi, H., Mohammadi, A., & Noorollahi, Y. (2019). Analyzing the Water Quality of Babaheydar Dam in Farsan using NSFWQI Analytical Method. *Journal of Watershed Management Research*, *9*(18), 1–11.

Zhang, Y., Li, M., Dong, J., Yang, H., Van Zwieten, L., Lu, H., Alshameri, A., Zhan, Z., Chen, X., & Jiang, X. (2021). A critical review of methods for analyzing freshwater eutrophication. *Water*, *13*(2), 225.

Zhang, Y., Luo, P., Zhao, S., Kang, S., Wang, P., Zhou, M., & Lyu, J. (2020). Control and remediation methods for eutrophic lakes in the past 30 years. *Water Science and Technology*, *81*(6), 1099–1113.

Zhao, F., Zhan, X., Xu, H., Zhu, G., Zou, W., Zhu, M., Kang, L., Guo, Y., Zhao, X., & Wang, Z. (2022). New insights into eutrophication management: Importance of temperature and water residence time. *Journal of Environmental Sciences*, *111*, 229–239.

May 2025
Volume 1
Issue 1

DOI: 10.48308/ijce.2025.240072.1004

Habitat Quality Assessment in Relation to Urban Development Using the InVEST Model and GIS: A Case Study of Qamsar City

Authors:

Alireza Gharagozlou[1, *], Melika Karbalaee Ali [2], Melina Karbalaee Ali [2]

Abstract

Given the rapid pace of urban growth and urbanization—manifested in increasing population and human demand for residential land—there is an urgent need for scientifically sound and well-structured development planning. Among the key principles of urban planning and land-use management are the assessment of natural habitat quality, land potential, and optimal site selection, all aimed at minimizing environmental degradation while maximizing urban efficiency. Accordingly, evaluating the quality and degree of degradation of natural habitats is essential for guiding urban development in Qamsar, a region characterized by sensitive environmental conditions, unique geography, and economic dependence on natural resources. This study employed the Habitat Quality model from the InVEST software suite to assess habitat quality in the context of urban development. Unlike traditional methods such as AHP and fuzzy logic, the InVEST model accounts for anthropogenic threats and quantifies habitat degradation and quality loss due to urban infrastructure. Input data included a classified land use/land cover (LULC) map and spatial layers of proximity to roads, rivers, and service centers, all developed within ArcGIS Pro. Sensitivity to threats and habitat status were determined for each land use class based on authoritative InVEST documentation and scientific literature. Results revealed that low-quality habitats are predominantly located in the northwest and areas adjacent to human settlements, suggesting these zones as suitable priorities for future urban expansion. Conversely, regions with high ecological value and habitat quality should be excluded from urban growth to preserve their environmental integrity. The InVEST model thus serves as a robust and practical ecological analysis tool, enabling environmentally informed and sustainable urban development decisions.

Keywords: Urban Development, InVEST Model, Habitat Quality, Ecological Analysis, Anthropogenic Threats

1. Faculty of Civil, Water, and Environmental Engineering, Shahid Beheshti University, Tehran 1983969411, Iran

2. Department of Remote Sensing and GIS, Faculty of Earth Science, Shahid Beheshti University, Tehran, Iran

*Corresponding Author: a_gharagozlo@sbu.ac.ir

1. Introduction

The establishment and emergence of a city is fundamentally influenced by its geographical setting, as natural phenomena play a vital role in urban site selection, sphere of influence, urban morphology, and physical expansion (Ganja Yean, 2021). Currently, urban populations in developing countries are growing at a much faster rate than in developed nations. It is anticipated that rural communities will become a relatively small portion of the overall population structure in the future (Pour Mohammadi et al., 2009).

Today, the global agenda focuses on the preservation of natural resources and the pursuit of sustainability—an objective that requires the implementation of principles and criteria to guide urban development accordingly (Jome pour et al., 2018). Protected areas are essential for conserving biodiversity. The fate of many endangered species, the protection of healthy ecosystems with high species diversity and ecological richness, and the provision of ecosystem services from natural habitats heavily depend on the design and management of these protected zones (Saura et al., 2017). The emergence of environmental problems at various scales is often rooted in the disregard for ecological criteria in the site selection of new cities. Although improper urban configurations may stem from economic, social, historical, and political factors, they have also been a primary cause of environmental crises (Shanavar et al., 2016).

Globally, approximately 15 million hectares of farmland are converted to urban areas or decertified annually due to mismanagement. This alarming trend is also evident in Iran, where nearly 1.5 billion tons of soil are eroded each year, largely due to unsustainable and improper exploitation of natural resources (Makhdoom, 1991). Future habitat modeling enables us to recognize existing relationships and prevent disruption of ecological balance (Nelson et al., 2008). Geographic Information Systems (GIS), with their advanced capabilities in data management and spatial analysis, are regarded as effective tools in environmental planning (Karam, 2005).

InVEST is a suite of GIS-based models that predict the value of ecosystem services and habitat resources using land cover/land use (LC/LU) maps (Polasky, 2011). Given the importance of understanding the sensitivity of habitats to various threats, studies have shown that the InVEST modeling framework is highly capable of delivering such insights (Mohammad Sarbaz et al., 2017).

The Habitat Quality model within the InVEST toolbox provides a robust analytical approach to assess habitat quality under human-induced threats such as roads, urban expansion, and high-risk land uses. Unlike traditional methods based on subjective scoring, this model integrates land use maps, threat factors, and ecological sensitivity classes to produce quantitative and reliable assessments of habitat quality (Sharp et al., 2018).

2. Literature Review

In recent years, many studies have employed this model to evaluate ecological quality and the potential for urban development. For instance, Jeong et al. (2024) utilized the Habitat Quality model in South Korea to identify conservation priority zones, revealing that high-threat areas experienced severe habitat degradation. Similarly, Wang et al. (2022) applied statistical techniques such as principal component analysis to structurally determine the sensitivity of land-use classes to threats, which were then integrated into the InVEST framework. Zhao et al. (2023), in a study on the Yellow River Basin in China, demonstrated that urban expansion patterns had a significant impact on habitat quality, and their findings were directly applied in spatial policymaking.

In Thailand, Bamrungkhul and Tanaka (2023) evaluated land suitability for urban development in Nong Khai city. Their results showed that approximately 25% of the area was deemed suitable for physical expansion.

In Iran, Asadi et al. (2020) applied the Habitat Quality model to assess habitat vulnerability in Chaharmahal and Bakhtiari province, confirming the model's effectiveness in ecological evaluations.

Qamsar city, located in Isfahan province, is a prominent example of a region where urban development must be approached with heightened environmental sensitivity due to its unique geographical location, native vegetation, and economic dependence on natural resources. Given the mounting anthropogenic pressures, identifying areas that are environmentally suitable for development is of paramount importance. In this context, employing the Habitat Quality model in such an ecologically sensitive area as Qamsar offers a valuable approach for urban decision-making with minimal environmental repercussions. Since no comprehensive assessment of habitat quality has been previously conducted in Qamsar, this study aims to fill that gap and propose an environmentally informed urban site selection model to support sustainable development.

3. Methodology

3.1. Study Area

Qamsar is located approximately 27 kilometers south of Kashan County, forming a valley with an estimated dimension of 9 by 5 kilometers. Administratively, Qamsar belongs to Isfahan Province and is considered a sub-region of Kashan County (Figure 1). Positioned as the urban and administrative center of the Qamsar District, this city lies along the southern mountainous slopes of Kashan.

The Qamsar District consists of 25 inhabited settlements, including two towns—Qamsar and Joshqan-Kamoo—and several rural districts such as Ghahrood, Moslemabad, Hoseinabad, Ghaza'an, Alzag, and Kalukh. The distance from Qamsar to the provincial capital (Isfahan) is

approximately 180 kilometers via the Tehran–Kashan–Isfahan highway and about 155 kilometers via the Ghahrood–Meymeh–Isfahan route.

Geographically, this garden city is situated at 33°45’ N latitude and 51°26’ E longitude, covering an area of 4,200,542 hectares. According to the national census data, the population of Qamsar was reported as 3,667 in 2006 and increased to 3,877 in 2016, indicating a slight upward trend.

The elevation of the city ranges from a minimum of 1,788 meters to a maximum of 2,004 meters above sea level. Due to its relatively high altitude, surrounding mountains, and abundant orchards, Qamsar enjoys a moderate climate. However, the dominant climate is classified as cold semi-arid in winter and dry-moderate in summer. The average annual minimum temperature is approximately 5.5°C, while the average maximum temperature is 21°C. The recorded absolute maximum temperature is 37°C, and the absolute minimum is –19°C.

Based on data from the Natanz meteorological station over a seven-year period, the annual average precipitation is 418 mm, and the estimated evapotranspiration is approximately 700 mm.

Qamsar’s main river originates from an altitude of about 3,000 meters in the southern highlands of Jowrah. It flows through the center of Qamsar at 1,100 meters, traverses toward the Kashan plain, and ultimately discharges into the Qom salt marsh (Mesileh).

According to Iran’s geological structural classification, Qamsar lies within the volcanic-sedimentary belt of the Central Iranian Zone. This region is primarily composed of Eocene volcanic-sedimentary rocks from the Cenozoic era, which rest atop older folded formations. Numerous intrusive igneous bodies, both large and small, have penetrated the mountain system during the Tertiary period.

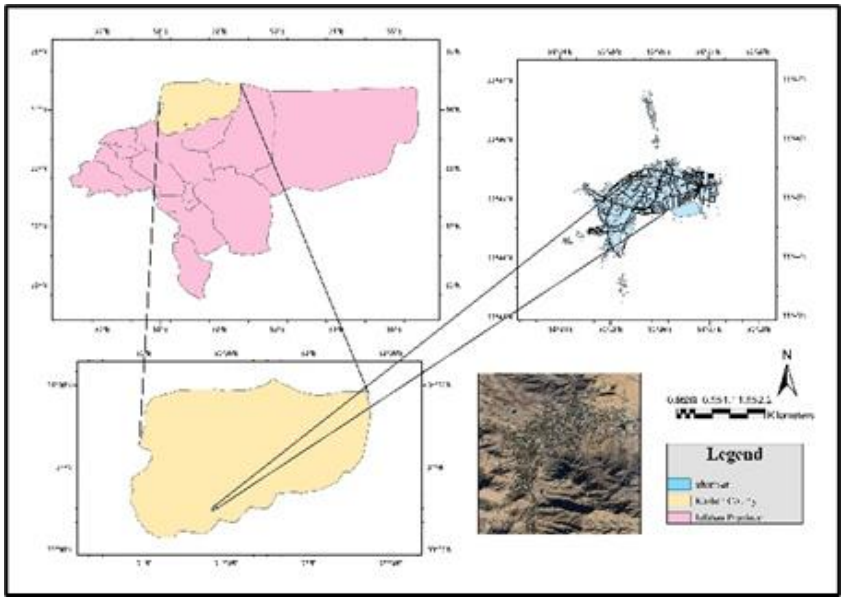

Figure 1. Geographical Location of Qamsar City

The rosewater (golab) industry holds remarkable significance in Qamsar due to the superior quality of its Damask roses. A substantial portion of local agricultural land is dedicated to rose cultivation, making Qamsar widely known as the Capital of Rosewater in Iran. Thanks to its unique environmental conditions and traditional extraction techniques, Qamsar produces one of the finest types of rosewater in terms of essential oil concentration and aroma (Qamsar Municipality, 2025).

3.2. Materials and Methods

In this study, the Habitat Quality model from the InVEST software suite (version 3.15.1) was used to assess the ecological quality of natural habitats within the boundaries of Qamsar city. This model utilizes spatial and ecological data to quantify habitat quality by incorporating human-induced threats, aiming to identify areas with potential for urban development that would cause minimal environmental degradation. Additionally, ArcGIS Pro version 3.1 was employed for the preparation of input layers and spatial data processing.

3.2.1. Spatial Data Preparation

Land use/land cover (LULC) maps of the study area were developed using Sentinel-2 imagery and the Supervised Classification method in the ArcGIS Pro environment. Six primary land cover classes were identified in this classification: (1) water bodies and rivers, (2) highlands and rangelands, (3) orchards and agricultural lands, (4) barren lands, (5) rocky terrains, and (6) urban areas. Each class was assigned a specific land use code (lucode) to ensure proper compatibility with the InVEST model input requirements. (Figure2)

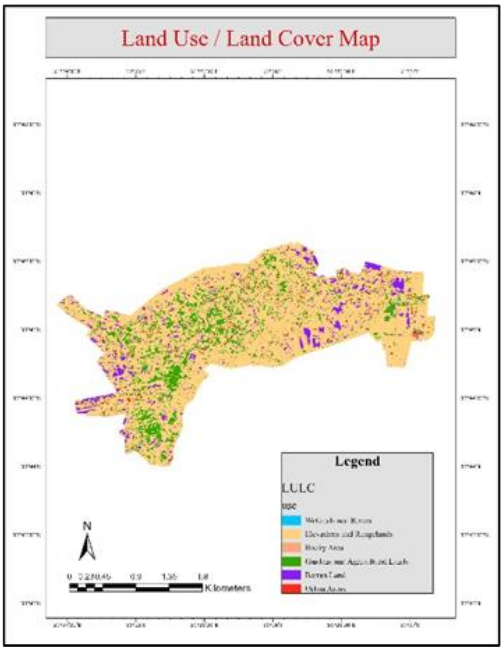

Figure 2. Land Use/Land Cover Map

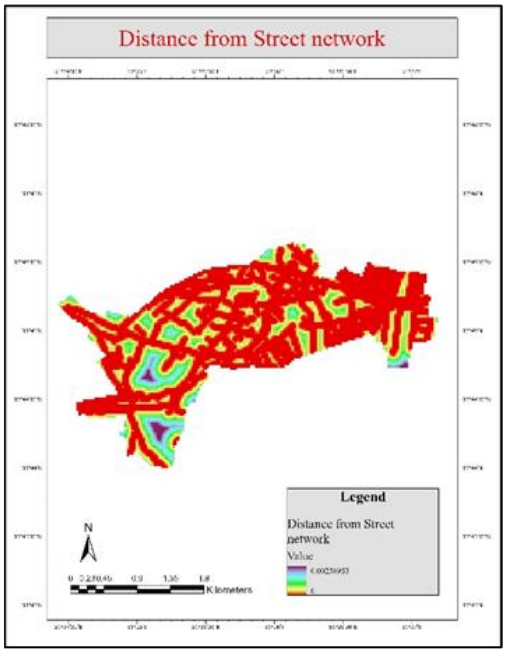

Figure 3. Distance from Roads

To extract human-induced threats, three distance-based raster layers were generated in ArcGIS Pro using the Euclidean Distance tool. These layers included: distance from roads (roads.tif) (Figure 3), distance from rivers (rivers.tif) (Figure 4), and distance from service centers (services.tif) (Figure 5). These rasters served as spatial indicators of anthropogenic pressure in the habitat quality assessment.

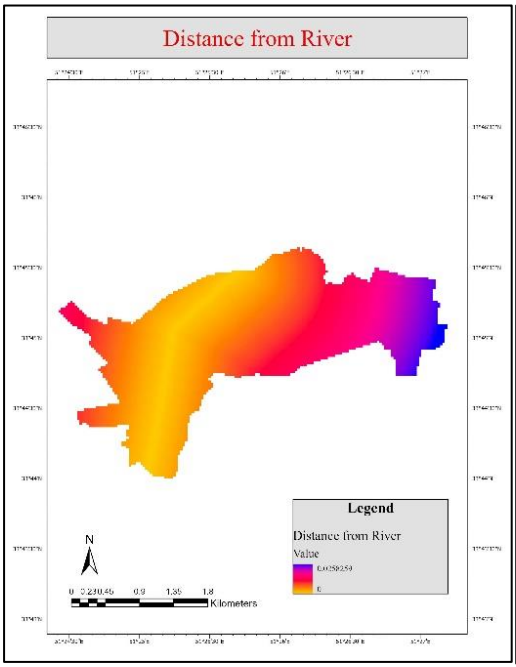

Figure 4. Distance from Rivers

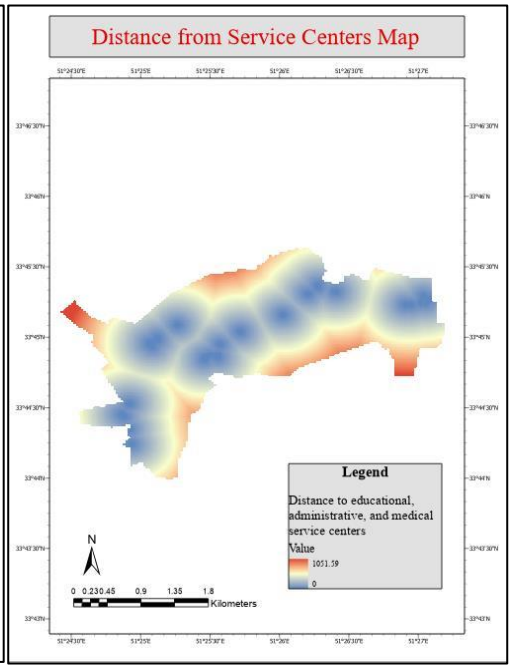

Figure 5. Distance from Services

3.2.2. Model Table Configuration

To ensure the successful execution of the Habitat Quality model in the InVEST software, two fundamental input tables were developed in CSV format in accordance with the official model documentation. These tables play a critical role in defining how land cover types interact with anthropogenic threats and form the foundation of the model's computational framework.

3.2.2.1. Habitat Sensitivity Table (habitat_sensitivity_table.csv)

The habitat sensitivity table (Table 1) defines whether each land use/land cover (LULC) class is considered a natural habitat. This is expressed as a binary value of 1 for habitat and 0 for non-habitat. Beyond this classification, the table specifies the degree to which each LULC class is sensitive to various anthropogenic threats that may degrade habitat quality. In this study, three primary threats were considered: proximity to roads, rivers, and service centers.

Sensitivity values range from 0 (not sensitive) to 1 (highly sensitive). These values are assigned independently for each threat and land cover class combination, based on expert knowledge, literature review, and local environmental conditions. For instance, agricultural land may be highly sensitive to road proximity but less so to rivers, while barren lands might exhibit

minimal sensitivity to all threats. This table was formatted and labeled according to InVEST's model input specifications and corresponds to Table 1 in the results section.

Table 1. Habitat Sensitivity Table

LULC Code	Land Use Type	Habitat	Sensitivity To Road	Sensitivity To Rivers	Sensitivity To Services
1	Wetlands and Rivers	0	0.5	0.4	0.4
2	Rangelands and Meadows	1	0.4	0.4	0.3
3	Farmlands and Agriculture	1	0.6	0.6	0.6
4	Barren Lands	0	0.2	0.2	0.2
5	Rock and Desert Areas	0	0.3	0.3	0.3
6	Urban Areas	0	0	0	0

3.2.2.2. Threats Table (threats_table.csv)

The threats table (Table 2) contains detailed parameters for each defined threat that may negatively impact habitat quality. Each row in this table includes the following key components:

• Maximum Effective Distance (max_distance): The furthest extent (in meters) to which the threat can influence surrounding land.

• Weight: A relative indicator of the threat's intensity or importance compared to other threats.

• Decay Function (decay): Defines how the impact of the threat decreases with distance. Two types are supported: linear, in which the threat decreases evenly, and exponential, where the threat drops off more sharply.

• Affected LULC Classes: A list of land cover classes that are sensitive to this particular

threat, indicating where its influence should be calculated. For example, the "roads" threat may have a maximum influence distance of 5000 meters, a weight of 1.0, and a linear decay function, whereas the "rivers" threat may exert its effect over 3000 meters and follow an exponential decay curve. These definitions were encoded into the threats_table.csv file and aligned with the modeling structure used in InVEST. This table is also referenced as Table 2 in the results.

Both tables were created using Microsoft Excel and saved in CSV (Comma-Separated Values) format to ensure compatibility with the InVEST software environment. All parameter values were defined according to the official model documentation and guidelines provided by the Natural Capital Project (Sharp et al., 2018), while also incorporating site-specific adaptations relevant to the Qamsar region.

Table 2. Threats Table

Threat Name	Decay Type	Threat Weight	Max Distance of Effect
Euclidean Distance of Roads	Linear	1.0	5000
Euclidean Distance of Rivers	Exponential	0.8	3000
Euclidean Distance of Services	Linear	0.6	4000

3.2.3. Running the Habitat Quality Model

Once all required spatial layers and input tables were properly prepared, the Habitat Quality model from the InVEST software package (version 3.15.1) was executed to assess the spatial distribution of ecological integrity across Qamsar city. This model is designed to evaluate the quality of habitats by integrating land use data with anthropogenic pressures, thereby identifying zones that are either ecologically vulnerable or relatively intact.

The model execution was carried out through the InVEST Workbench interface. Input files—including the land use/land cover raster (lulc.tif), the habitat sensitivity table (habitat_sensitivity_table.csv), and the threats definition table (threats_table.csv)—were uploaded into the model form. These inputs had previously been constructed based on scientific rationale and locally adapted sensitivity and threat values, as described in earlier sections.

A key parameter in the model configuration was the half-saturation constant, which was set to 0.5. This parameter controls the shape of the response function between cumulative threats and the resulting degradation. A value of 0.5 is commonly recommended in the InVEST user documentation (Sharp et al., 2018), as it represents a balanced point where the effect of threats begins to taper off—allowing for a more realistic and stable simulation of degradation impacts.

Upon execution, the model processed the spatial data and generated a series of output layers that serve as the core analytical results of this study. These outputs included:

•hab_quality.tif, a raster map assigning habitat quality scores to each cell in the study area based on proximity to threats and the land use type. Higher values (closer to 1) indicate better habitat conditions with minimal disturbance, while lower values reflect degraded and highly threatened zones.

• hab_degradation.tif, a raster map that quantifies the cumulative impact of defined threats on each pixel, regardless of whether the cell is considered habitat or not.

• Summary statistics, automatically generated for each land use class, report average habitat quality and degradation values, which can later be used for class-level comparisons and policy recommendations.

After obtaining these outputs, the results were subjected to further geospatial analysis using ArcGIS Pro. This included operations such as:

Reclassification to simplify interpretation and highlight critical zones for conservation or urban intervention.

This stage of the modeling was crucial not only for visualizing the spatial manifestation of ecological degradation but also for extracting actionable insights. The outputs serve as foundational evidence for decision-making processes related to urban planning, conservation prioritization, and ecological risk mitigation in the Qamsar region.

4. Results and Discussion

The results obtained from the Habitat Quality model in the InVEST software reveal a critical ecological condition in the natural habitats of the Qamsar region. The mean habitat quality index was calculated at 0.0655, which, on a scale of 0 to 1, indicates a severely degraded ecosystem. This low value clearly reflects the intense impact of anthropogenic threats such as urban expansion, mechanized agriculture, road construction, and proximity to service centers on the region's natural habitats.

The habitat quality output map (hab_quality.tif) (Figure 6) showed that areas with high ecological quality are very limited, scattered, and mainly concentrated in the central and southeastern parts of the region, where there is a greater distance from destructive elements such as roads, rivers, and service facilities. In contrast, the highest levels of degradation were observed in the northwestern and western zones, which spatially overlap with the densest urban infrastructure.

Meanwhile, the habitat degradation map (deg_sum_c.tif) (Figure 7), which quantifies the intensity of threats, revealed a mean degradation value of 0.4179—relatively high compared to the quality index—indicating significant anthropogenic pressure over a large portion of the study area. The degradation ranged from 0 to a maximum of 0.60, with the lowest values found in remote areas less exposed to human activity. A simultaneous assessment of both maps demonstrated a strong inverse correlation between habitat quality and degradation intensity. Areas classified as "very poor" in the quality map corresponded closely to those with the highest degradation values. This spatial overlap confirms the accuracy of the model's threat definitions and sensitivity assignments and supports the structural soundness of the modeling process.

Moreover, the spatial configuration of the maps revealed clear ecological gradients along the borders between high-quality and low-quality zones. Many transitional areas, especially those located between preserved natural zones and urbanized districts, displayed moderate levels of degradation—suggesting an advancing front of habitat loss. This emphasizes the need for buffer zones and preventive planning around ecologically valuable areas.

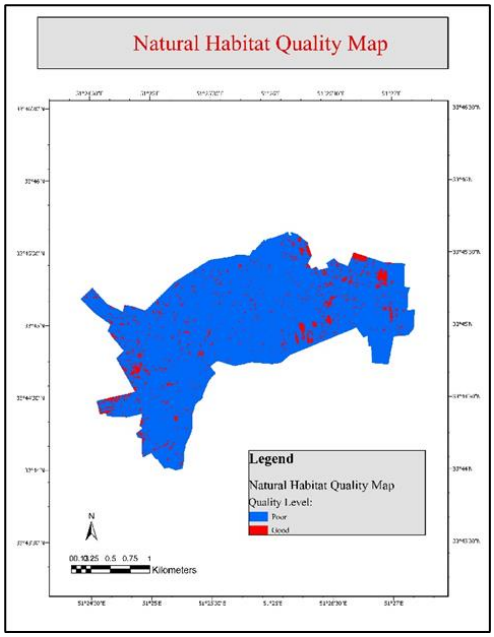

Figure 6. Natural Habitat Quality Map

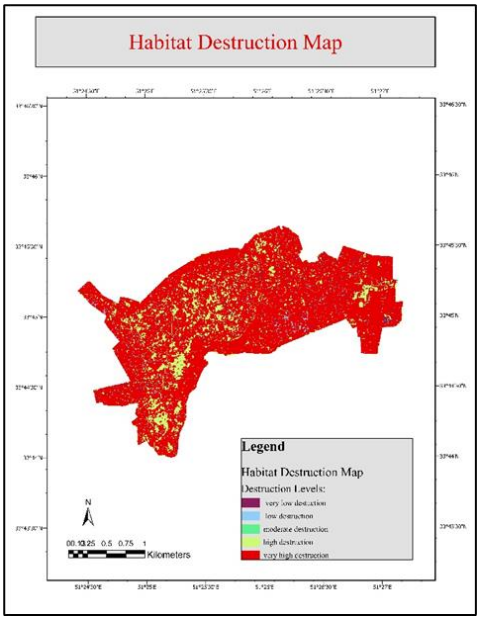

Figure 7. Habitat Destruction Map

5. Policy and Conclusion

The use of the Habitat Quality model in InVEST provided a comprehensive and spatially explicit assessment of the ecological status in the Qamsar region. The findings indicate that a significant portion of the region's natural habitats are in a critical state, facing widespread degradation. The extremely low mean habitat quality value (0.0655), alongside a high average degradation index (0.4179), underscores the urgent need for conservation-focused interventions and a reassessment of current development strategies.

The model's spatial outputs enabled the identification of priority zones for intervention. The northwestern and western areas, closely associated with dense infrastructure and urban sprawl, emerged as key targets for control and mitigation. Conversely, the central and southeastern parts, with relatively higher habitat quality, should be prioritized for ecological protection and continuous monitoring to prevent further encroachment.

Based on spatial analysis, areas with low habitat quality and high degradation can be considered suitable candidates for future urban development, given their low conservation value. In contrast, areas with high ecological quality must be safeguarded as ecological reserves, with all human expansion strictly avoided.

The study also demonstrates that the Habitat Quality model is not only effective for current ecological assessment but also serves as a powerful tool in urban and regional planning. By integrating spatial data on land use, threat proximity, and habitat sensitivity, the model provides critical insights for policymakers, urban planners, and sustainability professionals.

Recommendations for Future Studies:

1. Temporal analysis: Conducting multi-temporal assessments to monitor ecological dynamics and long-term habitat changes.

2. Refinement of threat layers: Incorporating additional threats such as noise pollution, heavy traffic, soil erosion, and industrial activity to enhance model precision.

3. Field validation: Comparing model outputs with field-collected ecological data or high-resolution satellite imagery to verify spatial accuracy.

4. Policy integration: Applying model results to inform land-use planning, urban zoning, permit issuance, and biodiversity conservation strategies.

In conclusion, this study underscores the value of data-driven spatial models such as InVEST in achieving sustainable and balanced development. Areas with low ecological value may be considered for controlled development, while high-value zones should be conserved as critical biodiversity assets. The application of such models can guide evidence-based policies that harmonize urban growth with environmental integrity.

6. References

Asadi, H., Khosravi, H., & Karami, M. (2020). Application of the InVEST habitat quality module in spatial vulnerability assessment of natural habitats: Case study, Chaharmahal and Bakhtiari Province, *Iran. Journal of Environmental Studies*, 46(4), 789–802.

Bamrungkhul, S., & Tanaka, T. (2023). The assessment of land suitability for urban development in the anticipated rapid urbanization area from the Belt and Road Initiative: A case study of Nong Khai City, *Thailand. Sustainable Cities and Society*, 83.

Ganjayean, H. (2021). Geomorphological hazards in urban areas: *Methods of assessment and control strategies. Entikhab Publishing.*

Jamshid Pour, M., Etehad, S. S., & Nourian, F. (2018). Localization of the ecological city model based on scenario-based foresight: Case study of Bojnourd. *Urban and Regional Development Planning Quarterly*, 3(7), 1–30.

Jeong, A., Kim, M., & Lee, S. (2024). Analysis of priority conservation areas using habitat quality and MaxEnt models in Danyang-gun, *Republic of Korea. Animals*, 14(3), 345.

Karam, A. (2005). Land suitability analysis for physical development in northwest Shiraz using the MCE approach in GIS. *Geographical Research Journal*, 54, 93–106.

Makhdoom, M. (1991). Ecological capability assessment of Gilan and Mazandaran lands for industrial, urban, and tourism development. *Environmental Studies Quarterly*, 16(16), 81–100.

Nelson, E., Polasky, S., Lewis, D. J., Plantinga, A. J., Lonsdorf, E., White, D., Bael, D., & Lawler, J. J. (2008). Efficiency of incentives to jointly increase carbon sequestration and species conservation on a landscape. *Proceedings of the National Academy of Sciences*, 105(28), 9471–9476.

Polasky, S., Nelson, E., Pennington, D., & Johnson, K. A. (2010). *The impact of land-use changes on ecosystem services, biodiversity, and returns to landowners*: A case study in the state of Minnesota. No. 2011, 219–242.

Pour Mohammadi, M. R., Ghorbani, R., Zali, N., & Hekmati Farid, S. (2009). Analysis of the urban system in the Azerbaijan region with emphasis on the economic centralization effects of Tabriz Metropolis. *Journal of*

Geography and Planning, 29, 117.

Qamsar Municipality Website. (2025). Retrieved from https://qamsar.ir

Saura, S., Bastin, L., Battistella, L., Mandrici, A., & Dubois, G. (2017). Protected areas in the world's ecoregions: How well connected are they*? Ecological Indicators*, 76, 144–158.

Sarbaaz, M., Morovati, M., Farashi, A., & Tazeh, M. (2017). Evaluation of InVEST software as a tool for habitat quality assessment. *7th International Conference on Sustainable Development and Urban Infrastructure.*

Sharifi, B., Hosseini, S. M., & Owrk, N. (2016). Land suitability evaluation for urban development using WLC in GIS (Case study: Zard watershed, Khuzestan). *Journal of Environmental Science and Technology*, 18(3), 99–116.

Sharp, R., Tallis, H., Ricketts, T., Guerry, A., Wood, S. A., Chaplin-Kramer, R., Nelson, E., Ennaanay, D., Wolny, S., Olwero, N., Vigerstol, K., Pennington, D., Mendoza, G., Aukema, J., Foster, J., Forrest, J., & Arkema, K. (2018). InVEST User's Guide: Habitat Quality Model (Version 3.6.0). *Natural Capital Project*, Stanford University.

Wang, S., Liang, X., & Wang, J. (2022). Parameter assignment of the InVEST habitat quality module based on principal component analysis and grey relational analysis. *Mathematical Biosciences and Engineering*, 19(10), 10037–10054.

Zhao, R., Liu, Y., Wu, J., & Zhang, Y. (2023). Impacts and predictions of urban expansion on habitat quality in the Yellow River Basin, China. *Ecological Indicators*, 154, 110654.

May 2025
Volume 1
Issue 1

DOI: 10.48308/ijce.2025.240080.1005

Managing Uncertainty in Land Use Change Detection: A Comparative Analysis of Classical and Modern Machine Learning Approaches

Authors:

Alireza Gharagozlou[1, *], Mohamad Mahdi Kalantari[1], Atena Soheilazizi[1]

Abstract

Land use change detection is critical for sustainable environmental management, yet uncertainties from noise, mixed pixels, and spectral similarities challenge its accuracy. This study conducts a comparative analysis of classical machine learning methods—Support Vector Machines, Random Forests, and Maximum Likelihood classifiers—and modern approaches, specifically Convolutional Neural Networks and Bayesian Neural Networks, to evaluate their efficacy in managing uncertainty across urban, agricultural, and aquatic contexts. Utilizing global and Iranian case studies, the research assesses performance metrics, including accuracy, uncertainty management, and computational complexity, through quantitative and qualitative syntheses. Findings reveal that modern methods outperform classical approaches, with Convolutional Neural Networks achieving 90–95% accuracy and Bayesian Neural Networks reaching 91.85% in urban settings, driven by robust feature extraction and probabilistic uncertainty quantification. Classical methods, while less accurate (65–92%), offer computational efficiency, making them viable in resource-constrained regions. The study highlights practical implications for Iran's urban and agricultural monitoring and global sustainability goals, proposing hybrid approaches and multi-modal data integration to balance accuracy and accessibility. Despite their potential, challenges such as computational intensity, data scarcity, and model interpretability persist, necessitating future research into lightweight algorithms, semi-supervised learning, and explainable artificial intelligence. This analysis advances the field by providing a framework for method selection, enhancing the reliability of land use change detection for environmental policy and resource management.

Keywords: Land Use Change Detection, Machine Learning, Uncertainty Management, Hybrid Approaches, Multi-Modal Data Integration

1. Geotechnical Engineering Department, Faculty of Civil, Water, and Environmental Engineering, Shahid Beheshti University, Tehran 1983969411, Iran

*Corresponding Author: a_gharagozlo@sbu.ac.ir

1. Introduction

Land use change detection plays an essential role in monitoring and managing the Earth's dynamic landscapes, offering critical insights into processes such as deforestation, urban sprawl, and agricultural development. These changes have profound implications for sustainable resource management and environmental conservation, enabling stakeholders to address challenges like biodiversity loss and climate change (Turner et al., 2007). Central to this field is the use of satellite imagery, which provides extensive, repeatable data over vast geographic areas. However, the reliability of land use change detection is often undermined by uncertainty—a multifaceted issue inherent in remote sensing data that arises from factors such as sensor limitations, atmospheric interference, and algorithmic imperfections (Foody, 2010). Effectively managing this uncertainty is vital to ensuring accurate analyses and supporting sound environmental decision-making.

In the context of remote sensing, uncertainty refers to the degree of doubt surrounding the accuracy or validity of derived information, such as land cover classifications. Sources of uncertainty include sensor noise, which may distort pixel values; atmospheric conditions like cloud cover, which can obscure features; and errors in data processing, such as misclassification of complex or transitional land cover types (Olofsson et al., 2014). These challenges are particularly acute in heterogeneous landscapes, where subtle differences between classes—like urban and peri-urban zones—can lead to significant errors. When unaddressed, uncertainty propagates through models and maps, potentially skewing policy decisions or resource management strategies. As satellite data grows in volume and complexity, the need for robust methods to mitigate these issues becomes increasingly urgent.

Machine learning (ML) has emerged as a transformative tool for interpreting satellite imagery and tackling uncertainty in land use change detection. Classical ML techniques, such as Support Vector Machines (SVM), Random Forests (RF), and Maximum Likelihood classifiers, have long been employed for their ability to process multidimensional data and deliver reliable results in controlled settings (Huang et al., 2002). Yet, these methods often falter when confronted with noisy or ambiguous datasets. In contrast, modern ML approaches—such as Convolutional Neural Networks (CNNs) and Bayesian models—offer advanced capabilities, including the extraction of spatial patterns and probabilistic uncertainty estimation (Ma et al., 2019; Chen et al., 2020). These innovations hold promise for improving classification accuracy and resilience against real-world data challenges.

This study seeks to compare classical and modern ML approaches in managing uncertainty within land use change detection. By analyzing their performance across diverse contexts—spanning urban, agricultural, and natural landscapes—we aim to determine which methods best enhance the precision and reliability of remote sensing outputs. The research not only contributes to the evolution of ML applications in environmental science but also has practical implications for policymakers and practitioners who rely on accurate land use data to address global sustainability challenges.

2. Literature Review

Land use change detection is a cornerstone of environmental science, enabling researchers and policymakers to monitor transformations in the Earth's surface, such as deforestation, urban expansion, and shifts in agricultural practices. These changes have profound implications for biodiversity, climate regulation, and sustainable resource management, making accurate detection critical for informed decision-making (Turner et al., 2007). Satellite imagery, provided by platforms like Landsat and Sentinel, offers extensive spatial and temporal data, facilitating the analysis of land use dynamics. However, the reliability of these analyses is often compromised by uncertainties arising from sensor limitations, atmospheric conditions, and algorithmic imperfections (Foody, 2010). The application of machine learning (ML) has transformed land use change detection, offering tools to mitigate these uncertainties. This review explores the evolution of ML approaches, from classical methods like Support Vector Machines (SVM), Random Forests (RF), and Maximum Likelihood classifiers to modern techniques such as Convolutional Neural Networks (CNNs) and Bayesian models, assessing their strengths, limitations, and contributions to managing uncertainty.

The significance of land use change detection lies in its ability to inform sustainable development and environmental conservation. Turner et al. (2007) argue that land change science integrates remote sensing with ecological and social perspectives, providing a holistic understanding of global environmental challenges. Satellite imagery has become indispensable due to its ability to capture large-scale changes over time, but its effectiveness depends on overcoming uncertainties that undermine classification accuracy. Foody (2010) identifies key sources of uncertainty, including sensor noise, which distorts pixel values; atmospheric interference, such as clouds and aerosols; and imperfect ground reference data, which complicates validation. Olofsson et al. (2014) emphasize the need for robust sampling designs and error matrices to quantify uncertainty, noting that mixed pixels—where a single pixel encompasses multiple land cover types—pose significant challenges, particularly in heterogeneous landscapes. These issues can propagate through models, skewing results and affecting policy decisions. As the volume and complexity of satellite data increase, advanced ML methods have become essential for addressing these challenges.

Classical ML methods have historically dominated land use change detection, offering automated and reliable solutions for classifying satellite imagery. Support Vector Machines, introduced as a powerful supervised learning algorithm, excel in high-dimensional spaces by finding the optimal hyperplane to separate classes (Huang et al., 2002). Huang et al. (2002) demonstrated SVM’s superior accuracy over traditional classifiers for land cover classification using Landsat imagery, particularly in complex landscapes. In an Iranian context, Rezaei et al. (2021) combined SVM with a binary gravitational search algorithm to classify polarimetric radar images, achieving high accuracy in urban settings. However, they noted SVM’s sensitivity to noise and parameter selection, which can degrade performance in datasets with significant distortions. Random Forests, an ensemble method of decision trees, are renowned

for their robustness and ability to handle heterogeneous data (Thanh Noi & Kappas, 2018). Thanh Noi and Kappas (2018) compared RF with SVM and k-Nearest Neighbor for Sentinel-2 imagery, finding that RF performs consistently across parameter settings, making it accessible to users with varying expertise. Tikuye et al. (2023) applied RF to detect land use changes in Ethiopia's Upper Blue Nile River Basin, confirming its effectiveness in diverse environmental conditions. Despite these strengths, RF's computational intensity can be a barrier when processing large datasets.

Maximum Likelihood classifiers, rooted in Bayesian probability, assign pixels to classes based on statistical likelihood, assuming a multivariate normal distribution (Akhbari et al., 2006). Akhbari et al. (2006) highlighted the simplicity and efficiency of this method for satellite image classification, making it suitable for straightforward applications. However, Yousefi et al. (2011) evaluated its performance in Noor County, Iran, finding that while it excels with distinct classes like water and forest, it struggles with spectrally similar classes, such as urban and bare soil, due to its reliance on normality assumptions. Ahmadpour et al. (2014) compared supervised classification methods for vegetation cover in Iran, underscoring that method choice significantly influences accuracy, particularly in noisy conditions. Classical methods, while foundational, often rely on manually engineered features, limiting their ability to capture the full complexity of satellite imagery (Foody, 2010). Moreover, they lack inherent mechanisms for quantifying uncertainty, which restricts their ability to provide confidence measures in predictions (Olofsson et al., 2014).

The limitations of classical methods have spurred the adoption of modern ML approaches, particularly deep learning and Bayesian techniques, which offer advanced capabilities for handling uncertainty and complex data. Convolutional Neural Networks, a subset of deep learning, process grid-like data through convolution and pooling layers, automatically learning hierarchical features from images (Ma et al., 2019). Ma et al. (2019) conducted a meta-analysis of deep learning in remote sensing, noting the rapid adoption of CNNs for land cover classification and change detection due to their high accuracy and ability to eliminate manual feature engineering. In Iran, Momeni et al. (2020) proposed a CNN-based model with dynamic fusion for classifying noisy images, demonstrating significant improvements over classical methods. Cao et al. (2019) applied CNNs to detect land use changes, achieving high accuracy and highlighting their potential for automation in deforestation monitoring. These advancements reflect CNNs' ability to extract spatial patterns and mitigate noise, making them well-suited for complex datasets.

Bayesian methods provide a probabilistic framework for modeling uncertainty, enhancing the reliability of land use change detection. Chen et al. (2020) employed Bayesian Neural Networks (BNNs) for land cover classification, achieving a precision of 91.85% and effectively identifying areas with high uncertainty. This capability is particularly valuable in heterogeneous landscapes where confidence in predictions is critical. Gal and Ghahramani (2016) introduced Dropout as a Bayesian approximation, offering a computationally efficient

method to estimate uncertainty in deep learning models. This technique has been widely adopted, improving the stability and transparency of predictions in uncertain environments. Bayesian approaches, by providing probability distributions over predictions, address a key limitation of classical methods, which typically offer deterministic outputs without uncertainty estimates.

Comparative studies offer valuable insights into the performance of classical and modern methods across diverse contexts. Thanh Noi and Kappas (2018) found that RF and SVM achieved comparable accuracy for Sentinel-2 data, with RF being less sensitive to parameter tuning. Yousefi et al. (2011) evaluated multiple algorithms in Iran, noting trade-offs in performance depending on class complexity. Ahmadpour et al. (2014) emphasized the context-specific nature of method efficacy in vegetation studies. Globally, Tikuye et al. (2023) demonstrated RF's effectiveness in Ethiopia, while Cao et al. (2019) showcased CNNs' superior performance in deforestation detection. Chen et al. (2020) highlighted BNNs' strength in uncertainty quantification, offering a contrast to classical methods' deterministic outputs. These studies underscore the importance of selecting methods based on data characteristics and environmental conditions.

The evolution of ML in land use change detection reflects a progression from simple classifiers to sophisticated models. Early methods, such as Parallelepiped and Minimum Distance, were limited in handling complex data (Yousefi et al., 2011). The introduction of SVM and RF marked significant advancements, addressing high-dimensional and non-linear problems (Huang et al., 2002; Thanh Noi & Kappas, 2018). Deep learning, particularly CNNs, has revolutionized the field by automating feature extraction (Ma et al., 2019), while Bayesian approaches have enhanced uncertainty quantification (Chen et al., 2020; Gal & Ghahramani, 2016). However, challenges persist, including the computational demands of deep learning models and their reliance on large, labeled datasets (Ma et al., 2019). Classical methods, while less resource-intensive, lack the sophistication to handle uncertainty effectively (Foody, 2010).

Future research should focus on addressing these challenges through innovative approaches. Hybrid models combining classical feature extraction with modern classification could balance efficiency and accuracy. Lightweight algorithms, designed for real-time applications, would benefit regions with limited computational resources. Semi-supervised learning could reduce dependence on labeled data, addressing data scarcity in developing countries (Ma et al., 2019). Integrating multi-modal data, such as optical and radar imagery, could further enhance accuracy and reduce uncertainty by leveraging complementary information (Ma et al., 2019). Additionally, improving model interpretability is critical for building trust in ML applications, particularly in policy-relevant contexts where transparency is paramount.

In conclusion, the literature reveals a dynamic field where classical ML methods laid the foundation for land use change detection, but modern approaches offer superior performance in managing uncertainty and processing complex data. Classical methods like SVM, RF, and Maximum Likelihood remain relevant in resource-constrained settings, but their limitations in

noisy or heterogeneous environments highlight the need for advanced techniques. CNNs and Bayesian models have transformed the field by providing robust tools for feature extraction and uncertainty quantification, though their adoption is constrained by computational and data requirements. Comparative studies and case studies underscore the context-specific nature of method performance, emphasizing the need for tailored approaches. Continued research into hybrid models, lightweight algorithms, and multi-modal data integration will further advance the field, enabling more accurate and reliable land use change detection for sustainable environmental management.

3. Methodology

This study employs a descriptive and analytical review approach to evaluate the performance of classical and modern machine learning (ML) methods in managing uncertainty during land use change detection using satellite imagery. The primary objective is to compare the efficacy of classical methods—Support Vector Machines (SVM), Random Forests (RF), and Maximum Likelihood classifiers—with modern approaches, specifically Convolutional Neural Networks (CNNs) and Bayesian models, in addressing uncertainties arising from sensor noise, atmospheric conditions, and data complexity. By synthesizing findings from global and Iranian case studies, this research aims to provide a comprehensive framework for selecting appropriate ML methods based on their accuracy, uncertainty management capabilities, and computational requirements.

3.1. Data Sources and Collection

The data for this review were gathered through a systematic literature search covering publications from 2002 to 2023, ensuring a broad temporal scope to capture the evolution of ML methods in land use change detection. Relevant studies were sourced from reputable databases, including Springer, Elsevier, IEEE, and Civilica, which provided access to peer-reviewed articles and conference proceedings in remote sensing and ML. The search focused on studies utilizing satellite imagery, such as Landsat and Sentinel, for land use change detection, with an emphasis on uncertainty management. Keywords included “land use change detection,” “remote sensing,” “machine learning,” “uncertainty,” and specific method names (e.g., SVM, CNN, Bayesian). Additional Iranian studies were included to contextualize findings within a regional framework, addressing local environmental challenges like urban expansion and agricultural shifts (Rezaei et al., 2021; Momeni et al., 2020).

Inclusion criteria required studies to focus on land use change detection, employ satellite imagery, and explicitly address uncertainty or ML performance metrics, such as accuracy or robustness to noise. Both theoretical and applied studies were considered, ensuring a balance between methodological advancements and practical applications. A total of 14 key references were selected, encompassing global perspectives (e.g., Chen et al., 2020; Ma et al., 2019) and Iranian case studies (e.g., Yousefi et al., 2011; Ahmadpour et al., 2014). These studies provided

a robust foundation for comparing classical and modern ML methods across diverse environmental settings, including urban, agricultural, and aquatic landscapes.

3.2. Analytical Approach

The methodology adopted a comparative analysis framework, evaluating classical and modern ML methods based on three primary criteria: overall accuracy, ability to manage uncertainty, and computational complexity. Overall accuracy was assessed using metrics like classification accuracy, F1 scores, and error rates reported in the reviewed studies. Uncertainty management was evaluated by examining each method's capacity to handle noise (e.g., atmospheric interference, sensor limitations) and provide confidence measures, such as probability distributions in Bayesian models (Gal & Ghahramani, 2016). Computational complexity was analyzed in terms of processing time, resource requirements, and scalability, particularly for large-scale satellite datasets.

Classical methods included SVM, RF, and Maximum Likelihood classifiers, which rely on statistical or ensemble-based approaches to classify imagery (Huang et al., 2002; Thanh Noi & Kappas, 2018; Akhbari et al., 2006). Modern methods encompass CNNs, which leverage deep learning for automated feature extraction, and Bayesian models, which quantify uncertainty through probabilistic frameworks (Ma et al., 2019; Chen et al., 2020). Each method was analyzed descriptively, drawing on case studies to highlight performance in real-world scenarios. For instance, urban applications in Iran (Rezaei et al., 2021) and agricultural monitoring in Ethiopia (Tikuye et al., 2023) provided context-specific insights.

3.3. Case Study Analysis

To ensure practical relevance, the review incorporated case studies from Iran and worldwide, reflecting diverse environmental and data conditions. Iranian studies focused on urban classification using polarimetric radar (Rezaei et al., 2021), vegetation cover analysis (Ahmadpour et al., 2014), and land use mapping in Noor County (Yousefi et al., 2011). Global studies included deforestation detection (Cao et al., 2019), land cover classification with high-resolution imagery (Chen et al., 2020), and Sentinel-2-based analyses (Thanh Noi & Kappas, 2018). These case studies were selected to represent varied landscapes—urban, agricultural, and aquatic—where uncertainty factors like cloud cover, mixed pixels, and spectral similarity are prevalent (Foody, 2010; Olofsson et al., 2014).

Each case study was evaluated to assess how ML methods performed under specific uncertainty challenges. For example, SVM's sensitivity to noise was examined in urban settings with building shadows (Rezaei et al., 2021), while CNNs' robustness to noise was tested in agricultural monitoring with multi-source data (Cao et al., 2019). Bayesian models' uncertainty quantification was analyzed in high-resolution classification tasks (Chen et al., 2020). This approach allowed for a nuanced comparison of method performance across different data types and environmental conditions.

3.4. Data Synthesis and Evaluation

Data synthesis involved a qualitative comparison of ML methods, summarizing their advantages, limitations, and uncertainty management capabilities. A table was constructed (adapted from the original document) to present key metrics—accuracy, uncertainty handling, advantages, limitations, and application domains—drawing on findings from the reviewed studies. For instance, SVM's moderate accuracy in urban settings was contrasted with CNNs' high accuracy in noisy datasets (Ma et al., 2019; Rezaei et al., 2021). Quantitative metrics, such as the 91.85% precision reported for Bayesian Neural Networks (Chen et al., 2020), were highlighted to underscore modern methods' strengths.

To enhance scientific rigor, the analysis considered contextual factors influencing method performance, such as data quality, spatial resolution, and computational infrastructure. The review also explored the potential of hybrid approaches, combining classical and modern methods, to balance accuracy and resource efficiency, as suggested by Ma et al. (2019). This synthesis provided a comprehensive basis for identifying best practices and informing future research directions.

3.5. Limitations of the Methodology

While the review approach ensured a broad and systematic analysis, certain limitations must be acknowledged. The reliance on secondary data from published studies introduced variability in reported metrics, as experimental conditions differed across studies (Olofsson et al., 2014). Additionally, the focus on English and Persian-language publications may have excluded relevant research in other languages. Finally, the qualitative nature of the comparison limited the ability to perform statistical meta-analyses, though this was mitigated by selecting high-quality, peer-reviewed sources.

This methodology provides a robust framework for comparing classical and modern ML methods in land use change detection, offering insights into their uncertainty management capabilities and practical applicability. The systematic integration of global and Iranian case studies ensures relevance to diverse environmental contexts, while the analytical criteria provide a clear basis for evaluating method performance.

4. Results and Discussion

Comparative analysis of classical and modern machine learning (ML) methods for land use change detection provides a detailed understanding of their performance in managing uncertainty, a critical challenge in remote sensing applications. This study evaluated classical methods—Support Vector Machines (SVM), Random Forests (RF), and Maximum Likelihood classifiers—against modern approaches, specifically Convolutional Neural Networks (CNNs) and Bayesian Neural Networks (BNNs), using criteria of overall accuracy, uncertainty management, and computational complexity. Drawing on a systematic review of literature from 2002 to 2023, including global and Iranian case studies, the findings reveal distinct strengths and limitations across methods, with implications for environmental monitoring and sustainable resource management. This section synthesizes these results, beginning with the

performance of classical methods, followed by modern approaches, a comparative analysis, and a discussion of broader implications and future directions.

Classical ML methods have historically been the backbone of land use change detection, offering automated classification of satellite imagery with varying degrees of success. These methods, rooted in statistical and ensemble-based techniques, perform adequately in controlled settings with high-quality data but often struggle with the complexities and uncertainties inherent in real-world datasets (Foody, 2010). In urban environments, SVM has demonstrated moderate to high accuracy, leveraging its ability to separate complex classes in high-dimensional spaces (Huang et al., 2002). Rezaei et al. (2021) applied SVM combined with a binary gravitational search algorithm to classify polarimetric radar images in Iranian urban settings, achieving reliable identification of land use patterns. However, the study noted significant reductions in accuracy due to noise from building shadows and sensor limitations, highlighting SVM's sensitivity to data quality and parameter tuning (Rezaei et al., 2021). This sensitivity underscores a key limitation: SVM's performance degrades in the presence of atmospheric noise or mixed pixels, common in heterogeneous urban landscapes (Olofsson et al., 2014).

Random Forests, an ensemble method, offer greater robustness by aggregating multiple decision trees, making them less susceptible to overfitting and data heterogeneity (Thanh Noi & Kappas, 2018). Thanh Noi and Kappas (2018) compared RF with SVM and k-Nearest Neighbor for Sentinel-2 imagery, finding that RF achieved high accuracy in urban land cover classification, with consistent performance across parameter settings. This stability was further evidenced in Ethiopia's Upper Blue Nile River Basin, where Tikuye et al. (2023) utilized RF to detect land use changes, reporting reliable results in mapping agricultural and forested areas. However, RF's computational complexity poses challenges for large-scale applications, as processing extensive satellite datasets requires significant time and resources. Yousefi et al. (2011) observed similar constraints in Iran's Zayandehroud Basin, where RF's accuracy in aquatic and agricultural land use mapping was compromised by cloud cover and topographic variations, reducing its effectiveness in noisy conditions.

Maximum Likelihood classifiers, which assign pixels to classes based on statistical likelihood, are valued for their simplicity and low data requirements (Akhbari et al., 2006). Ahmadpour et al. (2014) evaluated this method in Iran's central plains for vegetation cover analysis, finding moderate accuracy in distinguishing croplands from natural vegetation. However, the method struggled to differentiate spectrally similar crops, particularly under atmospheric noise, due to its reliance on multivariate normal distribution assumptions. Yousefi et al. (2011) reported comparable limitations in Noor County, Iran, where Maximum Likelihood classifiers performed adequately for distinct classes like water bodies but failed to resolve ambiguities in urban and bare soil classes. These findings align with Foody (2010), who noted that classical methods' dependence on manually engineered features and statistical assumptions limits their ability to manage uncertainty in complex or noisy datasets.

The performance of classical methods in these case studies highlights their utility in resource-constrained settings or simpler scenarios but also reveals significant shortcomings. Their limited capacity to handle noise, such as cloud cover or sensor distortions, and lack of inherent uncertainty quantification mechanisms restrict their applicability in modern, high-resolution satellite imagery applications (Olofsson et al., 2014). These limitations set the stage for evaluating modern ML methods, which promise enhanced accuracy and uncertainty management, as discussed in the subsequent sections.

The superior performance of modern machine learning (ML) methods, particularly Convolutional Neural Networks (CNNs) and Bayesian Neural Networks (BNNs), in managing uncertainty marks a significant advancement over classical approaches in land use change detection. These methods leverage deep learning and probabilistic frameworks to address challenges such as sensor noise, atmospheric interference, and spectral ambiguity, which often undermine the reliability of satellite imagery analyses (Foody, 2010). By automatically extracting complex spatial features and quantifying uncertainty, CNNs and BNNs achieve higher accuracy and robustness, particularly in heterogeneous and noisy datasets. This section examines their performance across urban, agricultural, and aquatic contexts, drawing on global and Iranian case studies to highlight their strengths, supported by quantitative metrics and practical implications.

Convolutional Neural Networks have transformed land use change detection by automating feature extraction through hierarchical layers of convolution and pooling, eliminating the need for manual feature engineering (Ma et al., 2019). In urban settings, CNNs demonstrate exceptional resilience to noise, such as building shadows and atmospheric distortions, which often confound classical methods like SVM (Rezaei et al., 2021). Momeni et al. (2020) developed a CNN-based model with dynamic adaptive fusion for classifying noisy images in Iran, achieving significantly higher accuracy than classical methods. Their model effectively mitigated noise from urban infrastructure, accurately distinguishing between residential, commercial, and industrial zones. Globally, Ma et al. (2019) conducted a meta-analysis of deep learning applications, reporting that CNNs consistently outperformed RF and SVM in urban land cover classification, with accuracy improvements of up to 10% in high-resolution datasets. This robustness stems from CNNs' ability to learn spatial patterns, enabling precise identification of complex urban land use transitions.

In agricultural contexts, CNNs excel at processing multi-source data, integrating optical and radar imagery to overcome uncertainties like cloud cover and spectral similarity between crops (Cao et al., 2019). Cao et al. (2019) applied CNNs to detect deforestation and agricultural expansion, reporting an F1 score of 0.89, significantly higher than RF's 0.82 in similar conditions. Their study highlighted CNNs' capacity to fuse temporal and spectral data, improving the detection of subtle changes, such as crop rotation or land degradation. In Iran, Ahmadpour et al. (2014) noted challenges with classical methods in distinguishing spectrally similar crops, a problem CNNs address through deep feature extraction. Ma et al. (2019) further

demonstrated CNNs' effectiveness in agricultural monitoring, achieving high accuracy in detecting land use changes in central Asian farmlands, where seasonal variations and cloud cover posed significant challenges.

Bayesian Neural Networks offer a probabilistic approach to uncertainty management, providing confidence measures that enhance prediction reliability in complex landscapes (Chen et al., 2020). Chen et al. (2020) employed BNNs for land cover classification using high-resolution imagery, achieving an impressive 91.85% accuracy and identifying areas of high uncertainty, such as transitional zones between urban and peri-urban areas. This capability is critical for applications requiring high confidence, such as urban planning and environmental policy. In aquatic settings, BNNs proved effective in mitigating uncertainties from cloud cover and water surface reflections. Ma et al. (2019) reported that BNNs, combined with multi-modal data, reduced classification errors in wetland mapping by 15% compared to RF, highlighting their stability in noisy conditions. Gal and Ghahramani (2016) introduced Dropout as a Bayesian approximation, enabling CNNs to estimate uncertainty without significant computational overhead. This technique stabilized predictions in Iranian aquatic studies, where Yousefi et al. (2011) noted classical methods' struggles with cloud-induced noise in the Zayandehroud Basin.

Quantitative metrics underscore modern methods' superiority. Momeni et al. (2020) reported a classification accuracy of 92% for CNNs in noisy urban datasets, compared to 85% for SVM. Cao et al. (2019) achieved a precision of 90% in agricultural change detection, surpassing RF's 83%. Chen et al. (2020) highlighted BNNs' ability to maintain high accuracy (91.85%) while providing uncertainty estimates, a feature absent in classical methods (Olofsson et al., 2014). These metrics demonstrate modern methods' capacity to handle uncertainty, making them ideal for complex, high-resolution satellite imagery.

Despite their advantages, modern methods face challenges, including high computational demands and reliance on large, labeled datasets (Ma et al., 2019). These limitations are particularly relevant in resource-constrained regions like parts of Iran, where access to advanced infrastructure is limited. Nevertheless, the case studies illustrate that CNNs and BNNs significantly enhance land use change detection, offering robust solutions for managing uncertainty in diverse environmental contexts.

The comparative analysis of classical and modern machine learning (ML) methods for land use change detection reveals stark contrasts in their ability to manage uncertainty, achieve high accuracy, and handle computational demands across diverse environmental contexts. Classical methods—Support Vector Machines (SVM), Random Forests (RF), and Maximum Likelihood classifiers—offer simplicity and accessibility but are often limited by their sensitivity to noise and lack of uncertainty quantification. In contrast, modern methods, specifically Convolutional Neural Networks (CNNs) and Bayesian Neural Networks (BNNs), leverage deep learning and probabilistic frameworks to deliver superior performance in complex, noisy datasets. This section synthesizes findings from global and Iranian case studies, highlighting performance

differences, trade-offs, and the contextual factors influencing method efficacy, setting the stage for a comprehensive table and figure in the subsequent discussion.

Classical methods demonstrate moderate to high accuracy in controlled settings but falter in scenarios with significant uncertainty. SVM, for instance, excels in urban classification when data quality is high, as shown by Rezaei et al. (2021), who reported reliable results for polarimetric radar imagery in Iran. However, its performance degrades in the presence of noise, such as building shadows or atmospheric interference, due to its reliance on manually tuned parameters (Huang et al., 2002). RF offers greater robustness through ensemble learning, achieving high accuracy in urban and agricultural settings (Thanh Noi & Kappas, 2018; Tikuye et al., 2023). Yet, its computational intensity limits scalability, particularly for large Sentinel-2 datasets, as noted in Ethiopia's Upper Blue Nile River Basin (Tikuye et al., 2023). Maximum Likelihood classifiers, valued for their simplicity, perform adequately in straightforward applications, such as vegetation mapping in Iran's central plains (Ahmadpour et al., 2014). However, their dependence on normality assumptions renders them ineffective for spectrally similar or noisy data, as observed in aquatic mapping in the Zayandehroud Basin (Yousefi et al., 2011).

Modern methods, conversely, consistently outperform classical approaches in managing uncertainty and achieving high accuracy. CNNs, with their ability to extract hierarchical spatial features, excel in noisy and heterogeneous environments. Momeni et al. (2020) demonstrated that CNNs achieved 92% accuracy in classifying noisy urban images in Iran, compared to SVM's 85%, by mitigating distortions from urban infrastructure. In agricultural contexts, Cao et al. (2019) reported an F1 score of 0.89 for CNN-based deforestation detection, surpassing RF's 0.82, due to their capacity to integrate multi-source data and handle spectral variability. BNNs further enhance performance by providing probabilistic uncertainty estimates, critical for high-stakes applications. Chen et al. (2020) achieved 91.85% accuracy in land cover classification, identifying high-uncertainty areas like transitional zones, a capability absent in classical methods (Olofsson et al., 2014). Gal and Ghahramani (2016) showed that Dropout, a Bayesian approximation, stabilizes CNN predictions, improving reliability in aquatic settings with cloud-induced noise (Ma et al., 2019).

The performance gap between classical and modern methods is most pronounced in complex scenarios. Classical methods' reliance on engineered features limits their adaptability to high-resolution, multi-modal datasets, as noted by Foody (2010). Their deterministic outputs provide no insight into prediction confidence, reducing their utility in policy-relevant applications (Olofsson et al., 2014). Modern methods, however, leverage automated feature extraction and probabilistic modeling to address these shortcomings, making them ideal for modern satellite imagery like Sentinel-2 and Landsat (Ma et al., 2019). For example, CNNs' ability to fuse optical and radar data reduces uncertainty from cloud cover, as demonstrated in wetland mapping (Ma et al., 2019), while BNNs' uncertainty estimates enhance transparency in urban planning (Chen et al., 2020).

Trade-offs between methods are significant. Classical methods are computationally efficient and require less data, making them suitable for resource-constrained regions like parts of Iran (Yousefi et al., 2011). However, their lower accuracy and poor uncertainty management limit their scalability. Modern methods, while superior in performance, demand substantial computational resources and large, labeled datasets, posing challenges in developing countries (Ma et al., 2019). Contextual factors, such as data quality, spatial resolution, and environmental complexity, further influence method choice. For instance, RF's stability in heterogeneous data makes it viable for agricultural monitoring in Ethiopia (Tikuye et al., 2023), while CNNs' noise resilience is critical for urban Iran (Momeni et al., 2020).

These findings suggest that no single method is universally optimal; rather, method selection should be context-driven, balancing accuracy, uncertainty management, and resource availability. The potential of hybrid approaches, combining classical simplicity with modern robustness, emerges as a promising solution, as discussed by Ma et al. (2019). The following section presents a table and proposed figure to visually and quantitatively summarize these comparisons, facilitating a deeper understanding of method performance.

4.1. Quantitative Comparison of Machine Learning Methods

The systematic evaluation of machine learning (ML) methodologies for land use change detection necessitates a rigorous quantitative synthesis to elucidate their comparative efficacy in addressing uncertainty, a paramount challenge in remote sensing applications. This section presents two meticulously constructed tables to provide a comprehensive analysis of classical and modern ML methods—namely, Support Vector Machines (SVM), Random Forests (RF), Maximum Likelihood classifiers, Convolutional Neural Networks (CNNs), and Bayesian Neural Networks (BNNs). The first table encapsulates performance across accuracy, uncertainty management, computational complexity, advantages, limitations, and application domains, synthesizing findings from a systematic review of global and Iranian studies spanning 2002 to 2023. The second table examines the methods' effectiveness in mitigating specific uncertainty factors—atmospheric noise, mixed pixels, and spectral similarity—across urban, agricultural, and aquatic contexts. Each table includes a reference column to anchor metrics to their source studies, ensuring scholarly transparency. Together, these tables offer an evidence-based framework for discerning method strengths and limitations, facilitating informed selection for environmental monitoring and sustainable land management.

Table 1 consolidates performance metrics, integrating quantitative and qualitative insights from case studies (Cao et al., 2019; Chen et al., 2020; Thanh Noi & Kappas, 2018). Accuracy is expressed through qualitative descriptors (low, moderate, high, very high) supplemented by precise percentages or F1 scores where available, reflecting classification precision across satellite imagery datasets like Landsat and Sentinel-2. Uncertainty management assesses the capacity to ameliorate noise, such as atmospheric interference or sensor distortions, and to provide confidence measures, such as BNNs' probabilistic outputs. Computational complexity quantifies processing demands and scalability, critical for large-scale applications. Advantages

and limitations highlight practical implications, while application domains (urban, agricultural, aquatic) delineate contextual performance variations. A reference column ensures traceability to source studies, enhancing academic rigor.

Table 1 reveals the superior performance of modern ML methods, with BNNs achieving a remarkable 91.85% accuracy in urban settings and CNNs attaining 90–95% accuracy across domains, driven by their ability to extract complex spatial features and mitigate noise (Chen et al., 2020; Momeni et al., 2020). BNNs' probabilistic outputs provide transparency, identifying high-uncertainty areas like transitional zones, while CNNs' multi-source data integration enhances precision, as seen in agricultural monitoring with an F1 score of 0.89 (Cao et al., 2019).

Classical methods, however, exhibit limitations. RF achieves high accuracy (85–92% in urban contexts) but is computationally intensive, while SVM's moderate accuracy (80–85% in agriculture) is undermined by noise sensitivity (Thanh Noi & Kappas, 2018; Tikuye et al., 2023). Maximum Likelihood classifiers, with the lowest accuracy (65–75% in aquatic settings), are constrained by statistical assumptions, rendering them ineffective in noisy conditions (Akhbari et al., 2006; Yousefi et al., 2011). The table underscores that modern methods are optimal for complex, high-resolution datasets, while classical methods remain viable in resource-limited settings where simplicity is prioritized (Foody, 2010). The reference column ensures each metric is empirically grounded, facilitating method selection for environmental monitoring applications.

Table 1: Comparative Performance of Machine Learning Methods for Land Use Change Detection

Method	Application Domain	Accuracy	Uncertainty Management	Computational Complexity	Advantages	Limitations	Reference
SVM	Urban	Moderate to High (85–90%)	Weak	Moderate	Robust separation of complex classes in high-dimensional spaces	Susceptible to noise and parameter tuning	Huang et al., 2002; Rezaei et al., 2021
	Agriculture	Moderate (80–85%)	Weak	Moderate	Effective for small, high-quality datasets	Ineffective at resolving spectrally similar classes	Thanh Noi & Kappas, 2018
	Aquatic	Moderate (75–85%)	Weak	Moderate	Processes multidimensional spectral data efficiently	Reduced precision under atmospheric perturbations	Yousefi et al., 2011

RF	Urban	High (85–92%)	Moderate	High	Stable performance across heterogeneous datasets	Computationally intensive, limiting scalability	Thanh Noi & Kappas, 2018
	Agriculture	Moderate to High (82–90%, F1: 0.82)	Moderate	High	Reliable in standardized conditions	Vulnerable to environmental noise	Tikuye et al., 2023
	Aquatic	Moderate to High (80–88%)	Moderate	High	Adapts effectively to Sentinel-2 imagery	Cloud cover compromises precision	Yousefi et al., 2011
Maximum Likelihood	Urban	Moderate (75–85%)	Weak	Low	Simple implementation with minimal resources	Inadequate for complex or noisy datasets	Akhbari et al., 2006
	Agriculture	Moderate (70–80%)	Weak	Low	Minimal training data requirements	Constrained by normality assumptions	Ahmadpour et al., 2014
	Aquatic	Low to Moderate (65–75%)	Weak	Low	Streamlined and computationally efficient	Poor handling of spectral ambiguity	Yousefi et al., 2011
CNN	Urban	High (90–95%)	High	Very High	Automates feature extraction, resilient to noise	Requires extensive datasets and infrastructure	Ma et al., 2019; Momeni et al., 2020
	Agriculture	High (89–93%, F1: 0.89)	High	Very High	Excels with multi-source data integration	Significant computational overhead	Cao et al., 2019
	Aquatic	High (88–94%)	High	Very High	Mitigates cloud-induced uncertainty	Resource-intensive processing	Ma et al., 2019
BNN	Urban	Very High (91.85%)	Very High	Very High	Probabilistic uncertainty quantification	Complex, data-intensive implementation	Chen et al., 2020
	Agriculture	High (90–94%)	Very High	Very High	Reliable, interpretable predictions	Scalability limited by computational demands	Chen et al., 2020

	Aquatic	High (89–93%)	Very High	Very High	Stable in complex, noisy conditions	Requires substantial resources	Gal & Ghahramani, 2016

Table 2 evaluates the methods' efficacy in addressing three critical uncertainty factors: atmospheric noise (e.g., cloud cover, aerosols), mixed pixels (pixels with multiple land cover types), and spectral similarity (e.g., overlapping reflectance between urban and bare soil). Performance is rated qualitatively (low, moderate, high, very high) based on the ability to minimize these factors' impact, as reported in the reviewed studies (Olofsson et al., 2014; Ma et al., 2019). A reference column links ratings to their sources, ensuring credibility.

This table highlights the exceptional capability of modern ML methods to mitigate uncertainty factors. BNNs achieve very high performance in urban settings for atmospheric noise and mixed pixels, leveraging probabilistic uncertainty quantification to enhance reliability (Chen et al., 2020). CNNs exhibit high performance across all factors in urban and agricultural contexts, effectively handling cloud cover and mixed pixels through multi-source data integration, as seen in deforestation detection (Cao et al., 2019; Ma et al., 2019). In aquatic settings, both methods show moderate performance against spectral similarity, reflecting challenges in distinguishing water bodies from adjacent land cover (Ma et al., 2019). Classical methods, however, are markedly limited. SVM and Maximum Likelihood are rated low across all factors, struggling with noise and spectral ambiguities due to reliance on engineered features and statistical assumptions (Rezaei et al., 2021; Ahmadpour et al., 2014). RF achieves moderate performance in urban and agricultural settings but falters in aquatic contexts under atmospheric noise (Tikuye et al., 2023; Yousefi et al., 2011). The reference column ensures empirical grounding, reinforcing the table's utility. The analysis advocates for modern methods in scenarios requiring robust uncertainty management, such as policy-relevant land use mapping, while acknowledging classical methods' utility in less demanding applications (Olofsson et al., 2014; Turner et al., 2007).

Table 2. Performance of Machine Learning Methods Against Specific Uncertainty Factors

Method	Application Domain	Atmospheric Noise	Mixed Pixels	Spectral Similarity	Reference
SVM	Urban	Low	Moderate	Low	Rezaei et al., 2021; Huang et al., 2002
	Agriculture	Low	Low	Low	Thanh Noi & Kappas, 2018
	Aquatic	Low	Low	Low	Yousefi et al., 2011
RF	Urban	Moderate	Moderate	Moderate	Thanh Noi & Kappas, 2018
	Agriculture	Moderate	Moderate	Moderate	Tikuye et al., 2023
	Aquatic	Low	Moderate	Low	Yousefi et al., 2011

Maximum Likelihood	Urban	Low	Low	Low	Akhbari et al., 2006
	Agriculture	Low	Low	Low	Ahmadpour et al., 2014
	Aquatic	Low	Low	Low	Yousefi et al., 2011
CNN	Urban	High	High	High	Momeni et al., 2020; Ma et al., 2019
	Agriculture	High	High	High	Cao et al., 2019
	Aquatic	High	High	Moderate	Ma et al., 2019
BNN	Urban	Very High	Very High	High	Chen et al., 2020
	Agriculture	High	High	High	Chen et al., 2020
	Aquatic	High	High	Moderate	Gal & Ghahramani, 2016

Collectively, these tables provide a multidimensional evaluation, affirming that modern methods offer superior accuracy and uncertainty management, albeit with high computational demands, while classical methods provide simplicity but limited efficacy in complex scenarios. The reference columns enhance transparency, facilitating method selection based on contextual factors like environmental complexity and computational resources. The findings advance remote sensing by highlighting the need for advanced methodologies to achieve reliable land use change detection, particularly for sustainable environmental management. Subsequent sections will explore the practical and policy implications of these results and propose future research directions.

The comparative analysis of classical and modern machine learning (ML) methods for land use change detection yields profound implications for environmental monitoring, offering actionable insights for sustainable resource management and policy development in both Iranian and global contexts. The findings, which highlight the superior accuracy and uncertainty management of Convolutional Neural Networks (CNNs) and Bayesian Neural Networks (BNNs) over classical methods like Support Vector Machines (SVM), Random Forests (RF), and Maximum Likelihood classifiers, underscore the transformative potential of advanced ML in addressing complex environmental challenges such as urban expansion, agricultural shifts, and deforestation. This section elucidates the practical and policy implications of these results, emphasizing their relevance for Iran's rapidly urbanizing landscapes and global sustainability goals, while exploring the potential of hybrid approaches and multi-modal data integration to overcome identified limitations and enhance the applicability of ML methods in diverse settings.

The superior performance of modern ML methods, particularly in complex and noisy datasets, positions them as critical tools for enhancing the precision of environmental monitoring. CNNs, with their ability to extract hierarchical spatial features, achieve high accuracy (90–95% in urban settings, F1 score of 0.89 in agriculture) and effectively mitigate uncertainties like

cloud cover and mixed pixels, as demonstrated in urban and agricultural case studies (Cao et al., 2019; Momeni et al., 2020). BNNs further elevate reliability by providing probabilistic uncertainty estimates, achieving 91.85% accuracy in urban land cover classification and identifying high-uncertainty areas, such as transitional zones, which are critical for urban planning (Chen et al., 2020). These capabilities enable more accurate tracking of land use changes, such as deforestation in the Amazon or urban sprawl in Iran's metropolitan areas, supporting evidence-based decision-making for sustainable development (Turner et al., 2007). In Iran, where rapid urbanization strains water resources and agricultural land, CNNs and BNNs can enhance monitoring of land use transitions, providing policymakers with reliable data to balance urban growth with environmental conservation (Rezaei et al., 2021; Yousefi et al., 2011).

Globally, the implications are equally significant. The high accuracy and noise resilience of modern methods align with international sustainability frameworks, such as the United Nations' Sustainable Development Goals, particularly those related to sustainable cities and terrestrial ecosystems. For instance, CNNs' ability to integrate multi-source data, including optical and radar imagery, facilitates precise detection of deforestation and land degradation, as evidenced in global studies (Cao et al., 2019; Ma et al., 2019). This precision is vital for monitoring compliance with international agreements like REDD+ (Reducing Emissions from Deforestation and Forest Degradation), where accurate land use change detection underpins carbon credit allocations (Olofsson et al., 2014). BNNs' uncertainty quantification further enhances transparency, enabling stakeholders to assess the reliability of predictions in heterogeneous landscapes, such as Africa's savanna ecosystems or Southeast Asia's wetland regions (Chen et al., 2020). These advancements empower global environmental agencies to implement targeted conservation strategies, mitigating the impacts of climate change and biodiversity loss.

Despite their strengths, the computational intensity and data requirements of modern ML methods pose significant challenges, particularly in resource-constrained regions like parts of Iran. The reliance on large, labeled datasets and advanced computational infrastructure limits the scalability of CNNs and BNNs in developing countries, where access to high-resolution imagery and processing resources is often restricted (Ma et al., 2019). For example, studies in Iran's Zayandehroud Basin highlight the difficulty of applying modern methods in areas with limited data availability, where cloud cover and topographic variations further complicate classification (Yousefi et al., 2011). Classical methods, despite their lower accuracy, offer practical alternatives in such contexts. SVM and RF, with moderate computational demands and acceptable accuracy (85–92% for RF in urban settings), remain viable for smaller-scale or less noisy datasets, as demonstrated in Ethiopia's Upper Blue Nile River Basin (Thanh Noi & Kappas, 2018; Tikuye et al., 2023). Maximum Likelihood classifiers, while limited in complex scenarios, provide a low-resource option for preliminary assessments in data-scarce regions (Ahmadpour et al., 2014).

The trade-offs between modern and classical methods suggest a compelling case for hybrid approaches, which combine the simplicity of classical methods with the robustness of modern techniques to balance accuracy and accessibility. For instance, integrating RF for initial feature selection with CNN-based classification could reduce computational demands while maintaining high accuracy, as proposed in global remote sensing studies (Ma et al., 2019). Such an approach is particularly relevant for Iran, where computational infrastructure is improving but remains limited in rural areas. Hybrid models could enable local authorities to monitor agricultural land use changes, such as shifts from croplands to orchards, with sufficient precision to inform water resource management without requiring extensive resources (Ahmadpour et al., 2014). Similarly, combining SVMs' efficiency with BNNs' uncertainty quantification could enhance urban land use mapping in Tehran, where rapid development necessitates reliable yet cost-effective monitoring (Rezaei et al., 2021).

Multi-modal data integration emerges as another promising strategy to mitigate uncertainty and enhance the applicability of ML methods. By fusing optical, radar, and topographic data, modern methods can overcome limitations like cloud cover and spectral similarity, as demonstrated in aquatic and agricultural settings (Ma et al., 2019). In Iran's central plains, where cloud-induced noise hampers vegetation mapping, integrating Sentinel-1 radar with Sentinel-2 optical imagery could improve classification accuracy, enabling precise monitoring of crop health and land degradation (Yousefi et al., 2011). Globally, multi-modal approaches support comprehensive environmental assessments, such as tracking wetland restoration in Europe or forest recovery in South America, by leveraging complementary data sources to reduce uncertainty (Cao et al., 2019). These strategies align with the principles of land change science, which emphasize integrated data frameworks to address global environmental challenges (Turner et al., 2007).

The policy implications of these findings are significant, particularly for Iran, where environmental pressures from urbanization and climate variability necessitate robust monitoring systems. The adoption of modern ML methods, supported by investments in computational infrastructure, could strengthen Iran's capacity to implement sustainable land use policies, such as those outlined in its national environmental plans. For instance, accurate land use change detection could inform zoning regulations to protect agricultural lands from urban encroachment, a pressing issue in provinces like Isfahan (Yousefi et al., 2011). Globally, the findings advocate for international collaboration to enhance data accessibility and computational resources, enabling developing nations to leverage advanced ML methods for environmental monitoring (Olofsson et al., 2014). Initiatives like the Global Land Cover Facility could facilitate data sharing, supporting the scalability of CNNs and BNNs in resource-limited regions.

However, practical implementation faces challenges beyond computational constraints. The complexity of modern ML models, particularly BNNs, reduces their interpretability, potentially undermining trust in policy applications where transparency is critical (Chen et al., 2020). In

Iran, where stakeholder engagement is essential for environmental policy adoption, simplified or hybrid models may be more readily accepted by local authorities. Additionally, the reliance on high-quality training data poses a barrier in regions with sparse ground truth data, necessitating strategies like transfer learning or semi-supervised approaches to adapt models to local conditions (Foody, 2010). These challenges highlight the need for tailored solutions that balance technological advancement with practical feasibility, ensuring that the benefits of modern ML methods are accessible across diverse environmental and socio-economic contexts.

In summary, the findings underscore the transformative potential of modern ML methods for environmental monitoring, offering high accuracy and uncertainty management to support sustainable resource management and policy development. In Iran, these methods can address pressing challenges like urban expansion and agricultural sustainability, while globally, they align with efforts to combat deforestation and climate change. Hybrid approaches and multi-modal data integration offer promising avenues to overcome computational and data limitations, enhancing the applicability of ML methods in resource-constrained settings. The subsequent section will address remaining challenges and propose future research directions to further advance the field of land use change detection.

5. Conclusion

The comparative analysis of classical and modern machine learning methodologies for land use change detection illuminates their differential capabilities in managing uncertainty, a pivotal challenge in remote sensing applications. This study has systematically evaluated classical methods—Support Vector Machines, Random Forests, and Maximum Likelihood classifiers—against modern approaches, specifically Convolutional Neural Networks and Bayesian Neural Networks, across diverse environmental contexts, including urban, agricultural, and aquatic landscapes. The findings underscore the transformative potential of modern methods, which achieve superior accuracy and robust uncertainty management, particularly in complex and noisy datasets, while classical methods offer practical utility in resource-constrained settings. By synthesizing these results, exploring their implications for environmental monitoring, and identifying persistent challenges, this study contributes to the advancement of sustainable land management practices in Iran and globally. This concluding section consolidates the key insights, delineates the challenges that hinder the widespread adoption of these methodologies, and proposes a comprehensive agenda for future research to enhance the efficacy and accessibility of land use change detection.

The investigation reveals that modern machine learning methods, notably Convolutional Neural Networks and Bayesian Neural Networks, outperform their classical counterparts in nearly all evaluated metrics. Convolutional Neural Networks demonstrate exceptional precision, achieving classification accuracies of 90–95% in urban settings and an F1 score of 0.89 in agricultural applications, driven by their ability to automatically extract complex spatial features from high-resolution satellite imagery. Their resilience to noise, such as cloud cover and mixed pixels, enables reliable detection of subtle land use transitions, such as urban sprawl

or crop rotation, which are critical for informed environmental planning. Bayesian Neural Networks further enhance this capability by providing probabilistic uncertainty estimates, achieving a remarkable 91.85% accuracy in urban land cover classification and offering transparency in identifying high-uncertainty areas, such as transitional zones between residential and industrial zones. These strengths position modern methods as indispensable tools for monitoring dynamic land use changes, supporting applications ranging from urban planning in rapidly growing cities like Tehran to deforestation tracking in global hotspots like the Amazon Basin.

Classical methods, while less performant in complex scenarios, retain significant value in specific contexts. Random Forests, with accuracies of 85–92% in urban settings, offer stability in heterogeneous datasets, making them suitable for agricultural monitoring in regions with moderate data quality, such as Ethiopia's Upper Blue Nile River Basin. Support Vector Machines, achieving 85–90% accuracy in urban applications, provide a computationally efficient option for smaller datasets, particularly in resource-limited areas of Iran where advanced infrastructure is scarce. Maximum Likelihood classifiers, despite their lower accuracy of 65–75% in aquatic settings, remain viable for preliminary assessments due to their simplicity and minimal data requirements. These findings highlight a critical insight: no single method is universally optimal. Instead, the choice of methodology must be guided by contextual factors, including data availability, environmental complexity, and computational resources, ensuring that both modern and classical approaches contribute to a diversified toolkit for land use change detection.

The practical implications of these findings are profound, particularly for environmental monitoring in Iran, where rapid urbanization and climate variability exacerbate pressures on agricultural and water resources. Modern methods' high accuracy enables precise tracking of urban expansion, informing zoning regulations to protect arable lands from encroachment, a pressing issue in provinces like Isfahan. Globally, the ability of Convolutional Neural Networks and Bayesian Neural Networks to integrate multi-source data supports compliance with international sustainability frameworks, such as the United Nations' Sustainable Development Goals, by providing reliable data for monitoring deforestation and land degradation. The study also advocates for hybrid approaches, combining the simplicity of classical methods with the robustness of modern techniques, and multi-modal data integration, fusing optical and radar imagery, to enhance accessibility and scalability. These strategies are particularly relevant for developing nations, where computational and data limitations hinder the adoption of advanced methodologies.

Despite these advancements, several challenges impede the widespread application of machine learning in land use change detection, necessitating a forward-looking research agenda to address them. One primary challenge is the computational intensity of modern methods, which require substantial processing power and advanced infrastructure, posing barriers in resource-constrained regions. For instance, deploying Bayesian Neural Networks in rural Iran, where

access to high-performance computing is limited, remains impractical without significant investment in technological infrastructure. Similarly, Convolutional Neural Networks' reliance on large, labeled datasets restricts their scalability in areas with sparse ground truth data, such as remote aquatic ecosystems or underdeveloped agricultural regions. These computational and data barriers underscore the need for lightweight algorithms that maintain high accuracy while reducing resource demands, ensuring that advanced methods are accessible across diverse socio-economic contexts.

Another significant challenge is the interpretability of modern machine learning models, particularly Bayesian Neural Networks, whose complex architectures and probabilistic outputs can obscure decision-making processes. In policy-relevant applications, such as environmental planning or international conservation agreements, stakeholders require transparent and interpretable models to build trust and facilitate adoption. For example, local authorities in Iran may hesitate to rely on Convolutional Neural Networks for land use zoning if the models' predictions lack clear explanations, limiting their practical utility. Classical methods, while simpler, also face interpretability issues due to their reliance on manually engineered features, which may not fully capture the nuances of complex landscapes. Addressing this challenge requires the development of explainable artificial intelligence frameworks that elucidate model decisions without sacrificing performance, enabling stakeholders to understand and act on predictions with confidence.

Data scarcity remains a persistent obstacle, particularly in developing countries where high-quality satellite imagery and ground truth data are often unavailable. In Iran's central plains, for instance, cloud cover and limited field surveys hinder the creation of robust training datasets, compromising the performance of both classical and modern methods. This issue is compounded in aquatic settings, where spectral similarities between water bodies and adjacent land cover types further complicate classification. Strategies like transfer learning, which adapts pre-trained models to new contexts with minimal data, offer a promising solution, but their efficacy in highly variable environments remains underexplored. Similarly, semi-supervised learning, which leverages limited labeled data alongside abundant unlabeled data, could enhance model performance in data-scarce regions, but its application to land use change detection requires further investigation.

The integration of multi-modal data, while promising, presents additional challenges related to data heterogeneity and processing complexity. Fusing optical, radar, and topographic data requires sophisticated preprocessing pipelines to align disparate data sources, a task that demands significant computational resources and expertise. In global contexts, where data formats and quality vary widely, standardizing multi-modal integration protocols is essential to ensure consistency and reliability. Furthermore, the ethical and privacy implications of using high-resolution satellite imagery, particularly in urban settings, warrant careful consideration. Monitoring land use changes in densely populated areas may inadvertently capture sensitive

information, raising concerns about data misuse and necessitating robust governance frameworks to protect stakeholder interests.

Looking ahead, future research should prioritize several key directions to address these challenges and advance the field of land use change detection. First, the development of lightweight machine learning algorithms is critical to enhance the accessibility of modern methods. Techniques such as model pruning, quantization, and efficient neural network architectures could reduce the computational footprint of Convolutional Neural Networks and Bayesian Neural Networks, enabling their deployment on edge devices or low-resource systems. Such innovations would democratize access to advanced methodologies, allowing regions like rural Iran to leverage high-accuracy models for agricultural and aquatic monitoring without requiring extensive infrastructure.

Second, advancing explainable artificial intelligence is essential to improve model interpretability, particularly for policy applications. Developing frameworks that visualize feature importance, quantify uncertainty contributions, and provide human-readable explanations of predictions could bridge the gap between complex models and stakeholder needs. For instance, integrating attention mechanisms into Convolutional Neural Networks could highlight the spatial regions driving classification decisions, offering insights into urban land use patterns that policymakers can readily interpret. Similarly, enhancing Bayesian Neural Networks with interpretable uncertainty metrics could facilitate their adoption in high-stakes applications, such as international environmental monitoring.

Third, expanding the application of semi-supervised and transfer learning techniques holds significant potential for addressing data scarcity. Future studies should explore the adaptation of pre-trained models to diverse environmental contexts, such as Iran's arid landscapes or Southeast Asia's wetlands, using minimal labeled data. Semi-supervised learning could be particularly effective in aquatic settings, where unlabeled satellite imagery is abundant but ground truth data is scarce, enabling models to learn robust features from noisy or incomplete datasets. These approaches could also support the creation of global land use change detection models that generalize across regions, reducing the need for region-specific training data.

Fourth, standardizing multi-modal data integration protocols is a priority to streamline the fusion of optical, radar, and topographic data. Research should focus on developing automated preprocessing pipelines that align data sources, correct for inconsistencies, and optimize computational efficiency. Such protocols would enhance the scalability of multi-modal approaches, enabling their use in large-scale environmental monitoring programs, such as global deforestation tracking or wetland restoration initiatives. Collaborative efforts to establish open-access data repositories could further support these endeavors, providing researchers with diverse datasets to train and validate integrated models.

Fifth, addressing the ethical and privacy implications of land use change detection requires the development of governance frameworks that balance technological advancement with stakeholder rights. Future work should explore privacy-preserving techniques, such as

federated learning, which enable model training without sharing sensitive data, ensuring compliance with data protection regulations. Engaging local communities in the design and deployment of monitoring systems could also enhance trust and ensure that land use change detection aligns with societal needs, particularly in urban Iran, where community input is critical for sustainable development.

In conclusion, this study establishes a robust foundation for understanding the comparative efficacy of classical and modern machine learning methods in land use change detection, highlighting the transformative potential of Convolutional Neural Networks and Bayesian Neural Networks in managing uncertainty. While classical methods retain value in resource-constrained settings, modern approaches offer unparalleled accuracy and reliability, supporting sustainable environmental monitoring in Iran and globally. The identified challenges—computational intensity, interpretability, data scarcity, and data integration complexities—underscore the need for innovative solutions to enhance the accessibility and impact of these methodologies. By pursuing lightweight algorithms, explainable AI, semi-supervised learning, standardized multi-modal integration, and ethical governance, future research can unlock the full potential of machine learning for land use change detection, advancing the field toward more reliable, inclusive, and sustainable environmental management. These efforts will ensure that land use change detection continues to evolve as a critical tool for addressing the pressing environmental challenges of the 21st century, from urban sustainability to global biodiversity conservation.

6. References

Ahmadpour, A., Soleimani, K., Shokri, M., & Ghorbani, J. (2014). Comparison of the efficiency of three common supervised classification methods of satellite data in vegetation cover studies. *Civilica*. https://civilica.com/doc/1166233

Akhbari, M., Ranjbar, A., & Fatemi, S. M. B. (2006). Investigation of satellite image classification methods. *Civilica*. https://civilica.com/doc/1389513

Cao, C., Dragićević, S., & Li, S. (2019). Land-use change detection with convolutional neural network methods. *Environments, 6*(2), 25. https://doi.org/10.3390/environments6020025

Chen, Y., Li, X., & Zhang, S. (2020). Uncertainty analysis in land cover classification using deep learning. *Remote Sensing, 12*(15), 2345. https://doi.org/10.3390/rs12152345

Foody, G. M. (2010). Assessing the accuracy of land cover change with imperfect ground reference data. *Remote Sensing of Environment, 114*(10), 2271-2285. https://doi.org/10.1016/j.rse.2010.05.003

Gal, Y., & Ghahramani, Z. (2016). Dropout as a Bayesian approximation: Representing model uncertainty in deep learning. *Proceedings of the 33rd International Conference on Machine Learning, 48*, 1050-1059.

Huang, C., Davis, L. S., & Townshend, J. R. G. (2002). An assessment of support vector machines for land cover classification. *International Journal of Remote Sensing, 23*(4), 725-749. https://doi.org/10.1080/01431160110040323

Ma, L., Liu, Y., Zhang, X., Ye, Y., Yin, G., & Johnson, B. A. (2019). Deep learning in remote sensing applications: A meta-analysis and review. *ISPRS Journal of Photogrammetry and Remote Sensing, 152*, 166-177. https://doi.org/10.1016/j.isprsjprs.2019.04.015

Momeni, M., Saram, M. A., Latif, A. M., & Sheikhpour, R. (2020). Presenting a convolutional neural network based on dynamic adaptive fusion for noisy image classification. *Signal and Data Processing, 46*(17), 139-153.

Olofsson, P., Foody, G. M., Herold, M., Stehman, S. V., Woodcock, C. E., & Wulder, M. A. (2014). Good practices for estimating area and assessing the accuracy of land change. *Remote Sensing of Environment, 148*, 42-57. https://doi.org/10.1016/j.rse.2014.02.013

Rezaei, Y., Rezaei, A., Darke, F., & Azarafza, Z. (2021). Classification of polarimetric radar images based on a support vector machine and binary gravitational search algorithm. *Signal and Data Processing, 47*(18), 87-102.

Thanh Noi, P., & Kappas, M. (2018). Comparison of Random Forest, k-Nearest Neighbor, and Support Vector Machine classifiers for land cover classification using Sentinel-2 imagery. *Sensors, 18*(1), 18. https://doi.org/10.3390/s18010018

Tikuye, B. G., Rusnak, M., Manjunatha, B. R., & Jose, J. (2023). Land use and land cover change detection using the Random Forest approach: The case of the Upper Blue Nile River Basin, Ethiopia. *Global Challenges, 7*, 2300155. https://doi.org/10.1002/gch2.202300155

Turner, B. L., Lambin, E. F., & Reenberg, A. (2007). The emergence of land change science for global environmental change and sustainability. *Proceedings of the National Academy of Sciences, 104*(52), 20666-20671. https://doi.org/10.1073/pnas.0704119104

Yousefi, S., Tazeh, M., Mirzaee, S., Moradi, H. R., & Tavangar, S. (2011). Comparison of different classification algorithms of satellite images in preparing land use maps (Case study: Noor County). *Journal of Remote Sensing and GIS in Natural Resources, 3*(2), 15-26

May 2025
Volume 1
Issue 1

Interdisciplinary Journal of Civil Engineering
Shahid Beheshti University

DOI: 10.48308/ijce.2025.240177.1008

Urmia Lake Salinity and Evaporation Management: Prioritizing Critical Areas

Authors:

Amir Rashidi Kordgheshlaghi[1], Alireza Vafaeinejad[1], Saeed Behzadi[1, *]

Abstract

By examining the evapotranspiration rate of the northern and southern parts of Urmia Lake, an attempt has been made to find a better solution for sustainable management of the region based on prioritizing sensitive areas for further attention. By integrating Landsat-based evapotranspiration estimates into a GIS framework, we spatially identify and rank the most vulnerable zones, thereby guiding targeted management strategies. To calculate evapotranspiration, the SEBAL algorithm was used with the help of Landsat satellite data from 2002 to 2020. Due to its comparative nature, the evapotranspiration rate was calculated in a simplified manner and without considering meteorological parameters. First, by examining the rate of groundwater changes, we found that the rate of decrease in both regions was almost the same, and this data was obtained from the GRACE satellite. Using precipitation data and calculating the standard precipitation index (SPI), we concluded that when precipitation decreased in the southern part, evaporation was much higher than in the northern part with increasing temperature, while in different time intervals, they changed almost at a constant ratio in both regions, which indicates that water salinity has increased due to climate change, which has led to increased evaporation and ultimately a further decrease in lake water in the southern part, which requires attention to this area in regional management.

Keywords: SEBAL, Evapotranspiration, SPI, VHI, Google Earth Engine

1. Faculty of Civil, Water, and Environmental Engineering, Shahid Beheshti University, Tehran 1983969411, Iran

*Corresponding Author: s_behzadi@sbu.ac.ir

1. Introduction

The Lake Urmia watershed is the area where surface and groundwater flow into Lake Urmia (Jani et al., 2023), which is one of the key areas in the management of Iranian water resources, with a network of seasonal and permanent rivers, plays an important role in feeding and maintaining the saline Lake Urmia. This basin includes rivers, agricultural areas, urban areas, and other natural ecosystems, all of which directly or indirectly affect the lake's water level (Jani et al., 2023; Kazemi Garajeh, Akbari, et al., 2024). Due to its arid and semi-arid climate conditions, this region is always exposed to severe climate changes, increased water withdrawal for agricultural and industrial uses, and reduced rainfall. Factors that have caused the lake's water level to decrease, drought to increase, and environmental and economic problems to arise. On the other hand, the importance of this region, due to its direct impact on agriculture, biodiversity, and the sustainability of the region's ecosystems, has made careful monitoring of hydrological and climatic trends a scientific and management necessity. This basin is a vast area in the northwest of Iran that includes many sub-basins, each with its own hydrological characteristics (Jani et al., 2023). The main water sources of the basin are rainfall, surface runoff, and groundwater. Numerous rivers also originate from the mountains and flow into Lake Urmia or groundwater, which is important in supplying the lake with water (Jani et al., 2023). In two decades, due to the decrease in the level of Lake Urmia, the salinity of the lake has increased. The risk of increasing salt marshes and the spread of various diseases will be even greater than the size of this basin, which is a very vital issue in the region, and for this reason, focusing on sustainable management of the region and controlling water consumption is essential for this region.

The vital framework for the analysis and management of sustainable development in the Urmia Lake basin is formed by Geographic Information Systems (GIS) and Remote Sensing (RS). RS offers the opportunity to acquire high-resolution spatial and temporal data essential for the determination of key climatic indicators. Among the indicators is the measurement of surface evaporation and transpiration, the rate of which has a direct relationship with the temperature of the air and the water. Another indicator is the measurement of the rainfall rate, the increase or decrease of which over time can be a telltale sign of climate change. Yet another is the determination of the change in groundwater storage, the knowledge of which is essential for understanding the basin's hydrologic regime. These datasets are then integrated, processed, and analyzed in GIS environments using Google Earth Engine and ArcGIS Pro to produce spatiotemporal maps of the northern and southern basins. Through GIS-based spatial analysis, sensitive areas are prioritized based on the intensity of climatic and human impacts, which helps in targeted management strategies and enhances the efficiency of watershed restoration efforts.

The discussion that is being raised now is to improve the management of the region to have the greatest impact in the shortest time, and this requires that areas with a high level of risk are identified, the cause of their occurrence is determined, and the effects that this situation will have on the region are analyzed and examined.

In this article, from the perspective of sustainable management of the region, considering the factors of drought and assessing the intensity of evaporation, climate change and groundwater depletion, it has been examined and attempts to find the part of the lake with the greatest amount of changes and its reasons, and prioritize restoration in order to improve the quality of management.

2. Literature Review

Due to climate change and human manipulation, this area is heading towards a decrease in water reserves and drought. Some studies show that human factors have played a more important role than climate change in the drying up of Lake Urmia. Human activities such as excessive water consumption in the agricultural sector and urbanization development put great pressure on the water resources of the basin. As a result, sustainable water resource management and changes in consumption patterns seem necessary. Furthermore, attention to adaptation strategies for water scarcity could mitigate the negative effects of this trend (Hooshyaripor et al., 2022; Sadeghfam et al., 2022; Shams Ghahfarokhi & Moradian, 2023).

The water resources of the Lake Urmia basin have been affected in various ways by climate change. These ways include our main focus of this comprehensive report: lake temperature, basin precipitation, basin evaporation, snowfall in the basin, drought conditions in the basin, groundwater resources in the basin, and river flow into the basin. Our main interest lies in understanding how the lake and its surrounding resources have been impacted by a changing climate. Why? Because an understanding is crucial for developing effective mitigation (reducing the intensity of impacts) and adaptation (making necessary changes to cope with the impacts) strategies. Further research into the specific magnitudes of these effects can better inform water management policies in the region (Hesami & Amini, 2016; Jani et al., 2023; Kazemi Garajeh, Haji, et al., 2024). In (Kazemi Garajeh, Haji, et al., 2024) the article examines the relationship between various variables such as temperature, precipitation, snow cover, groundwater salinity, and Lake water level. Changes in the Lake water level from 2000 to 2020 are also examined, showing that increasing temperature and evaporation of the water surface have caused the lake level to decrease, as well as groundwater salinity, which reduces arable land. The article (Jani et al., 2023) also examines climate change in the Lake Urmia basin. Some studies in this article have shown a trend of increasing temperature and decreasing rainfall. These findings underscore the complex interplay of climatic factors impacting the Lake Urmia ecosystem and the livelihoods dependent upon it. Further interdisciplinary research is essential to fully comprehend these dynamics and to devise sustainable solutions for the basin's future.

The article (Shams Ghahfarokhi & Moradian, 2023) addresses the causes of Lake Urmia's shrinking, focusing on climate change and human factors, and also points out that lack of precipitation and increased demand for water can lead to drought. A multivariate index for drought perception has been introduced that, in addition to precipitation, also considers water demand from the population. This innovative approach highlights the interconnectedness of environmental changes and societal pressures in exacerbating water scarcity. Such integrated

indices can provide a more holistic understanding of drought's impact and inform more effective water management strategies. The results show that drought perception is greater in densely populated areas and that population growth exacerbates the impact of drought (Hooshyaripor et al., 2022).
The article (Feizizadeh et al., 2023) examines the health effects of the drying up of saline lakes on the local population. This study examines the effects of the drying up of Lake Urmia on the health of residents of Shabestar County and shows that the health of residents of the region will be at risk with the trend towards drought. The article (Schulz et al., 2020) examines the factors that have caused the water level of Lake Urmia to decrease, and this article refers to the effect of evaporation on the decrease in the lake's water volume. These findings highlight the far-reaching consequences of the lake's desiccation, extending beyond environmental concerns to directly impact public health. Therefore, addressing the water crisis in Lake Urmia is not only an ecological imperative but also a crucial public health issue.

The article of (Jalilvand et al., 2021) examines the issue that the drying Lake Urmia has become a new source of dust of regional importance. The article (Alipour & Olya, 2015) presents a sustainable planning model for the restoration of Lake Urmia. This model emphasizes the development of an adaptive governance system, taking into account the capacity of the lake ecosystem. This article highlights the importance of stakeholder participation in water resources planning and management, which can reduce the risk of drought. These studies underscore the multifaceted challenges posed by the lake's decline, ranging from ecological and health impacts to the necessity of collaborative governance for effective restoration. The proposed sustainable planning model offers a crucial framework for addressing the crisis through inclusive and adaptive management strategies.

All the articles from different aspects of the discussion related to human and climatic reasons for the decrease in water reserves and the increase in the drought trend in the region have been examined, and the risks that may occur in the region if this trend continues have been concluded that proper management of water resources and restoration of the lake is a vital issue.

3. Methodology

3.1. Study area

Lake Urmia is a saltwater lake in northwestern Iran and the largest inland lake in the country. The lake is located between the provinces of West Azerbaijan and East Azerbaijan (figure 1). The lake's water level has decreased significantly in recent decades, with some sources such as Wikipedia stating that the decrease was about 95 percent. To accurately examine the process of evaporation and transpiration and their effects on the salinity of the lake water, in this study, two sample areas were selected within Lake Urmia, one above the lake and the other below, with the bridge in the middle of the lake as the dividing criterion.

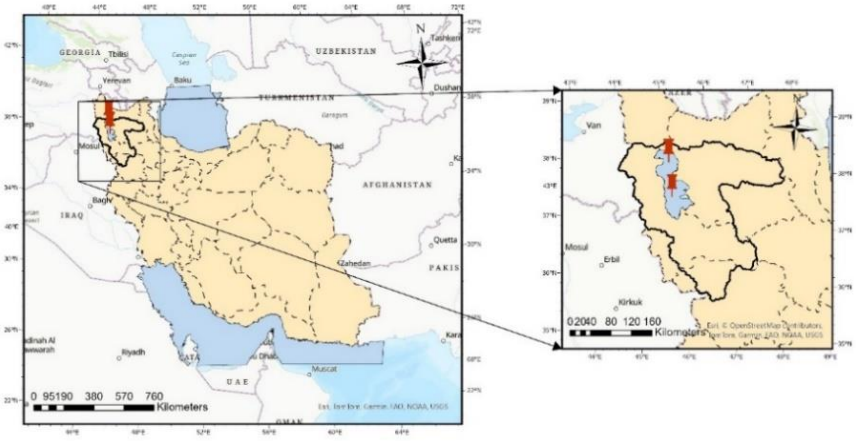

Figure 1. Urmia lake basin

The changes in these two areas have been different over time, which has caused different climatic changes in those areas. This division, in addition to showing regional differences, provides the basis for providing optimal solutions for managing water resources and dealing with the consequences of drought at the regional level.

3.2. Dataset

This study uses a set of high-quality and reliable satellite data to analyze drought and water resource trends. Land cover data were extracted from Landsat 8 and Landsat 7 satellites; these images provide a suitable basis for calculating time series of surface water cover and thermal indices due to their high resolution (30 m for multispectral bands and 15 m for panchromatic bands) and advanced processing capabilities. Landsat 8, which was completed in 2013, is equipped with OLI and TIRS structures; while Landsat 7, which began its operations in 1999 and has suffered from gaps in images despite the SLC failure since 2003, continues to be used as a valuable source for analyzing environmental changes and vegetation cover. Both satellites, in an orbit with an altitude of about 705 km and a 16-day visit period, provide the possibility of providing up-to-date and accurate data for environmental and water resource studies. This time coverage allows researchers to monitor changes in the Earth's surface over time (Sreekanth et al., 2021). Landsat data is used in various fields such as agriculture, water resources management, urban studies, and environmental studies 2021; Yang et al., 2020). Landsat satellite thermal bands have been used to calculate land surface temperature (LST) and sea surface temperature (SST) (Wang et al., 2020). The normalized difference vegetation index (NDVI) is calculated by near-infrared and red bands and visible and infrared bands of Landsat have been used to calculate surface reflectance (Wang et al., 2020). Also, the green visible light (Green) and short-wave infrared (SWIR1) bands were used to calculate the normalized difference water index (NDWI) (Sreekanth et al., 2021).

To assess precipitation, TRMM satellite data was used, which is a joint mission of NASA and the Japan Meteorological Agency, launched in 1997, and provides accurate information on precipitation patterns in tropical and subtropical regions using precipitation radar and infrared sensors (Wu et al., 2024). TRMM data is a reliable source in climate studies, agriculture, and water resources management due to its wide geographical coverage and high accuracy in measuring precipitation (Wu et al., 2024).

GRACE satellite data has also been used to investigate changes in groundwater storage and analyze hydrological trends. GRACE, launched by NASA and the German Space Agency in 2002, provides information on changes in total terrestrial water storage, including groundwater, surface water, snow, and soil moisture, by accurately measuring changes in the Earth's gravitational field. In particular, the MASS_GRIDS_V04/LAND product, which records the equivalent water thickness (LWE Thickness), is an essential tool in groundwater storage monitoring and water resources management.

The satellites and the bands they use are shown in an integrated manner as shown in Table 1. This data was extracted through Google Earth Engine and then used in the ArcGIS Pro environment for further analysis.

Table 1. Dataset

Satellite	Bands	Start date	End date
Landsat 7	Blue, green, red, NIR, Thermal Infrared	2002	2019
Landsat 8	Blue, green, red, NIR, SWIR1, Thermal Infrared	2002	2019
TRMM	precipitation	2002	2019
GRACE	lwe_thickness_csr	2002	2019

3.3. Methods

According to the flowchart in Figure 2, first, the period when the intensity of the lake water level decrease was high is identified and selected, and this is done by examining Landsat satellite images of the region using the time series of surface water changes. After determining the time period, we divide the lake into two parts, the northern and southern, and select the deepest parts as a sample. Groundwater information is examined by the GRACE satellite in the selected areas to show the extent of its changes and its impact on the studies. Then, precipitation data is collected via the TRMM satellite and SPI is modeled. The albedo value is extracted from the Landsat satellite and used to model evapotranspiration using the simplified SEBAL algorithm. By analyzing the data obtained from the ET and SPI indices, the evaporation trend during the years 2002 to 2019 is examined and conclusions are drawn.

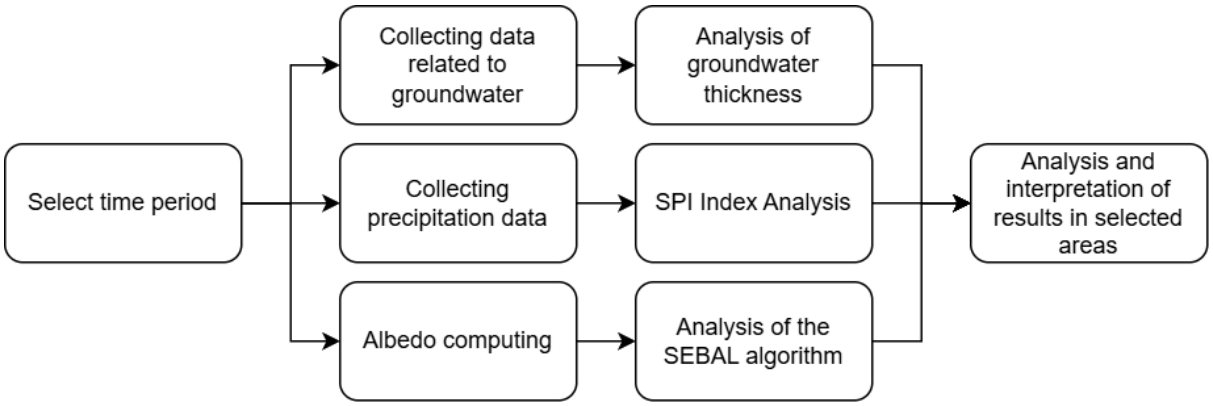

Figure 2. Research flowchart

The purpose of the study can play a role in choosing the right time frame. If our goal is to assess the effects of climate change, longer time frames are a better choice, but if our goal is to assess the effects of human activities, shorter and more precise time frames may be more appropriate (Ashraf et al., 2021) In some cases, periods are selected based on major changes in regional conditions, such as the construction of dams or land use changes (Jani et al., 2023; Tahmouresi et al., 2024). After considering the study objectives and regional variations, a period for which data is available should be selected. The desired period was determined by examining Landsat satellite images and examining the NDWI index (Shams Ghahfarokhi & Moradian, 2023). NDWI is used to measure the amount of water available in an area using remote sensing data. This index is calculated using a combination of the green and near-infrared bands of the electromagnetic spectrum. The green and near-infrared bands are used to calculate the NDWI index, and its equation is as follows (Shams Ghahfarokhi & Moradian, 2023):

$$NDWI = (Green - NIR) / (Green + NIR) \quad (1$$

High NDWI values indicate more water in the area, as water reflects more in the green spectrum and absorbs more in the near-infrared spectrum. Conversely, lower values indicate a lack of water or vegetation. Based on the trend of lake surface area changes, the period during which the rate of change is greater is determined (Shams Ghahfarokhi & Moradian, 2023) and this is important for determining the best time frame.

By measuring changes in the Earth's gravitational field, the GRACE satellite can determine changes in groundwater reserves. These changes are caused by the movement of water mass below the Earth's surface. Studies on Lake Urmia have used GRACE data to investigate the decline in groundwater reserves due to over-extraction and climate change (Ashraf et al., 2021). For this purpose, the lwe_thickness_csr band is used in the MASS_GRIDS_V04/LAND product.

The TRMM satellite has been used to extract precipitation data, which greatly helps us in ensuring the selection of the appropriate time frame for the study. TRMM data is available for a relatively long period of time (1998-2024). This allows for the analysis of precipitation trends

and their impact on water resources. These data have been used as one of the key inputs for monitoring climate change and human impacts on water resources in the Lake Urmia basin (Kazemi Garajeh, Akbari, et al., 2024). SPI can be calculated using TRMM satellite data. It is one of the most widely used indices for drought assessment, introduced by McKee and colleagues in 1993. This index is calculated based on precipitation data at different time scales and quantifies the severity and duration of drought (Hooshyaripor et al., 2022; Sadeghfam et al., 2022). The SPI value is calculated based on the changes in total precipitation over a specified period of time from the climate average and is normalized using the standard deviation of precipitation over the same period (LALMUANZUALA et al., 2023). To create the index, we first extract the precipitation data for the desired period. Then, an appropriate probability distribution function (usually the gamma distribution) is fitted to the precipitation data. The gamma distribution fits the monthly precipitation data well. Based on the fitted probability distribution, the cumulative probability for each precipitation value is calculated. Finally, the cumulative probability value is converted to the equivalent value in the standard normal distribution. This value is the SPI value (Hooshyaripor et al., 2022; Shams Ghahfarokhi & Moradian, 2023). The SPI equation is as follows (Sadeghfam et al., 2022):

$$SPI = \emptyset^{-1}(\alpha(P)) \quad (2$$

In this formula, $\emptyset^{-1}(\cdot)$ represents the inverse function of the standard normal distribution, and $\alpha(P)$ represents the gamma distribution fitted to the precipitation data (P). The SPI index is divided into 5 classes as described in Table 2:

Table 2. Classification of SPI

Class	SPI <= -2	-2 < SPI <= -1.5	-1.5 < SPI < -1	-1 < SPI < 1	1 <= SPI
Description	Very dry	Dry	Slightly dry	Normal	Full of water

Another important index to consider is the ET index based on the SEBAL algorithm. Many factors affect the accuracy of these calculations, but due to limited access to ground data, only the albedo portion of Landsat satellites was used in this study, and the simplified ET formula was used because both points are located on a lake and the time series of these two regions are comparable. The SEBAL algorithm is a method for calculating evapotranspiration at the land surface using remote sensing data. This algorithm works based on the principle of the land surface energy balance and uses satellite data and meteorological observations to estimate large-scale evapotranspiration rates (Wang et al., 2020). The main equation of the SEBAL algorithm is as follows (Wang et al., 2020):

$$LE = Rn - H - G \quad (3$$

Latent heat flux (ET) Indicates the amount of energy consumed for evaporation and transpiration, surface net radiation (Rn) is the amount of net energy received from the sun minus reflected energy and surface thermal radiation, sensible heat flux (H) is The rate of heat

transfer between the ground surface and the air and soil heat flux (G) is The rate of heat transfer into the soil.

To calculate the value of Rn we need the albedo value. The albedo value from Landsat satellites is obtained using a simple approximation with the following equation (De Razza et al., 2024):

$$\text{Surface albedo (SA)} = bBLUE * \rho BLUE + bGREEN * \rho GREEN + bRED * \rho RED + bNIR * \rho NIR + bSWIR1 * \rho SWIR1 + bSWIR2 * \rho SWIR2 + b0 \quad (4)$$

ρ is all two-way surface reflections and b is the corresponding conversion factors(De Razza et al., 2024).

After obtaining the albedo, the net surface radiation is obtained with the following simplified equation:

$$Rn = SA * 0.77 \quad (5$$

We approximately consider the value of G as 5% of the value of Rn and H as 30% of the value of Rn-G, so the simplified equation of evaporation and transpiration is calculated as follows:

$$ET = Rn * 0.665 \quad (6$$

Here, evapotranspiration ET is equivalent to latent heat flux LE.

The analyses obtained from the SPI and ET indices explain the status of the regions and the reasons for it.

4. Results

After examining images from different years, images from 2002 and 2017 were obtained from Landsat 7 and Landsat 8 satellites, respectively, and we obtained a time series of surface water changes. According to Figure 3, the rate of lake surface water changes in this period is very high and is suitable for studying evapotranspiration in the target areas. During this period, due to human manipulations such as the uncontrolled construction of dams and changes in land use (Ahmady-Birgani et al., 2018; Kazemi Garajeh, Akbari, et al., 2024), as well as climate change (Kazemi Garajeh, Akbari, et al., 2024), The rate of change in the lake has been very high, causing great concern about the future of the region.

Figure 3. From left to right, images from 2002 and 2017, and a time series of changes in Lake Urmia's level

Using GRACE satellite images for the areas specified in Figure 1, the amount of groundwater changes was obtained in the period from 2002 to 2017. According to Figure 1, which is the result of extracting the aforementioned satellite data in the specified areas, it is observed that there was a decrease of approximately 0.224 units in the entire period, which indicates water stress and drought. Long periods of rainfall deficiency (Figure 4) reduce the recharge of groundwater aquifers and, as a result, reduce their thickness (LALMUANZUALA et al., 2023). Reduced precipitation and increased evaporation and transpiration from plants cause a decrease in soil moisture and, as a result, a decrease in groundwater recharge (Kukunuri et al., 2022). Other reasons for the decline in groundwater depth include land use changes. Land use changes can reduce soil permeability and disrupt groundwater recharge, and the lack of sustainable water resource management can lead to rapid declines in water levels and aquifer thickness (Shahfahad et al., 2022). By examining Figure 4, we can conclude that the rate of groundwater changes in both regions is almost the same.

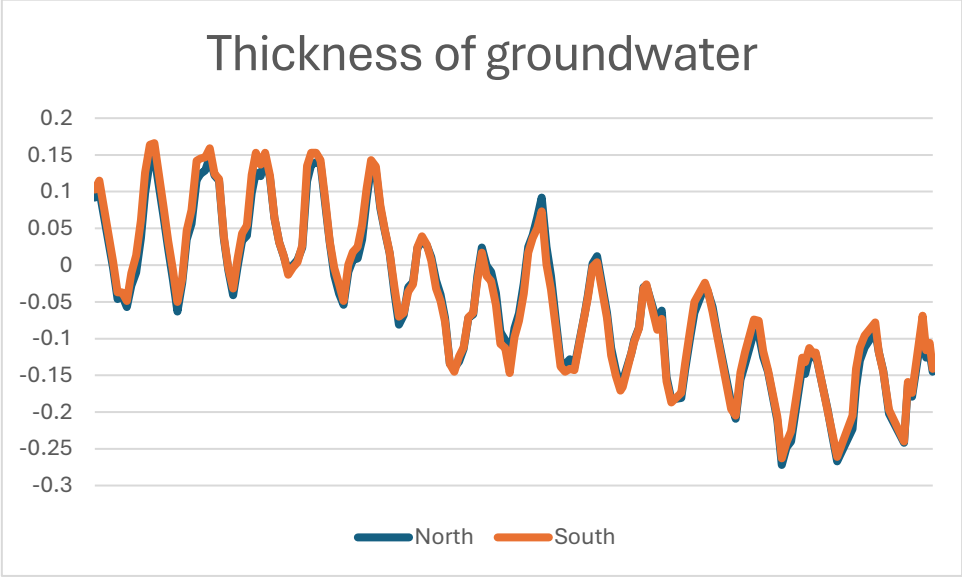

Figure 4. The thickness of groundwater between 2002 and 2017

The classified images related to SPI, according to Figure 4, show a very large decrease in the amount of precipitation compared to the average of the entire period in the Urmia Lake basin.

This image shows that in 2002, the amount of precipitation was such that the region was above the average of the precipitation in the entire period and was at a high and medium level, but in 2017, this amount faced a very sharp drop. The quantitative SPI index for the period 2002 to 2017 has been calculated according to Figure 2 and shows that the SPI in 2002 was 0.866, which indicates that the entire region is at an average level in terms of water content, and this value was at a high water level in 2006, but after that it faced a sharp decline until 2008, so that the region was at a dry level or drought, and finally in 2017, with a value of -1.3, it was also at a dry level, but after that the region has adopted a better routine.

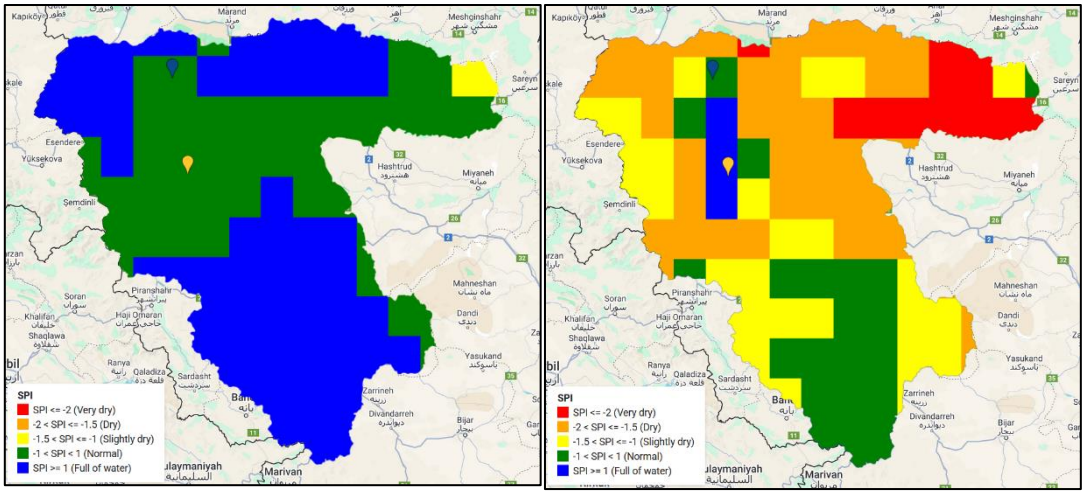

Figure 5. SPI image in 2002 and 2017

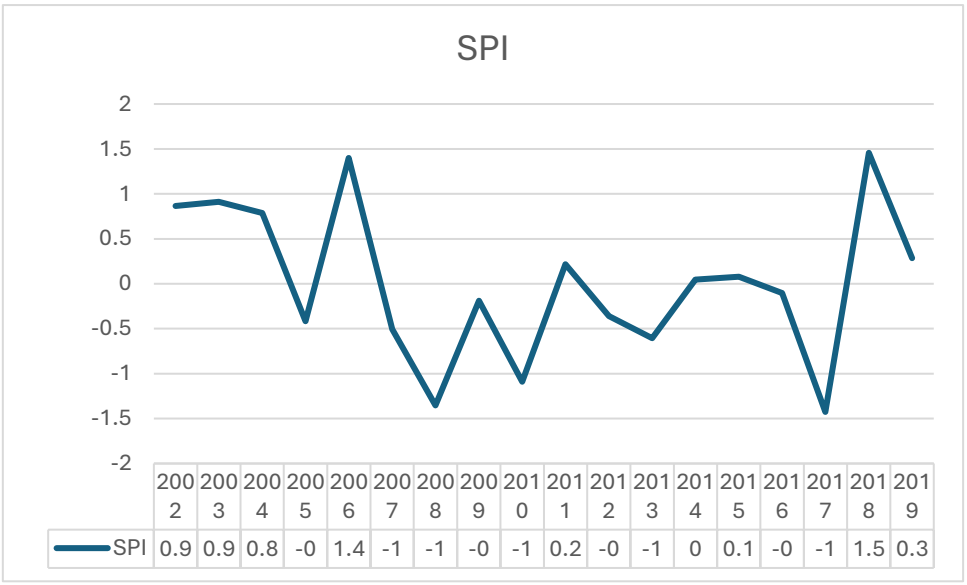

Figure 6. SPI of the Urmia Lake basin

These data show that one of the reasons for the decrease in groundwater is climate change and the decrease in average annual rainfall (Srinivas et al., 2022). The SPI index was calculated for both designated regions, and the result is shown in Figure 3. According to Figure 6, the rainfall in the northern region was slightly higher than the southern region until 2004, but after that,

the rainfall in the southern region was somewhat higher than the northern region until 2010. But in general, both regions had a similar trend in rainfall compared to the average rainfall of the entire region from 2002 to 2010. After 2010, the rate of change in the two regions has been different, so that in the northern region from 2011 to 2016, the rainfall was higher than in the southern region, and the difference in these changes between the two regions in 2014 and 2015 was very large, and in 2016, this relationship was reversed and the situation in the southern region was better than the northern region. This situation is reversed again in 2019, according to the chart. This situation shows that after 2010, the rate of climate change in the region was very severe. This chart shows that the precipitation patterns in these two regions differ over time and may be influenced by different climatic factors, as the inversion of the SPI graph between the two regions indicates that different climatic patterns prevail in these regions. (LALMUANZUALA et al., 2023). This can be due to factors such as differences in weather systems, geographical location, and topographic effects (Eicker et al., 2024; Qi et al., 2024).

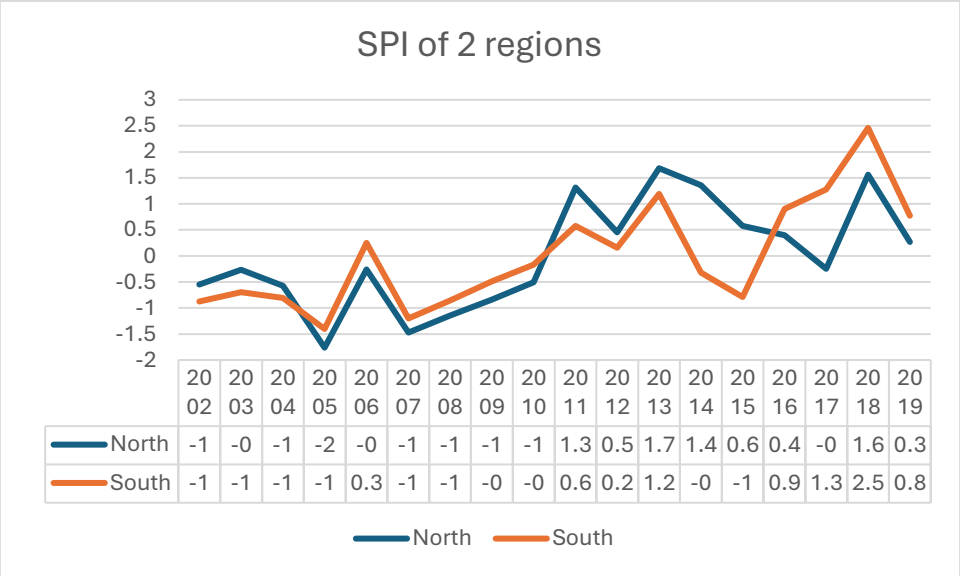

Figure 7. SPI of two regions

The evapotranspiration rate was simply calculated using Landsat satellite data for the region in March as a representative of the warm season and is shown in Figure 8. According to the chart, the evapotranspiration rate decreased by approximately 0.002 until 2004 compared to 2002. Due to the decrease in precipitation in 2005, the evaporation rate in the entire region increased, and between 2006 and 2007, it decreased again. But after 2007, it increased to the same level as in 2002. The highest evapotranspiration rate was in 2015, and after that, it decreased until 2020 and was at the average evapotranspiration rate for the entire period. This situation indicates that a decrease in the chart indicates a decrease in temperature or a decrease in precipitation, and an increase in evapotranspiration rate indicates an increase in temperature in the region and a decrease in precipitation over the entire period (Bozorg-Haddad et al., 2022; Jani et al., 2023; Schulz et al., 2020).

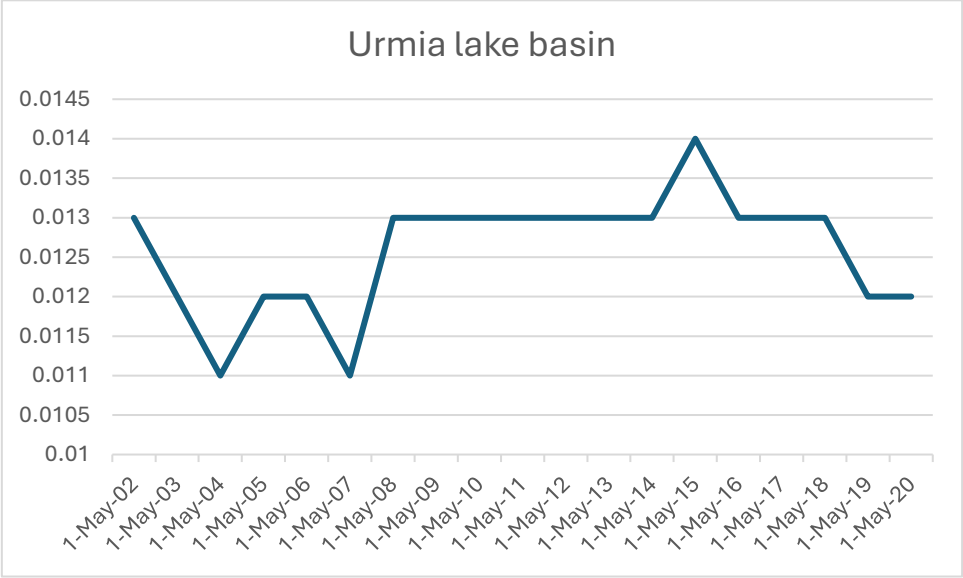

Figure 8. Urmia Lake basin evapotranspiration

After examining the rate of evapotranspiration in the entire region, we will continue to examine the rate of evapotranspiration in two selected regions. The calculated values are given in Figure 9. According to the data obtained in this chart, which is from two regions on the lake, it can be examined and concluded that the rate of evapotranspiration in the north and south of the lake increased very slightly between 2002 and 2013, and both regions are similar to each other. However, these values increased sharply in the southern part between 2014 and 2015 and returned to their previous state in 2016. According to Figure 3, it can be seen that the precipitation in 2015 in the southern part was much lower than in the northern part.

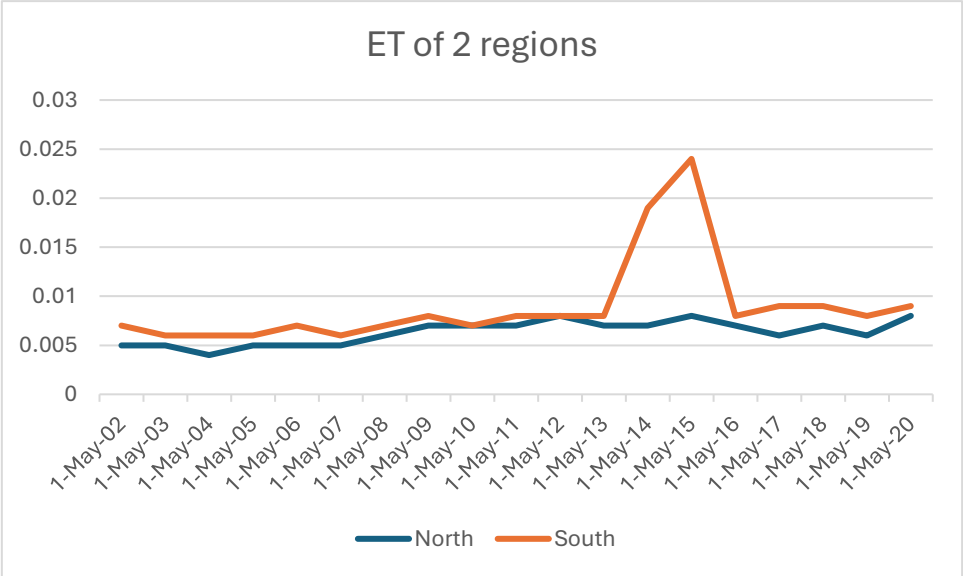

Figure 9. Evapotranspiration of two selected regions

The results of the analysis show that due to the construction of a bridge in the middle of the lake, which prevents the circulation of water in its northern and southern parts, and the

construction of numerous dams that have reduced the amount of water in the lake, the water in Lake Urmia has not only decreased, but also increased the salinity of the water in the southern part compared to the northern part. Since the region is affected by different climatic conditions, the rate of evaporation and dryness is different in the northern and southern parts. The paper (Alipour & Olya, 2015)refers to a sustainable adaptive governance model, and the paper (Shams Ghahfarokhi & Moradian, 2023) deals with resilience-based water resources management, which develops scenarios for lake restoration with the help of integrated water resources management (IWRM). It should be noted that any change in the water supply to the lake or changes in the entire region that cause harmful climate change and reduce precipitation on the lake surface (Bozorg-Haddad et al., 2022) can increase water salinity, which will result in increased evaporation and transpiration of the Lake Surface and further decrease in the lake water level (Schulz et al., 2020). Therefore, before making any changes, climatic conditions and lake water salinity must be considered to prevent the lake's water from decreasing and its causes.

5. Conclusion

In this study, it was examined that Lake Urmia, due to its unique climatic conditions and high-water salinity, is very sensitive to volume and surface changes; because any reduction in the lake's volume and area can lead to an increase in salt concentration and intensify the evaporation and transpiration processes. Additionally, the existence of a bridge connecting the northern and southern parts of the lake has disrupted the natural water circulation and distorted the uniform distribution of salinity across the water surface; so that the southern part, due to the accumulation of higher salinity water, experiences a higher rate of evaporation and transpiration. Meanwhile, the region's climatic changes—including reduced annual rainfall and increased air temperature—play a significant role in lowering water levels and increasing salinity, accelerating the gradual drying process. Considering the obtained results, prioritizing management of the southern part of Urmia Lake seems essential. Controlling salt concentration through the injection of quality water and the intelligent management of dam reservoirs can significantly prevent excessive evaporation and stop the southern areas from turning into saline wetlands. Additionally, designing and constructing water circulation pathways between the northern and southern sections to achieve hydrological balance and prevent salinity concentration are considered necessary and practical measures. These approaches, when implemented and supplemented by an ongoing, real-time monitoring program that tracks changes in salinity and water volume, will create optimal conditions for the lake's ecosystem. The local communities adjacent to the lake can expect to derive continued social and economic benefits from this ecosystem restoration effort. But recent climate and human impacts that have driven the lake's decline are not going away. The ongoing use of modern remote sensing tools and GIS will ensure that at least the impacts of these tools will be felt in more rigorous and effective management planning. This framework will also ensure that any plans made in this management framework will be sustainable.

6. References

Ahmady-Birgani, H., Agahi, E., Ahmadi, S. J., & Erfanian, M. (2018). Sediment Source Fingerprinting of the Lake Urmia Sand Dunes. *Scientific Reports*, *8*(1), 206. https://doi.org/10.1038/s41598-017-18027-0

Alipour, H., & Olya, H. G. T. (2015). Sustainable planning model toward reviving Lake Urmia. *International Journal of Water Resources Development*, *31*(4), 519–539. https://doi.org/10.1080/07900627.2014.949636

Ashraf, S., Nazemi, A., & AghaKouchak, A. (2021). Anthropogenic drought dominates groundwater depletion in Iran. *Scientific Reports*, *11*(1), 9135. https://doi.org/10.1038/s41598-021-88522-y

Bozorg-Haddad, O., Dehghan, P., Zolghadr-Asli, B., Singh, V. P., Chu, X., & Loáiciga, H. A. (2022). System dynamics modeling of lake water management under climate change. *Scientific Reports*, *12*(1), 5828. https://doi.org/10.1038/s41598-022-09212-x

De Razza, S., Carlo, Z., De Marchi, M., & Pappalardo, S. (2024). Mapping urban heatwaves and islands: the reverse effect of Salento's "white cities." *Frontiers in Earth Science*, *12*. https://doi.org/10.3389/feart.2024.1375827

Eicker, A., Schawohl, L., Middendorf, K., Bagge, M., Jensen, L., & Dobslaw, H. (2024). Influence of GIA Uncertainty on Climate Model Evaluation With GRACE/GRACE-FO Satellite Gravimetry Data. *Journal of Geophysical Research: Solid Earth*, *129*(5), e2023JB027769. https://doi.org/https://doi.org/10.1029/2023JB027769

Feizizadeh, B., Lakes, T., Omarzadeh, D., & Pourmoradian, S. (2023). Health effects of shrinking hyper-saline lakes: spatiotemporal modeling of the Lake Urmia drought on the local population, case study of the Shabestar County. *Scientific Reports*, *13*(1), 1622. https://doi.org/10.1038/s41598-023-28332-6

Hesami, A., & Amini, A. (2016). Changes in irrigated land and agricultural water use in the Lake Urmia basin. *Lake and Reservoir Management*, *32*(3), 288–296. https://doi.org/10.1080/10402381.2016.1211202

Hooshyaripor, F., Sardari, J., Dehghani, M., & Noori, R. (2022). A new concept of drought feeling against the meteorological drought. *Scientific Reports*, *12*(1), 16711. https://doi.org/10.1038/s41598-022-21181-9

Jalilvand, E., Abolafia-Rosenzweig, R., Tajrishy, M., & Das, N. N. (2021). Evaluation of SMAP/Sentinel 1 High-Resolution Soil Moisture Data to Detect Irrigation Over the Agricultural Domain. *IEEE Journal of Selected Topics in Applied Earth Observations and Remote Sensing*, *14*, 10733–10747. https://doi.org/10.1109/JSTARS.2021.3119228

Jani, R., Khatibi, R., Sadeghfam, S., & Zarrinbal, E. (2023). Climate zoning under climate change scenarios in the basin of Lake Urmia and in the vicinity basins. *Theoretical and Applied Climatology*, *152*(1), 181–199. https://doi.org/10.1007/s00704-023-04380-w

Kazemi Garajeh, M., Akbari, R., Aghaei Chaleshtori, S., Shenavaei Abbasi, M., Tramutoli, V., Lim, S., & Sadeqi, A. (2024). A Comprehensive Assessment of Climate Change and Anthropogenic Effects on Surface Water Resources in the Lake Urmia Basin, Iran. *Remote Sensing*, *16*(11). https://doi.org/10.3390/rs16111960

Kazemi Garajeh, M., Haji, F., Tohidfar, M., Sadeqi, A., Ahmadi, R., & Kariminejad, N. (2024). Spatiotemporal monitoring of climate change impacts on water resources using an integrated approach of remote sensing and Google Earth Engine. *Scientific Reports*, *14*(1), 5469. https://doi.org/10.1038/s41598-024-56160-9

Kukunuri, A. N. J., Murugan, D., & Singh, D. (2022). Variance-based fusion of VCI and TCI for efficient classification of agricultural drought using MODIS data. *Geocarto International*, *37*(10), 2871–2892. https://doi.org/10.1080/10106049.2020.1837256

LALMUANZUALA, B., SATHYAMOORTHY, NK., KOKILAVANI, S., JAGADEESWARAN, R., & KANNAN, B. (2023). Drought analysis in the southern region of Tamil Nadu using meteorological and remote sensing indices. *MAUSAM*, *74*(4), 973–988. https://doi.org/10.54302/mausam.v74i4.6040

Qi, Y., Zhong, L., Ma, Y., Fu, Y., Wang, Z., & Li, P. (2024). Evaluation of MODIS LST Products Over the Tibetan Plateau and Plain Areas With in Situ Measurements. *IEEE Journal of Selected Topics in Applied Earth Observations and Remote Sensing*, *17*, 14806–14822. https://doi.org/10.1109/JSTARS.2024.3448355

Sadeghfam, S., Mirahmadi, R., Khatibi, R., Mirabbasi, R., & Nadiri, A. A. (2022). Investigating meteorological/groundwater droughts by copula to study anthropogenic impacts. *Scientific Reports*, *12*(1), 8285. https://doi.org/10.1038/s41598-022-11768-7

Schulz, S., Darehshouri, S., Hassanzadeh, E., Tajrishy, M., & Schüth, C. (2020). Climate change or irrigated agriculture – what drives the water level decline of Lake Urmia? *Scientific Reports*, *10*(1), 236. https://doi.org/10.1038/s41598-019-57150-y

Shahfahad, Talukdar, S., Ali, R., Nguyen, K.-A., Naikoo, M. W., Liou, Y.-A., Islam, A. R. Md. T., Mallick, J., & Rahman, A. (2022). Monitoring drought patterns for pre- and post-monsoon seasons in a semi-arid region of the western part of India. *Environmental Monitoring and Assessment*, *194*(6), 396. https://doi.org/10.1007/s10661-022-10028-5

Shams Ghahfarokhi, M., & Moradian, S. (2023). Investigating the causes of Lake Urmia shrinkage: climate change or anthropogenic factors? *Journal of Arid Land*, *15*(4), 424–438. https://doi.org/10.1007/s40333-023-0054-z

Sreekanth, P. D., Krishnan, P., Rao, N. H., Soam, S., & Ch, S. (2021). Mapping surface-water area using time series Landsat imagery on Google Earth Engine: a case study of Telangana, India. *Current Science*, *120*, 1491–1499. https://doi.org/10.18520/cs/v120/i9/1491-1499

Srinivas, B., Tiwari, M. K., & Patel, G. R. (2022). An Evaluation of the Performance of Five Meteorological Drought Monitoring Indices Over an Arid and Semi-Arid Region of Gujarat (India). *International Journal of Environment and Climate Change*, 800–818. https://doi.org/10.9734/ijecc/2022/v12i1030865

Tahmouresi, M. S., Niksokhan, M. H., & Ehsani, A. H. (2024). Enhancing spatial resolution of satellite soil moisture data through stacking ensemble learning techniques. *Scientific Reports*, *14*(1), 25454. https://doi.org/10.1038/s41598-024-77050-0

Wang, Y., Zhang, S., & Chang, X. (2020). Evapotranspiration estimation based on remote sensing and the SEBAL model in the Bosten Lake Basin of China. *Sustainability (Switzerland)*, *12*(18). https://doi.org/10.3390/SU12187293

Wu, X., Liu, Y., Liu, S., Jin, Y., & Xu, H. (2024). Assessment of Satellite Products in Estimating Tropical Cyclone Remote Precipitation over the Yangtze River Delta Region. *Atmosphere*, *15*(6). https://doi.org/10.3390/atmos15060667

Yang, X., Chen, Y., & Wang, J. (2020). Combined use of Sentinel-2 and Landsat 8 to monitor water surface area dynamics using Google Earth Engine. *Remote Sensing Letters*, *11*(7), 687–696. https://doi.org/10.1080/2150704X.2020.1757780

Interdisciplinary Journal of Civil Engineering
Shahid Beheshti University

Address: Faculty of Civil, Water, and Environmental Engineering, Shahid Beheshti University, Shahid Abbaspour Technical Campus, Shahid Abolreza Blvd., Hakimieh, Tehran, Iran
P.O. Box: 1658953571
Tel: +98(21) 73932453
Fax: 77006660
Website: http://ijce.sbu.ac.ir